2021

Learning-based Predictive Control Approach for Real-time Management of Cyber-physical Systems

Roja Eini
Virginia Commonwealth University

Learning-based Predictive Control Approach for Real-time Management of Cyber-physical Systems

By

Roja Eini

A Dissertation
Submitted to the Faculty of
Virginia Commonwealth University
in Partial Fulfillment of the Requirements
for the Degree of Doctor of Philosophy
in Electrical and Computer Engineering
in the Department of Electrical and Computer Engineering

Richmond, Virginia

August 2021

Learning-based Predictive Control Approach for Real-time Management of Cyber-physical Systems

By

Roja Eini

Approved:

Sherif Abdelwahed
(Major Professor)

Carl Elks
(Committee Member)

Yanxiao Zhao
(Committee Member)

Changqing Luo
(Committee Member)

Milos Manic
(Committee Member)

Name: Roja Eini

Date of Degree: August , 2021

Institution: Virginia Commonwealth University

Major Field: Electrical and Computer Engineering

Major Professor: Dr. Sherif Abdelwahed

Title of Study: Learning-based Predictive Control Approach for Real-time Management of Cyber-physical Systems

Pages of Study: 128

Candidate for Degree of Doctor of Philosophy

Cyber-physical systems (CPSs) are composed of heterogeneous, and networked hardware and software components tightly integrated with physical elements [72]. Large-scale CPSs are composed of complex components, subject to uncertainties [89], as though their design and development is a challenging task. Achieving reliability and real-time adaptation to changing environments are some of the challenges involved in large-scale CPSs development [51]. Addressing these challenges requires deep insights into control theory and machine learning. This research presents a learning-based control approach for CPSs management, considering their requirements, specifications, and constraints.

Model-based control approaches, such as model predictive control (MPC), are proven to be efficient in the management of CPSs [26]. MPC is a control technique that uses a prediction model to estimate future dynamics of the system and generate an optimal control sequence over a prediction horizon. The main benefit of MPC in CPSs management comes from its ability to take the predictions of system's environmental conditions and disturbances

into account [26]. In this dissertation, centralized and distributed MPC strategies are designed for the management of CPSs. They are implemented for the thermal management of a CPS case study, smart building. The control goals are optimizing system efficiency (lower thermal power consumption in the building), and improving users' convenience (maintaining desired indoor thermal conditions in the building).

Model-based control strategies are advantageous in the management of CPSs due to their ability to provide system robustness and stability. The performance of a model-based controller strongly depends on the accuracy of the model as a representation of the system dynamics [26]. Accurate modeling of large-scale CPSs is difficult (due to the existence of unmodeled dynamics and uncertainties in the modeling process); therefore, model-based control approach is not practical for these systems [6]. By incorporating machine learning with model-based control strategies, we can address CPS modeling challenges while preserving the advantages of model-based control methods.

In this dissertation, a learning-based modeling strategy incorporated with a model-based control approach is proposed to manage energy usage and maintain thermal, visual, and olfactory performance in buildings. Neural networks (NNs) are used to learn the building's performance criteria, occupant-related parameters, environmental conditions, and operation costs. Control inputs are generated through the model-based predictive controller and based on the learned parameters, to achieve the desired performance. In contrast to the existing building control systems presented in the literature, the proposed management system integrates current and future information of occupants (convenience, comfort, activities), building energy trends, and environment conditions (environmental temperature, humidity,

and light) into the control design. This data is synthesized and evaluated in each instance of decision-making process for managing building subsystems. Thus, the controller can learn complex dynamics and adapt to the changing environment, to achieve optimal performance while satisfying problem constraints. Furthermore, while many prior studies in the filed are focused on optimizing a single aspect of buildings (such as thermal management), and little attention is given to the simultaneous management of all building objectives, our proposed management system is developed considering all buildings' physical models, environmental conditions, comfort specifications, and occupants' preferences, and can be applied to various building management applications. The proposed control strategy is implemented to manage indoor conditions and energy consumption in a building, simulated in EnergyPlus software. In addition, for comparison purposes, we designed and simulated a baseline controller for the building under the same conditions.

Keywords: Cyber-physical Systems, Smart Building Management System, Model Predictive Control, Machine Learning, Learning-based Control, Model-based Control

DEDICATION

I dedicate this work to my best friend and husband, Panos, who has always been there for me not only as a patient spouse, but also as an academic guide and support to lean on. I also dedicate this work to my beloved parents, Esmaeil and Minoo, my dear sister, Sara, and my beloved brother, Reza, who have always empowered me with their unconditional love and support.

ACKNOWLEDGEMENTS

First and foremost, I would like to express my deepest appreciation and sincere gratitude to my advisor, Dr. Sherif Abdelwahed for his endless support. I cannot thank him enough for supporting me during the past four years. This dissertation would not have been possible without his valuable comments, encouragement, guidance, and immense knowledge. I would also like to thank my committee members, Dr. Carl Elks, Dr. Yanxiao Zhao, Dr. Changqing Luo, and Dr. Milos Manic for their insightful suggestions and invaluable comments on this work. Lastly, special thanks go to my beloved family and all my friends for their continuous support, love, and blessings.

TABLE OF CONTENTS

LIST OF TABLES

LIST OF FIGURES

CHAPTER I

INTRODUCTION

1.1 Motivations

Cyber-physical systems (CPSs) are composed of heterogeneous, and networked hardware and software components tightly integrated with physical elements. Instances of CPS are present in many diverse technological areas, including energy, transportation, telecommunications, environmental monitoring, biomedical and biological systems [72]. In a CPS, real-world data from various physical parameters, is collected, analyzed, and monitored with the aim of optimizing resources, and enhancing users' safety and convenience [6].

Smart building management system is an example of CPSs, in which optimal decisions are made based on the information from physical world, to optimize the residents' comfort and operational costs [35]. Residential and commercial buildings account for 40% of the total energy use in the United States, 36% of the US total greenhouse gas emissions, and 12% of US fresh water consumption. A proper building management system can help reduce up to 30% of energy costs [97]. Moreover, according to [46], residents of the United States spend 90% of their lives indoors. Therefore, it is clear that an efficient building management system can save a great deal of time, money, and energy.

In a building management system, various components, such as heating, ventilation, and air conditioning (HVAC) and lighting systems, are being controlled. The control ap-

proaches for buildings management are classified into two main categories: classical control approaches and modern control techniques [35]. Classical controllers, such as on/off and proportional integral derivative (PID) controllers, have been extensively used for building management purposes; however, they are only sufficient for linear switching components, and they reveal poor performance for modulating, nonlinear, or noisy processes [75]. Furthermore, since system uncertainties and constraints are not considered in the classical controllers, deviations of the operating conditions from the tuning conditions can deteriorate control performance significantly, to the point that the system becomes unstable [13].

Modern control techniques are categorized into soft control, hard control, and hybrid control methods [94]. Hard control techniques include gain scheduling control, robust control, model predictive control (MPC), optimal control, and nonlinear control. Fuzzy logic control and artificial neural network (ANN)-based control methods are known as soft control approaches [38]. Hybrid control methods are developed by integrating soft and hard control methods. Adaptive-fuzzy control and fuzzy-PID control are examples of hybrid control techniques [92, 93]. In this essence, hard control methods are counted as model-based control techniques, and soft and hybrid control strategies are defined as learning-based techniques. MPC is one of the most commonly used control approaches for the management of CPSs. The main benefit of MPC in CPS management comes from its ability to take the predictions about the system's environmental conditions and disturbances into account [26]. Cyber-physical systems are usually subject to various changes in their structures [6]; for instance, a smart building is subject to disturbances such as occupancy profiles, occupants' behaviors, and weather conditions.

Depending on the requirements of the control problem, we can configure MPC in a centralized or distributed structure, each of which has its advantages and disadvantages. Using centralized MPC for real-world CPSs is impractical because these systems are innately large-scale and interconnected structures, which demand large centralized computational effort as well as complex communications [36]. Also, there are centralized modeling issues associated with global data collection and control actuation by a centralized agent [26]. Hence, applying distributed control methodologies for the management of real-world CPSs is considered a more suitable approach. The idea behind the distributed control approach is to split the centralized system into subsystems, that are controlled by local controllers [81]. Depending on the degree of interaction between the subsystems, agents may need to communicate to coordinate with each other. Using a distributed controller reduces the system's computational demand and eliminates the need for the system's global information. In addition, distributed control approaches are usually more accurate and tolerant to model inaccuracies and system failures [81].

From the modeling viewpoint, MPC can be designed based on a physical model of the system (known as model-based MPC), or based on a black-box model of the system (known as learning-based MPC) [71]. The majority of existing control approaches for building management systems are model-based [70, 11, 77, 21, 96, 74, 39, 44]. A model-based controller is designed based on a mathematical representation of the system dynamics. For instance, in a model-based building management system, it is assumed that each component is defined based on an accurate physical model [26]. A model-based control approach can be generalized and analyzed easily; however, it may lack sufficient accuracy for systems with

complex nonlinear dynamics [18]. To address this issue, learning-based control approaches are introduced for buildings management.

A learning-based controller is designed directly using online or off-line information of the system. An accurate mathematical representation of the system dynamics is not required for designing learning-based control approaches. Learning-based control methods can address various challenges in the control design [18]. Learning-based control strategies are utilized when (1) system's un-modeled dynamics and uncertainties can not be modeled mathematically, (2) modeling the system is time-consuming, complicated, and expensive, (3) an adequate control performance is infeasible through the model-based control design [18].

1.2 An Overview of Cyber-physical Systems

A cyber-physical system (CPS) consists of a collection of computing devices interacting with one another, and with the physical world via sensors and actuators in a feedback loop [6]. To meet their operational requirements, CPSs are expected to adapt to the changing environmental conditions and uncertainties. From the self-adaptation perspective, there are three categories of CPSs; human-operated CPSs, semi-autonomous CPSs, and autonomous CPSs [6]. Human-operated CPS learns from the environment and makes decisions in real-time with the help of human operator; a human operator remains an integral part of the system's decision-making process and interacts with the system when required. Semi-autonomous CPS operates independently in pre-defined conditions; for instance, semi-autonomous drones operate on their own, once the user has defined the flight path. Autonomous CPS is

capable of making decisions and operating independently, without any human intervention. At this point, most of the CPSs development is of the first two categories; human-operated and semi-autonomous CPSs [6].

Cyber-physical systems offer various opportunities for transforming traditional industries into smart industries, with a high level of efficiency, cost-effectiveness, and safety; smart healthcare systems, smart buildings, smart grids, and smart traffic systems are examples of CPSs. There are some challenges in CPS design and development; achieving robustness, stability, and reliability are some of these challenges [51]. Deep insights into control theory, machine learning, CPS specifications, and design requirements are required to address CPS challenges. In this dissertation, we have studied and addressed CPS challenges in smart building case studies, and we proposed control approaches for CPSs management. The following two subsections present a brief overview of CPS under study (smart buildings), and our proposed control approach for CPS management.

1.2.1 An overview of building management systems

In conventional buildings, subsystems, such as heating/cooling, ventilation, and lighting systems, are set through simple controllers which use the current measured and desired conditions to turn devices on or off. Furthermore, components in a conventional building operate independently without coordination, which means that even if each device satisfies comfort and energy savings in each zone individually, it might not meet the overall performance requirement in the entire building. Besides, environmental factors, such as outdoor climatic conditions, occupancy status, and occupants' behavior, are not considered in the

conventional building management systems. As a result, conventional building systems can not respond to the dynamically changing environmental factors in a space and can cause discomfort and energy inefficiency [24]. To address these issues, smart control strategies are used in the building management systems. For instance, using predictive control strategies in the thermal systems can reduce overheating and overcooling in a space by considering the future thermal conditions. Moreover, the occupant-related variables, such as the occupants' perception of comfort, can be included in smart building management systems.

1.2.2 An overview of the proposed control approach for CPSs management

Fig. 1.1 shows an overview of our proposed control structure for CPSs management. The structure consists of three main blocks; system module, environment module, and control module. The system module defines CPS dynamics as a function of environmental parameters, system states, and control inputs. The model can be tuned through model-based forecasting strategies or machine learning. In the environment module, the environment prediction model is trained off-line and online with the system's historical data. Moreover, the environment inputs are continuously sampled and fed into the prediction filter. The predicted environmental parameters obtained in this module are used for updating the environment parameters in the system module and control module.

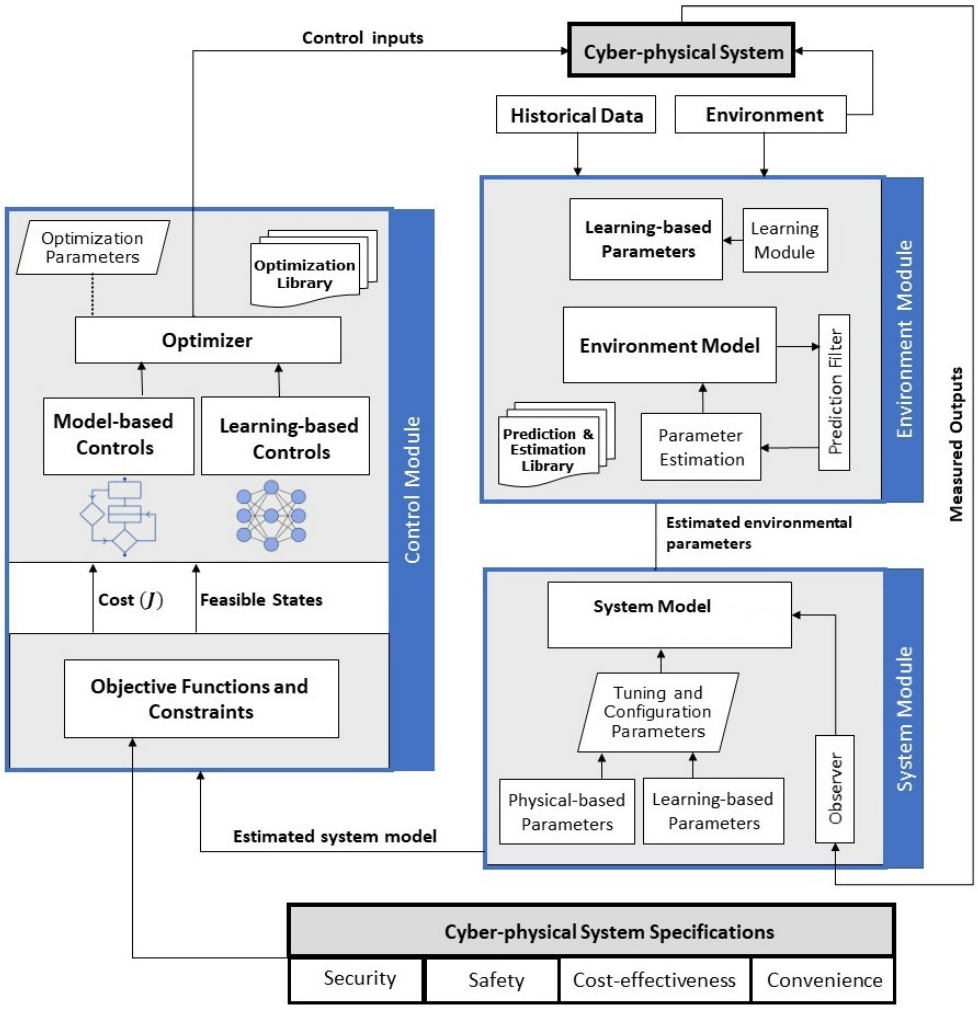

Figure 1.1: An overview of the proposed control structure for CPS management

In the control module, an objective function containing CPS performance specifications (in terms of safety, cost-effectiveness, and convenience) and its operating constraints is formulated. Optimal control inputs are generated through a learning-based or model-based optimizer. In this study, we developed predictive controllers, which utilize future states and environmental disturbances in making control decisions. Current and future control inputs

are injected to the cyber-physical system to minimize operating costs and meet the desired performance metrics.

1.3 Literature Review and Related Works

The following subsections present overviews of the related works.

1.3.1 MPC for CPS management

Literature [44, 11, 117, 96] applied centralized MPC to optimize energy consumption and thermal properties of a smart building. Authors in [11] proposed a simulation-based MPC to control an HVAC system in a multi-zone building; their results outperformed the results from a standard control strategy in terms of reducing operating costs and maintaining thermal comfort. In [117], an MPC approach is proposed to regulate the climatic condition and energy consumption in a building, considering occupancy status and outdoor temperature. Authors in [96] proposed a scenario-based MPC to control the CO_2 level and indoor temperature of a building. The main benefit of their work was reducing the complication of solving optimization problems in a regular implicit MPC.

Literature [40, 90, 79, 15] applied distributed MPC to the temperature regulation problem in a smart building. Authors in [90] proposed distributed MPC to control temperature in a three-zone building. However, the presented strategy does not include the open door situation, and only one information per time step is being exchanged. Authors in [79] applied distributed MPC to a simplified two-masses model of a building system; they did not consider the pressure and temperature dynamics in the control loop. Authors in [15]

studied the distributed control of building temperature, without considering the outdoor temperature.

1.3.2 Model-based Control for CPS management

Various control systems have been proposed for smart building management over the last few decades. Most of these efforts are focused on using model-based control approaches to achieve the goal of balancing two key factors in smart buildings; occupants' comfort, and energy-saving [112, 78, 100, 54, 20, 99, 22, 48]. The study in [112] introduced a multi-objective optimization approach for managing users' comfort and energy usage in a smart building. A mathematical model of the building energy system is first developed, then energy demand and consumption are predicted based on this model, and these predictions are utilized in a model-based cost function. Authors in [78] employed an off-line tuning methodology to find the optimum parameters (sampling period, prediction horizon, and control horizon) for the model predictive controller (MPC). The modified MPC approach is then used for the thermal control of a building. In [100], the authors utilized a modular model predictive control (MMPC) strategy to manage cooling and heating systems in an energy-efficient building. A thermal model of the building is considered through a nonlinear prediction model, and the heat flows are adjusted by the model-based controller such that energy efficiency and users' thermal comfort are optimized. The study in [54] proposed a management structure for controlling energy and thermal comfort in a building; authors used a meta-modeling approach to model the building attributes, then they optimized the building performance based on the developed meta-models. Authors in [20] proposed a

model-based predictive control approach for managing heating and cooling systems, energy storage devices, and photovoltaics (PV) cells in a smart building. In this work, a thermal model is used to predict the building zones' temperature six hours ahead; the forecasts are then utilized in the optimization problem. Various constraints, such as occupants' comfort, PV generation, and storage capacity, are considered in the control problem. Another model-based management system for smart building control is presented in [99]. The authors introduced an MPC-based approach that learns the building's energy system dynamics, and regulates its multiple energy sources. Their proposed approach provides fast response times to rapidly fluctuating energy production and consumption systems. The authors in [22] developed a model-based controller to optimally coordinate the heating system demand, renewable energy generation, and battery power. In this study, a simple lumped model is developed, which describes the building's future thermal dynamics. A model-based controller then takes into account these thermal dynamics, renewable energy status, battery charge, outdoor temperature, electricity price, energy demand, and occupants' satisfaction in order to regulate the zonal temperatures. The study in [48] investigated energy consumption estimation and management of different kinds of appliances in a smart building. In this research, the appliances' models are described by modular mathematical models in a simulator, and they are integrated into a model-based control structure.

From a conceptual viewpoint, model-based building management systems explained in literature [112, 78, 100, 54, 20, 99, 22, 48] are similar. In all of these studies, a mathematical representation of building dynamics is used to model the process. The process modeling is then utilized to minimize the deviation of the controlled variables from the desired values

[26]. In spite of the fact that a model-based control approach is a clear structure which can be generalized and analyzed easily, creating a mathematical model for the process with sufficient accuracy is a critical issue [18]. Furthermore, since buildings are usually large-scale systems with complex components, and subject to uncertainties, modeling such systems for a model-based control design is challenging [68].

1.3.3 Learning-based Control for CPS management

Data-driven or learning-based control approaches can be employed to address the issues in a model-based control design. Unlike model-based building management systems that require mathematical representation of the building components, learning-based building management systems do not utilize models to describe building characteristics, and therefore, their performance is not affected by modeling inaccuracies. Artificial intelligence and machine learning techniques are known to be efficient in the management and control of buildings due to their capability in capturing buildings' nonlinear and complex dynamics [66]. Machine learning algorithms are particularly exploited in building management systems to learn dynamic information of occupants' activities (e.g., presence), occupants' comfort, environmental conditions (e.g., weather, light), energy generation (e.g., load profile), and energy demand. Learning and integrating this information into the management system enables optimized building operations under environmental uncertainties. Researchers have proposed various learning-based control strategies for smart buildings management [43, 80, 88, 85, 84, 83, 50, 120, 41].

In [80], a neural network-based management system is proposed to control the per-

formance of boilers in a smart building. The proposed control strategy turns on/off the boilers at the optimum time based on the data from the surrounding environment (e.g., thermal comfort information, weather data, energy consumption trend). Authors in [88] proposed a data-driven modeling approach for capturing seasonal fluctuations in a building's thermal environment and in its occupants' thermal comfort. In their study, thermal comfort limits are first modified through their approach; then, an adaptive energy management system is developed, which is able to save energy up to 34.33% over the new comfort ranges. The study in [85] introduced an artificial neural network (ANN)-based technique for the energy management of a zero-energy building. The proposed management system learns from human behavior, and optimizes energy consumption/generation based on the forecasts of renewable energy sources. The performance of this method is validated on a real case study. Authors in [84] proposed a computational intelligence (CI)-based energy management system for controlling thermal energy storage (TES) units in a building. The proposed strategy is composed of three main parts: a building power requirement predictor, a utility load predictor, and a thermal energy storage control module. Both predictions and controls are performed based on ANN approach. The proposed system is tested under different thermal scenarios, with the aim of achieving an optimal balance between energy used from utility and energy used from TES. Authors in [83] compared the performance of three deep learning algorithms (standard long short-term memory (LSTM), LSTM-based sequence to sequence (S2S) architecture, and convolutional neural network (CNN)-based architecture) on building energy demand forecasting problem. They concluded that all three deep learning algorithms performed better than the baseline (standard ANN); they

claimed that ANN algorithm is not even able to follow the general trends. They have further shown that LSTM method failed in adapting to sudden variations in the data; however, LSTM S2S and CNN models followed all the changes. In [50], a periodic operation plan is introduced to use building thermal mass for energy-saving and thermal comfort management. Energy demand forecasts are provided by the neural networks. Using the building thermal inertia, the control strategy avoids air conditioning while the room is still within the human comfort zone. Another learning-based building management system is presented in [120]. ANN-based predictors are trained from historical energy consumption and environment data. The forecasts of load profiles are then utilized to monitor energy consumption, detect anomalies/faults, and locate energy-saving opportunities.

Although learning algorithms proposed in [80, 88, 85, 84, 83, 50, 120] enable real-time forecasting in building management systems, they ignore the knowledge embedded in the mathematical models of building dynamics, and they require large training datasets to cover the system behavior. Furthermore, relying only on real-time data makes it difficult to fully understand the inference mechanism learned, and to verify the credibility of learning. In particular, evaluating the learning algorithm performance from a holistic view is not sufficient, and its reliability in a specific task needs to be assessed.

1.3.4 Incorporating Learning with Model-based Control for CPS management

By integrating machine learning with model-based control strategies, we can utilize advantages of both worlds; on the one hand, we are capable of formulating system management tasks as optimal control problems in terms of performance metrics using the

model-based design, and on the other hand, online parameters tuning is integrated within the control structure to improve the quality of partially specified dynamical system models as well as to adapt to changes in the system model itself over time. Recently, a few studies are conducted on combining machine learning with model-based control techniques for buildings management [37, 65, 98]. Authors in [37] combined learning with a model-based predictive control approach to optimize energy consumption and control temperature in a building. Authors used a deep time delay neural networks (TDNN) to mimic the behavior of a model-based controller in the context of building control. In particular, learning is utilized to develop the computational efficiency of the model-based controller. Authors in [65] integrated learning within a model-based control approach to manage energy consumption in a building equipped with HVAC, energy storage, and photovoltaic. A deep learning approach is utilized to reduce the complexity of solving the non-convex model-based optimization problem. Authors in [98] presented a hybrid ANN-Genetic algorithm (ANN-GA) for the building energy management, in which building energy demand and indoor temperature are learned through ANN models, and GA calculates the future energy consumption trend. Then, a model-based controller determines the set-point schedules based on the learned data, such that the loads are shifted to the cheaper price periods. In summary, in all the above-mentioned related works, the integrated model-based and machine learning structure for the building management is utilized in one of the following three main aspects:

- Estimating the components' dynamics through learning-based approximations,
- Learning control laws from the training data instead of solving the actual model-based optimization problem,
- Updating the optimization cost function, performance-related parameters, and operating constraints through learning-based techniques.

1.4 Summary of Contributions

As found in the literature review, the works in [37, 65, 98] draw some similarities to our study. In particular, the authors integrated a machine learning algorithm into a model-based control design to develop a building management structure. However, these studies mainly focused on smart buildings' energy-saving aspect, aiming only to manage buildings' thermal conditions but leaving aside other subsystems of buildings which may highly affect their performance. In contrast, the focus of this dissertation is on designing a building management system that improves energy efficiency while considering all other important building subsystems and objectives, including buildings' physical models, environment conditions, comfort specifications, and occupants' preferences. Furthermore, in the mentioned literature on incorporating learning with model-based control, authors only utilized learning to include the estimations of occupancy profiles or energy consumption patterns in the control loop. However, there exists a wide variety of factors in a building that can be learned to improve control performance. For instance, building comfort parameters, such as thermal and visual comfort, can be learned and included in the management system. In addition, while we acknowledge the efforts of the previous studies in the context of building management and control [11, 117, 96, 90, 79, 15, 112, 78, 100, 54, 20, 99, 22, 48, 80, 88, 85, 84, 50, 120, 37, 65, 98], it is worth mentioning that, to the best of our knowledge, none of the previous studies have provided an integrated building management system that considers all the design aspects, performance requirements, and specifications of smart buildings.

This dissertation aims to develop efficient control architectures for real-time management of CPSs. It is attempted to address computational complexity, reliability, and adaptability

issues in CPSs management. Centralized and distributed MPC approaches are proposed for CPSs management. To address computational complexity, a coordination mechanism is introduced for the distributed MPC. The coordination mechanism is very important because control performance is highly dependent on the degree of interactions between subsystems [10]. Our proposed distributed MPC approach is applied to manage a CPS case study, smart building. To ensure reliability and adaptability in CPSs management, we incorporate machine learning with a model-based control strategy in three aspects: modeling CPS components' dynamics, generating control inputs, and real-time reconfiguration of the operating constraints and requirements. A model-based controller is utilized where there is a proper mathematical representation of CPS dynamics available, and learning is applied to learn and estimate subjective CPS parameters (for instance, occupants' behavior, building's energy consumption data, environmental conditions, and comfort in a smart building). The proposed real-time building management system leads to a more efficient design structure that: a) enables CPS subsystems to adapt to environment variations, b) allows systems to adapt to the subjective occupant-related parameters, and c) enables real-time model and specifications learning and improvement. To evaluate the performance of our proposed control strategies, we have implemented them on an actual building simulated in EnergyPlus building simulation software. The main contributions of this dissertation are:

1. Designing a centralized and a distributed model predictive control (MPC) for the management of CPSs, and implementing them for the thermal management of a multi-zone building, such that the maximum comfort and minimum energy consumption

are attained. A coordination mechanism is introduced for the distributed controller to minimize the computational complexity of the control problem.

2. Proposing a learning-based predictive management system for real-time control and monitoring of thermal, visual, and olfactory conditions in smart buildings (CPS case study), and implementing the system on an actual building simulated in EnergyPlus building simulation software. The proposed management system is developed not only for comfort management and energy efficiency, but also for addressing adaptability and reliability issues in CPS management.

3. In comparison to the previous building management systems presented in the literature, the proposed learning-based management structure uses a combination of model-based predictive control strategies and learning algorithms to include all building performance aspects (thermal, visual, auditory subsystems) in the design.

4. Compared to the previous works, the proposed management system includes a mechanism to integrate the current and future information of occupants (such as preferences, convenience, comfort criteria, activities), building energy trends (supply and demand), and environment conditions (such as environmental temperature, humidity, and light) into the control design. This data is synthesized and evaluated in each instance of decision-making process for scheduling building subsystems.

5. Unlike many prior studies in the field, which were typically developed for a particular building application with specific needs and requirements, the proposed manage-

ment system is a generic control structure which can be applied to various building management applications.

1.5 Dissertation Organization

The dissertation is organized as follows. Chapter 2 provides a detailed description of smart building components, their specifications, requirements, and constraints. In chapter 3, centralized and distributed model predictive control approaches are introduced for CPSs management, and they are implemented for the management of CPS case study; thermal management of smart building. The performance of distributed and centralized control approaches are also compared and analyzed in chapter 3. In chapter 4, our proposed learning-based management system is presented for the real-time control of CPSs, and it is applied to an actual building simulated in EnergyPlus software to optimize its performance (thermal, visual, and olfactory conditions) and energy consumption. Performance of the proposed learning-based control technique is also compared to that of a baseline controller in chapter 4. Finally, conclusions and future works are provided in chapter 5.

CHAPTER II

REQUIREMENT SPECIFICATION FOR CYBER-PHYSICAL SYSTEMS

Cyber-physical systems integrate physical dynamics with computational processes; they basically operate at three layers: perception layer, transmission layer, and application layer [82]. Perception layer contains physical devices, i.e., sensors and actuators. This layer captures real-time data (such as light, sound, and temperature), and performs commands received from the application layer. Transmission layer performs the networking and communication between the perception and application layers. Various network protocols and routing devices exist in the transmission layer. In the application layer, the received information from sensors is processed, and optimal control decisions are generated for the actuators [82]. The dynamics of CPS components and its specifications are included in the application layer, and they are utilized in the decision-making process. The mathematical representation of a CPS component is as follows:

$$\begin{aligned} &x(k+1) = f(x(k), u(k), k), \qquad x(0) = x_0 \\ &g(x(k), y(k)) = 0 \end{aligned} \tag{2.1}$$

where the first argument defines the system model, and the second one represents the system specifications. $x(k) \in \mathbb{R}^n$ is a vector of state variables that should be monitored or controlled (such as temperature, humidity, and sound level), and $u(k) \in U \subset \mathbb{R}^m$ denotes the control inputs, at time step k. $y(k) \in \mathbb{R}^m$ represents a vector of the algebraic state

variables as the system output. x_0 is a vector of initial values for state variables. Under this definition, we analyze the requirements, specifications, and mathematical models for CPSs; smart buildings.

Buildings are the largest energy-consuming sector in the world [97], and therefore their management and control are of crucial importance. The first step in designing a smart building management system is to define its components. Some building components can be defined in mathematical terms, such as the thermal models, HVAC systems, and comfort parameters. There are some dynamics in a building that can not be modeled explicitly, such as the time-varying thermal dynamics due to the changing occupancy status or occupants' behavior.

In this chapter, we aim at providing a formal description of the building's mathematical models, design requirements, and specifications. The models developed for smart buildings in this chapter are then utilized in the rest of the dissertation to design management systems for these plants.

2.1 Building Components' Models

Building components are modeled differently, using approaches suitable to their characteristics. For instance, HVAC systems are modeled based on the thermodynamic laws, while occupants' behaviors are defined based on probability functions [53, 95, 58, 45]. This section provides the formulations for modeling the building's thermal and humidity conditions, and occupants' behavior. Each model's characteristics, drawbacks, and advantages are also discussed in detail.

2.1.1 Thermal models

Thermal properties of a building can be modeled through three approaches: first-principles, data-driven, and hybrid modeling methods [17]. First-principles modeling methods are based on the physical knowledge to describe the system dynamics mathematically, e.g., thermal processes. In data-driven modeling, system's parameters are measured and fed into various mathematical algorithm, such as identification algorithm, to generate the model. The hybrid modeling approach combines the first-principles methods with data-driven approaches [17]. From the first-principles modeling methods, thermal models of a storage tank, heating coil, water thermal storage tank, and heat pump in a single-zone building are developed as follows [116]:

$$
\begin{aligned}
\frac{dT_z}{dt} &= \frac{1}{\rho_a C_{p,a} V_z}\left[\dot{m}_a C_{p,a}(T_{a,s} - T_z) + q_s + \alpha_z(T_{out} - T_z)\right] \\
\frac{dT_{w,r}}{dt} &= \frac{1}{\rho_w C_w V_{tk}}[-\dot{m}_w C_w(T_{w,s} - T_{w,r}) + U_{hp}U_{hp,m}COP + \alpha_h(T_{t,mr} - T_{w,s})] \\
\frac{dT_{a,s}}{dt} &= -\frac{h_t \eta_{s,ov} A_o}{\rho_a C_v A(Ta, s - \bar{T}_t)} - \frac{\gamma \dot{m}_a}{\rho_a A L_c(T_{a,s} - T_{w,r})} \\
\frac{dT_{w,s}}{dt} &= -\frac{h_{it} A_{it}}{m_w C_w(T_t - T_w)} + \frac{\dot{m}_w}{m_w L_c(T_{w,s} - T_{w,r})} \\
COP &= 1 + (COP_{max} - 1)(1 - T_{w,s} - \frac{T_o}{\Delta T_{max}})
\end{aligned}
\tag{2.2}
$$

In the thermal model above, the zonal heating system warms up the area using a water tank, heat pump, and a heating coil. The model parameters are defined in Table 2.1 [116]. There are three control variables in this model; air flow rate ($\dot{m}_a$), water flow rate ($\dot{m}_w$), and heat pump input (U_{hp}), and the control objective is to regulate the zone temperature (T_z).

Table 2.1: Thermal model parameters

Parameter	Description	Parameter	Description
T_z	Zone temperature	$\dot{m}_a$	Air flow rate
$\dot{m}_w$	Water flow rate	V_z	Zone volume
$T_{a,s}$	Supply air temperature	V_{tk}	Volume of tank
$T_{w,s}$	Supply water temperature	α_z	Zone heat loss
$T_{w,r}$	Return water temperature	α_h	Tank heat loss
$T_{t,mr}$	Mechanical room temperature	ρ_w	Water density
T_{out}	Outdoor air temperature	ρ_a	Air density
T_o	Source water temperature of heat pump	U_{hp}	Heat pump input
$\bar{T}_t$	Tube temperature	$U_{hp,m}$	Maximum heat pump capacity
COP	Performance coefficient of the heat pump	q_s	Internal heat gain
$C_{p,a}$	Air heat constant	A	Cross sectional area
C_w	Water heat constant	A_o	Total area of coil
h_t	Heat transfer coefficient of air	A_{it}	Inside area of tube
h_{it}	Heat transfer coefficient between water and tube	L_c	Heat coil length
$\eta_{s,ov}$	Overall efficiency of fins in sensible heat transfer	γ	Heat transfer ratio

Many researchers utilize the electro-thermal models of buildings for thermal control design purposes [15, 57, 16]. This kind of thermal design allows for easy modeling of buildings with various plans as well as considering the thermal interactions between the zones. In electro-thermal modeling, an equivalent electrical circuit, composed of resistors, capacitors, and current sources, represents the building's thermal model. The circuit's voltage and current represent the temperature and heat flux, respectively. Moreover, the

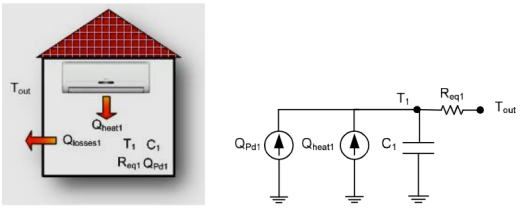

Figure 2.1: Electro-thermal circuit model of a single-zone building [15]

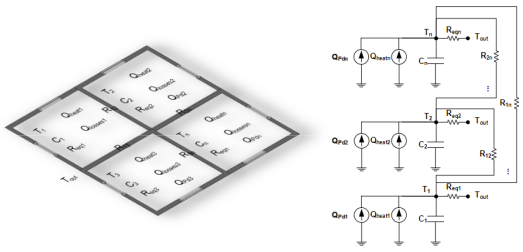

Figure 2.2: Electro-thermal circuit model of a multi-zone building [15]

thermal resistance and capacity of the building components are equivalent to the electrical resistance and capacitance of the circuit. Figures 2.1 and 2.2 present the electro-thermal circuit for a single-zone and a multi-zone building, respectively [15]. The thermal equations for the circuits in Figs. 2.1 and 2.2 are as follows [15]:

$$\begin{aligned} \frac{dT_i}{dt} &= \frac{1}{C_i}(Q_{heat_i} - Q_{loss_i} + Q_{pd_i}), \\ Q_{loss_i} &= \frac{T_{out} - T_i}{R_{eqi}} + \sum_{j=1}^{n} \frac{T_j - T_i}{R_{ij}}, \\ R_{eq_i} &= \frac{R_{wall_i} R_{window_i}}{R_{wall_i} + R_{window_i}} \end{aligned} \tag{2.3}$$

where Q_{loss_i}, T_i, C_i, Q_{heat_i}, and Q_{pd_i} are the heating/cooling loss, indoor temperature, thermal capacitance, heating/cooling power, and the thermal disturbances, respectively. R_{ij}, T_{out}, and R_{eq_i} denote the thermal resistance between the zones, outdoor temperature, and equivalent electrical (thermal) resistance of all the walls and windows, respectively. The electro-thermal model can be developed as a first-order model as expressed in equation (2.3), or more accurately as a second-order network with three resistors and two capacitors [32]. Studies have shown that the second-order model is more accurate in modeling the

building's thermal dynamics; however, using a higher-order model makes the control problem more complicated [32]. Using the provided thermal models in this subsection, the zonal temperature (as the state variable) is estimated at each instant, and it is utilized to generate optimal control inputs (airflow rate, water flow rate, and heat pump input) for the heating/cooling systems in the building. The parameters of thermal models can be tuned using a machine learning algorithm.

2.1.2 Humidity models

The dynamics of humidity in buildings can be defined based on the gas laws, i.e., the rate of humidity sorption and desorption [63]. Here, we present the two most commonly used humidity models for buildings, i.e., the American Society of Heating, Refrigerating, and Air-conditioning Engineers (ASHRAE) 160P humidity model [107], and Building Research Establishment (BRE) admittance humidity model [64]. The ASHRAE 160P humidity model [107] is presented in (2.4).

$$P_i = P_{o,24h} + \frac{cQ_{source}}{Q_{ventilation}} \tag{2.4}$$

where P_i and $P_{o,24h}$ are the indoor air vapour pressure (Pa) and outdoor air vapour pressure (Pa), respectively. c is a constant value, $1.36 \times 10^5 m/s$. Q_{source} and $Q_{ventilation}$ are the moisture generation rate (kg/s) and ventilation rate (m/s), respectively. In ASHRAE 160P humidity model, the moisture storage is not implicitly included in the humidity balance equation, and the 24-hour running average values are used to attain the indoor

vapour pressure. A more detailed humidity model is expressed based on BRE admittance formulations as follows [64]:

$$\frac{dh_i}{dt} = -\alpha h_i + \beta h_{sat} - nh_i + nh_o + \frac{Q_{source}}{\rho V_a} \tag{2.5}$$

where h_i, h_o, and h_{sat} denote the indoor humidity ($kg.kg^{-1}$), outdoor humidity ($kg.kg^{-1}$), and air saturation specific humidity ($kg.kg^{-1}$), respectively. α and β are the moisture admittance factors (s^{-1}). n, Q_{source}, ρ, and V_a are the air exchanging rate factor between inside and outside air (s^{-1}), moisture generation rate, air density ($kg.m^{-3}$), and indoor air volume (m^3), respectively. The first two terms in the BRE model represent the moisture balance between zone air and interior fabrics in the humidity sorption/desorption conditions. The next two terms express the impact of the inside and outside air exchange on the indoor humidity. The last term represents the impact of indoor moisture sources on the indoor humidity value.

The BRE model is developed for the building's humidity condition assuming that there is no HVAC system in the building, and the zone temperature is a constant value. To make the BRE model more compatible with modern buildings, two more terms are added to (2.5) as follows [115]:

$$\frac{dh_i}{dt} = -\alpha h_i + \beta h_{sat} - nh_i + nh_o + \frac{Q_{source}}{\rho V_a} + \epsilon(T_i - T_{surf}) \tag{2.6}$$

where T_i and T_{surf} are the indoor temperature (K) and inside wall surface temperature (K), respectively. The modified BRE model is more accurate than the standard BRE model since it includes the difference of indoor temperature and wall temperature; the indoor temperature is changing rather than being constant in the humidity balance equation.

For considering the impact of the HVAC system on the humidity model, equation (2.6) is updated to (2.7) [115]. During the initial cooling process of the HVAC system, the temperature at the evaporator is lower than the dew point of the indoor air. This condensed air causes the dehumidification of the air coming out of the evaporator. Thus, the model is updated by adding two major terms to (2.6), i.e., the HVAC's dehumidification effect term ($\delta S_{vent}(h_i - h_{vent})$) and the humidity loss in the condensation process term ($\frac{Q_L \dot{m}}{h_v \rho V_a}$).

$$\frac{dh_i}{dt} = -\alpha h_i + \beta h_{sat} - n h_i + n h_o + \frac{Q_{source}}{\rho V_a} + \epsilon(T_i - T_{surf}) + \delta S_{vent}(h_i - h_{vent}) + \frac{Q_L \dot{m}}{h_{vent} \rho V_a}$$
$$\dot{m} = k_1(h_i - h_{surf} + k_2(T_i - T_{surf}))$$
(2.7)

where S_{vent}, h_{vent}, and Q_L are the ventilation air flow speed ($m^3.s^{-1}$), specific humidity of air from ventilation system ($kg.kg^{-1}$), and latent cooling rate ($kg.kg^{-1}.s^{-1}$), respectively. k_1 and k_2 are the humidity driving force factor ($kg.s^{-1}$) and temperature driving force factor ($kg.K.s^{-1}$), respectively. Additionally, h_{surf} is the air humidity of wall's inside surface ($kg.kg^{-1}$). Using the humidity models, indoor humidity is estimated at each instant, and it is then utilized in formulating the humidity regulation problem in the control module (Fig. 1.1). The control input of the humidity model is the moisture generation rate.

2.1.3 Occupant behavior models

The occupants' behavior (e.g., presence, activities, changing the windows/blinds/shades status, clothing) alters the building parameters, including the heat gain, moisture gain, CO_2 emissions, comfort criteria, and actuators' performances. Studies have shown that human behavior variations can lead to 40% change in building energy usage [62]. Residents'

actions vary based on the season, time of the day, indoor and outdoor temperature, building orientation, state of presence (i.e., arriving, present, leaving), mood, personality, and culture. Predicting the residents' actions toward a specific situation is not easy; for instance, when an occupant feels cold, she or he might put on a sweater, increase the thermostat set-point, or close the blinds. The occupants' behavior can be modeled through the following steps:

- Collecting the environmental conditions and occupants' action data.
- Designing a probabilistic model by mapping the residents' actions to the environmental conditions. The probabilistic model should be built generic, i.e., not only for a specific type of building (commercial, residential, factory) or a specific season or location. The correlation between the indoor temperature and the window opening event is presented in Fig. 2.3 [58]. The model can be stated as a probability function, e.g., based on the Markov functions, that correlates the system's current state (affected by the resident's action) with the current environmental condition.
- Choosing an appropriate learning algorithm to refine the correlations.
- Testing and validating the model by comparing its outputs with the actual system's outputs.

The probability (P) that an occupant takes specific behavioral decisions or actions (A) is defined as a function of the occupant's characteristic (O) and the current environmental conditions (C), as (2.8). An occupant tends to take actions (e.g., switching lights or turning on AC) when the environmental conditions exceed the comfort zone limits. The more the environmental conditions exceed the occupant's comfort zone, the more likely the occupant will take an action (higher probability). In this regard, the probability function is cumulative and incremental as (2.9) [58].

$$P(A) = f(C, O) \tag{2.8}$$

$$f = \begin{cases} f_{inc}, & \text{if } C > h \\ 0, & \text{if } C \leq h \\ f_{dec}, & \text{if } C < l \\ 0, & \text{if } C \geq l \end{cases} \tag{2.9}$$

where h and l denote the upper and lower limit of occupant's comfort zone, respectively. f_{inc} and f_{dec} are the increasing and decreasing form of the probability function f, respectively.

In this study, we present the two most commonly used occupant behavior models: occupants' actions toward blinds and window status [53], and occupants' presence status [95]. The Haldi model, proposed in [53], specifies whether the operable windows are open or closed at each step of the simulation. The model is generated based on datasets collected during a seven-year simulation in Switzerland. The probability of the window/blind status change (P) is calculated through the model. If the probability is greater than the random distribution (R), the action will happen. If the action happens, the duration of the state to remain unchanged is predicted from the Weibull distribution [67]. The model is solely developed based on the indoor/outdoor temperature, rain level, occupancy state (arriving, present, leaving), and environmental conditions.

In [95], a Markov chain model is developed to predict the occupancy status (present, arriving, leaving). This model uses the daily probability profile to determine the occupancy at each time step. Higher probability values are given to the actions taken while the occupant is leaving or arriving; i.e., the predictions from this model are fed into the Haldi model. The advantage of this model over the fixed-schedule model is that this model considers the long

and short absence/presence due to possible breaks/incidents. Utilizing the provided models, we can include the occupants' behaviors in the building management system, for instance, the occupants' status information can be considered while generating the control inputs for the heating, cooling, and ventilation systems, considering that human bodies emit heat, carbon dioxide, odours, and water vapour pressure in an environment.

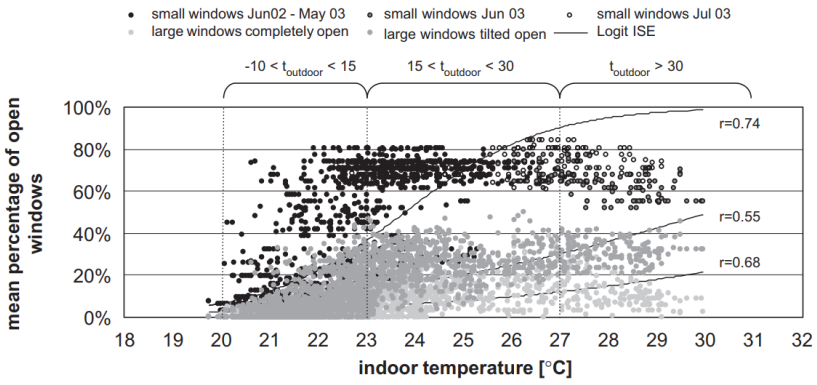

Figure 2.3: Likelihood of a window open considering the indoor temperature [58]

2.2 Building Comfort Specifications

Maintaining occupants' comfort is one of the essential control goals in building management systems. Thermal, visual, acoustic, olfactory, and hygienic comfort are the five categories of residents' comfort in buildings [23]. Building comfort parameters are evaluated based on two types of factors: environmental factors, such as the environment temperature, humidity, light, and personal factors, such as the subjective perception of comfort by individuals. Assessing comfort based on the environmental factors is way easier than evaluating it based on the occupant's personal characteristics because the environmental factors can be

measured analytically, but the personal factors are subjective parameters, which differ from one individual to another [23].

From the control viewpoint, the initial building management systems were developed with the aim of minimizing energy consumption and maintaining fixed set-points on environmental conditions; these systems did not consider the building comfort factors. Therefore, control designers utilize intelligent, adaptive, and predictive control techniques to design more efficient building management systems in which comfort specifications, occupants' preferences, and their behaviors are considered along with building energy saving aspects. Further descriptions of each of five performance criteria (thermal, visual, olfactory, auditory, and hygienic comfort) are provided in the following subsections. The models provided in this section compose the high-level specifications block in Fig. 1.1. We then extract the important environmental and personal parameters involved in each comfort criteria, and include them in the control loop.

2.2.1 Thermal comfort

One of the common scales for quantifying thermal sensation of building residents is the predicted mean vote (PMV) index, which was first introduced by the American Society of Heating, Refrigerating, and Air Conditioning Engineers (ASHRAE) [31]. PMV index is a nonlinear function, with values ranging from [-3-+3], representing cold, cool, slight cool,

neutral, slight warm, warm, and hot thermal states, respectively. PMV index equation is stated in (2.10) [31].

$$\begin{aligned} PMV = (0.303e^{-0.036M+0.028})[(M-W) - 3.05\times10^{-3}[5733 - 6.99(M-W) - P_a] \\ - 0.42[(M-W) - 58.15] - 1.7\times10^{-5}M(5867-P_a) - 0.0014M(34-T_{ai}) \\ - 3.96\times10^{-8}f_{cl}[(T_{cl}+273)^4 - (\bar{T}_r+273)^4] - f_{cl}h_c(T_{cl}-T_{ai})] \end{aligned} \tag{2.10}$$

where M,W, and P_a denote the occupant metabolic rate, external work, and water vapor pressure, respectively. T_{ai} and $\bar{T}_r$ represent the air temperature and radiant temperature, respectively. f_{cl} is the portion of body area covered with clothes, which is calculated from (2.11).

$$\begin{aligned} f_{cl} &= 1 + 1.29I_{cl} && I_{cl} \le 0.078 \\ f_{cl} &= 1.05 + 0.645I_{cl} && I_{cl} \ge 0.078 \end{aligned} \tag{2.11}$$

T_{cl} and h_c are the clothing surface temperature and convection coefficient, respectively, which are calculated from (2.12).

$$\begin{aligned} &T_{cl} = 35.7 - 0.028(M-W) - I_{cl}[3.96\times10^{-8}f_{cl}[(T_{cl}+273)^4 - (\bar{T}_r+273)^4] + f_{cl}h_c(T_{cl}-T_{ai})], \\ &h_c = 2.38(T_{cl}-T_{ai})^{0.25} && 2.38(T_{cl}-T_{ai})^{0.25} \ge 12.1\sqrt{V_a} \\ &h_c = 12.1\sqrt{V_a} && 2.38(T_{cl}-T_{ai})^{0.25} \le 12.1\sqrt{V_a} \end{aligned} \tag{2.12}$$

where V_a and I_{cl} are the air velocity and clothing thermal resistance, respectively. The radiant temperature, $\bar{T}_r$, is calculated though (2.13).

$$\bar{T}_r = [\frac{1.1\times10^8 {V_a}^{0.6}}{\epsilon D^{0.4}}(T_g - T_{ai}]) + (T_g+273)^4]^{0.25} - 273 \tag{2.13}$$

where T_g, D, and ϵ are the globe radiant temperature, diameter, and emissivity coefficient, respectively. The water vapour pressure, P_a, is calculated from (2.14).

$$P_a = 10 \times H_{ai} e^{(\frac{16.6536 - 4030.183}{T_{ai} + 235})} \tag{2.14}$$

where H_{ai} denotes the air humidity. Thus, thermal comfort standard (PMV) is a function of seven variables T_{ai}, $\bar{T_r}$, H_{ai}, V_a, I_{cl}, W, and M, as (2.15). In this study, we assess the thermal comfort value by learning the variables in PMV equation. The estimated parameters are then utilized to regulate the control variables (including air temperature (T_{ai}), and air humidity (H_{ai})) for the heating/cooling systems.

$$PMV = f(T_{ai}, \bar{T_r}, H_{ai}, V_a, I_{cl}, W, M) \tag{2.15}$$

2.2.2 Visual comfort

Visual comfort is difficult to measure due to the lack of a universal definition for it. Visual comfort is quantified based on three main factors: glare, luminance, and contrast [23]. Some common metrics for measuring glare, luminance, and contrast level are explained here.

Table 2.2: Comfort glare index (DGP and DGI) values

Glare rating	DGP average	DGP limits	DGI limits
Imperceptible	0.33	$0.314 - 0.352$	≤ 18
Perceptible	0.38	$0.356 - 0.398$	$18 - 24$
Disturbing	0.42	$0.39 - 0.448$	$24 - 31$
Intolerable	0.53	$0.464 - 0.59$	≥ 31

Table 2.3: Comfort luminance threshold levels

	Parallel to window	Facing the window
Comfortable luminance	$\leq 2000cd/m^2$	$\leq 1920cd/m^2$
Uncomfortable luminance	$\geq 4000cd/m^2$	$\geq 4500cd/m^2$

The most common glare metrics are daylight glare probability (DGP), daylight glare index (DGI), unified glare index (UGI), CIE glare index (CGI), and visual comfort probability (VCP). Among these glare metrics, DGP and DGI are the most commonly used and most reliable criteria for assessing the discomfort glare [61]. DGP index is introduced in [114], based on the subjective responses from 349 tests in a perimeter office with three window sizes and three shading systems. This metric is expressed based on the probability that a subject senses a disturbing glare, rather than measuring or quantifying the glare level. DGI metric is useful for evaluating the glare index of large glare-sources such as a window. DGI is calculated as the sum of glare contribution of each bright source [59]. The two metrics, DGP and DGI, are expressed in the following equations, respectively [114, 59].

$$DGP = 5.87 \times 10^{-5} E_v + 0.0918 \log\left(1 + \sum_i \frac{L_{s,i}^2 \omega_{s,i}}{{E_v}^{a_1} P_i^2}\right) + 0.16 \tag{2.16}$$

$$DGI = 10 \log 0.48 \sum_{i=1}^{n} \frac{{L_{s,i}}^{1.6} {\omega_{s,i}}^{0.8}}{L_b + 0.07 {\omega_{s,i}}^{0.5} L_{s,i}} \tag{2.17}$$

where $L_{s,i}$ and $\omega_{s,i}$ are the luminance (cd/m^2) and solid angle of the source, respectively. L_b, E_v, and P_i are the background luminance (cd/m^2), vertical eye illuminance (lux), and position index, respectively.

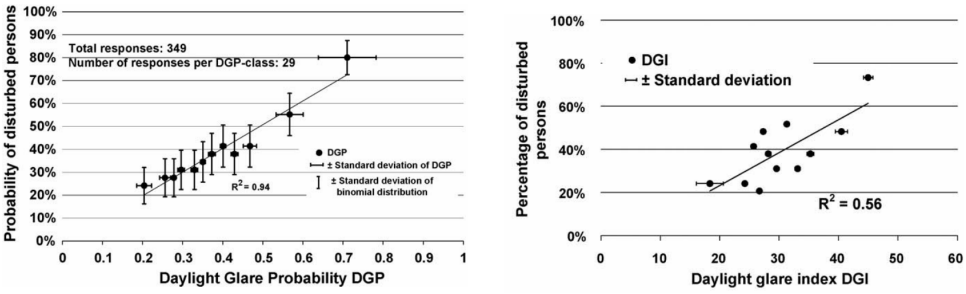

Figure 2.4: DGP and DGI glare indexes versus the percentage of residents disturbed [114]

Table 2.2 shows the recommended (minimum) DGP and DGI levels for comfortable glare [114, 59]. Fig. 2.4 presents the percentage of persons dissatisfied (PPD) metric versus the DGP and DGI values [114]. The comfortable luminance threshold range is dependent on the occupant's view direction, i.e., the thresholds for a person with a view direction parallel to or facing a window are different [60]. Furthermore, the suggested comfort/discomfort ranges vary slightly from one study to another [103, 104, 113, 109]; however, the comfortable and uncomfortable luminance thresholds shown in table 2.3 are the recommended levels by most of the related studies. The contrast between the luminance from an object and its background is an effective factor in determining visual satisfaction. Suggested contrast ratios for maintaining visual comfort vary from one study to another. For instance, authors in [101], suggested a contrast range of $3:1-40:1$ for the highest display quality. However, the Swedish National Board for Industrial and Technical Development (NUTEK) recommended a contrast range of $3:1-20:1$ for visual satisfaction. Also, a contrast ratio of $9:1-11:1$ is recommended as a comfortable display range in [121]. In this dissertation, we evaluate the visual comfort criterion by learning its

three essential contributing factors, i.e., glare, contrast, and luminance. The control inputs (source luminance ($L_{s,i}$)) for the lighting systems are generated based on the learned visual parameters.

2.2.3 Auditory comfort

The buildings' acoustical comfort is typically given low priority; however, the residents' comfort and productivity are highly dependent on their acoustical satisfaction, specifically in workspaces, conference rooms, and educational spaces. Unwanted noises cause various health issues for humans, such as cardiovascular diseases, sleep disorders, and hearing loss. According to the U.S. environmental protection agency (EPA), over 100 million people in the United States are exposed to traffic noises near their houses [106]. Furthermore, it is declared by the world health organization (WHO) that 120 million people worldwide are exposed to chronic noise pollution [19]. Although acoustic comfort is one of the essential assets in buildings, there is not any clear definition for it. Two main parameters for measuring the acoustical satisfaction/dissatisfaction are noise and loudness. The source of noise can be from outdoors or adjacent indoor spaces. Loudness can be the result of lacking a sound control in the building spaces.

There is a considerable amount of literature on the measurement and evaluation of auditory comfort. Two of the most commonly used acoustic standards in the U.S. are the sound transmission class (STC) and weighted Sound Reduction (RW) metrics [14, 2, 1]. The STC metric is introduced by the American Society for Testing and Materials, known as ASTM International [14]. STC is a standard for indicating the resistance of building

materials to airborne sound. Building materials with higher values of STC have a higher ability to reduce sound transmission. Different materials have different STC levels; for instance, STC range of glass is in the 20s or STC range of a regular wall is in the 30s. Generally, the desired range of STC for insulating the building from undesired noises is around 50s. The RW metric is also introduced by the international organization for standardization (ISO) [2, 1]. RW is similar to the STC rating, except it covers a larger frequency range than STC. RW indicates the amount of noise reduction in dB; for instance, $RW = 50$ dB means that the unwanted noise is reduced by 50 decibels. The desired amount of $RW = 53$ dB is usually suggested in the studies for residential buildings. Table 2.4 presents some other parameters that can be used for auditory comfort evaluation.

In literature [25, 87, 76], procedures are introduced in order to assess the buildings acoustical comfort. Authors in [25] evaluated the residents' acoustical comfort based on the residents' feedback. According to [25], since the STC parameter is profoundly affected by the noisy behavior of the neighbors, two other factors, the sleep awakening due to the neighbor's noise, and the subjective rating of the tenants for the building's sound insulation, should also be considered in measuring the residential acoustic comfort. The study eventually suggested $STC = 60$ dB as the lower bound of the acoustic comfort for the residents. Authors in [87] considered the footfall noise of overhead neighbors in evaluating the acoustic comfort; they suggested 55 dB as the lower bound for the apparent airborne sound reduction index (RW) value. Authors in [76] investigated the acoustic comfort based on feedback from the residents (n=800); they found out that the low-frequency noise induced by impact sound was the highest recorded source in both acoustic measurements

and self-reported noise annoyance. The comfort bound for the weighted impact sound pressure level ($L_{n,w}$) is suggested to be 53 dB in this study [76].

Although STC and RW values can be easily determined, they are not sufficient measures for evaluating the desired acoustic comfort because they do not consider the acoustic outcome or residents' opinions (i.e., satisfaction level). Furthermore, these ratings are not fully applicable to very low frequencies; i.e., a material with a high STC value may not provide soundproofing to a very low frequency sound caused by rumbling traffic, reverberating construction, or droning hubbub of office voices. The noise-caused percentage dissatisfied (NPD) is a more reliable acoustic comfort metric, which is calculated as follows [29]:

$$NPD = 4.35 \int_{-\infty}^{\text{noise level}} e^{(-(\frac{x-58.6}{13})^2)} dx \tag{2.18}$$

where x is the class of noise in dB. For a residential building, an NPD with a lower bound of 20% is suggested to be acoustically comfortable [29]. Once the acoustic comfort is evaluated, it is utilized as the system constraints of the control problem in the control module (in Fig. 1.1).

2.2.4 Olfactory comfort

Human beings breathe in and out 12000 liters of air everyday [108], and this air quality is evaluated based on the smell sense, which is an important sense in humans' body. The air quality of a building can be evaluated by measuring the amount of indoor and outdoor pollutants, such as tobacco smokes, combustion products, and micro organisms. The air quality is expressed as good, moderate, unhealthy for sensitive people, unhealthy, very

Table 2.4: Acoustic comfort parameters

STC	Sound transmission class
$D_{nT,w}$	Apparent standardized level difference index
$L_{n,w}$	Weighted impact sound pressure level
C	A-weighted pink noise spectrum adaption term
$C_{50,3150}$	C adaption term, frequency range 50-3150
RW	Apparent airborne sound reduction index

unhealthy, and hazardous, as shown in Table 2.5. Table 2.6 shows the impact of Carbon Dioxide on building residents' performance and productivity [47]. The olfactory comfort is usually measured based on the air pollutant concentration; however, this factor should be considered along with the occupants' own perception of smell. The intensity of air pollutants, considering the psychological characteristics of residents, can be defined through (2.19) [102].

$$S = kC^{\beta} \tag{2.19}$$

where C is the pollutant concentration in ppm and β denotes the psychological aspect of the resident; an exponent less than 1. To properly determine the residents' sensation of olfactory comfort, a standard known as the percentage of persons dissatisfied (PPD) with the air contaminant is utilized. The PPD equation is stated in (2.20) [102].

$$PPD = \begin{cases} 395 \ \exp\left(-3.66{L_p}^{0.36}\right), & \text{if } L_p \geq 0.3321/s. \\ 100, & \text{otherwise.} \end{cases} \tag{2.20}$$

where L_p is the air flow rate. In this study, the olfactory comfort criterion is assessed by learning the ventilator's air flow rate and pollutants intensity. The control inputs (air flow rate (L_p)) for the ventilators are generated based on the learned olfactory parameters.

Table 2.5: Air quality index levels

Air quality index	Health condition
$0 - 50$	Good
$51 - 100$	Moderate
$101 - 150$	Unhealthy for sensitive people
$151 - 200$	Unhealthy
$201 - 300$	Very unhealthy
$301 - 500$	Hazardous

Table 2.6: Impacts of excessive Carbon Dioxide on the residents' body

CO2 concentration	CO2 concentration	Impact
3%	$30000ppm$	Deep breathing
4%	$40000ppm$	Dizziness, headache
5%	$50000ppm$	Death after 0.5-1 hours
8-10%	$80000 - 100000ppm$	Death

2.2.5 Hygienic comfort

Hygienic comfort refers to creating and maintaining an environment that promotes human health [23]. The important distinction between the hygienic comfort and other comfort categories is that many hygienic hazards cannot be detected by human senses; e.g., carbon monoxide gas is colorless, odorless, and deadly. Inadequate hygienic comfort in the buildings may cause sick building syndrome (SBS) for its occupants. Headache and dizziness, aches and pains, eye/throat/skin irritations, nausea, fatigue, distraction problems, and breath shortness are the most commonly known SBS symptoms [49].

In the same vein as olfactory comfort, hygienic comfort is addressed in [7, 8] through the proper design of ventilation and handling of exhaust. The Health and Safety Executive (HSE) has provided required instructions on how to investigate the causes of SBS, diagnose it, and recover from the condition before it worsens [69]. According to HSE, the necessary parameters to be controlled for maintaining hygienic comfort are the conditions of air filters, humidifiers, and HVAC systems. Different scales are developed to calculate the hygienic comfort of buildings. Among these scales, the ASHRAE standard 62.1 (Ventilation for Acceptable Indoor Air Quality) [12] and the Indoor Air Quality Design Tool (IAQDT) [111] are the most widely used standards to express hygienic comfort. According to the ASHRAE standard 62.1 (Appendix D), hygienic comfort is determined based on the volumetric flow of outdoor air (V_o), volumetric flow of return air (V_r), volumetric flow of supply air from HVAC (V_s), recirculation flow (R), contaminant concentration in the outdoor air (C_o), contaminant concentration in a zone (C_s), filter efficiency (E_f), ventilation effectiveness (E_v), and contaminant generation rate (N) [12]. Assuming constant air flow for the HVACs,

contaminant concentration is calculated through equation (2.21), and then, it is compared with a concentration guideline for maintaining acceptable hygienic comfort level.

$$C_s = \frac{N + E_v V_o (1 - E_f) C_o}{E_v (V_o + R V_r E_f)} \tag{2.21}$$

IAQDT standard calculates contaminant concentration based on the HVAC system configuration. The main difference between IAQDT standard and ASHRAE standard 62.1 is that IAQDT does not assume steady conditions in the model, it calculates the transient concentration of contaminants [111]. Based on the IAQDT standard, contaminant concentration and supply flow rates are measured as follows:

$$\dot{m}_s c_s = \dot{m}_v (1 - \eta_v) c_o + \dot{m}_t (1 - \eta_t) c_z$$
$$\left(\frac{\rho_z V_z}{\Delta t} + \dot{m}_c \eta_c + \dot{m}_r + \dot{m}_x + \dot{m}_e + \sum R \right) c_{z,t} + \dot{m}_s \left(1 - \eta_s\right) c_{s,t} = \frac{\rho z V_z}{\Delta t} c_{z,t-\Delta t} + \dot{m}_i c_o + \sum G \tag{2.22}$$

Parameters in (2.22) are defined in Table 2.7 [111].

By calculating and collecting the contaminant concentrations throughout the day, we can learn and predict the hygienic comfort of buildings through machine learning algorithms. The estimated hygienic comfort values are then included in the control problem to regulate the HVACs, filters, and ventilation systems in buildings.

Performance of the five mentioned comfort aspects have inter-correlation; i.e., there exist conflicts between these comfort parameters. For instance, the higher rate of ventilation causes a higher level of olfactory comfort, but it may generate unwanted background noises, and causes occupants' acoustic discomfort. As another example, studies on acoustic comfort reveal that the overall acoustic satisfaction of occupants in green buildings is lower than

the same value for occupants of regular (not green) buildings [5]. Therefore, the building management system designers should consider these incompatibilities/inter-relations and create a balance between all these comfort parameters.

Table 2.7: Parameters of IAQDT standard

$\dot{m}_i$	Infiltration flow	c_o	Contaminant concentration in the outdoor air
$\dot{m}_e$	Exfiltration flow	c_s	Contaminant concentration in the mixed supply air
$\dot{m}_x$	Exhaust flow	c_z	Contaminant concentration in the zone and return air
$\dot{m}_c$	Air cleaner flow	η_v	Filter efficiency for the ventilation air stream
$\dot{m}_r$	Return flow	η_t	Filter efficiency for the recirculation air stream
$\dot{m}_s$	Supply flow	η_s	Filter efficiency for the air steam
$\dot{m}_u$	Spill flow	η_c	Filter efficiency for the air cleaner
$\dot{m}_t$	Recirculation flow	G	Contaminant generation rate
$\dot{m}_v$	Ventilation flow	R	Contaminant removal coefficient

2.3 Conclusion

In this chapter, the specifications of smart buildings (CPS case study), are described. The information provided in this chapter is utilized in the rest of this dissertation for design, development, and realization of management systems for these CPS infrastructures.

CHAPTER III

DISTRIBUTED AND CENTRALIZED MODEL PREDICTIVE CONTROL FOR CYBER-PHYSICAL SYSTEMS

In this chapter, we design centralized and distributed model predictive control (MPC) for the management of cyber-physical systems. The developed control approaches are then applied to a CPS case study; smart building. The performance of centralized and distributed control methods are compared on global and partitioned models, with different specifications. Simulation results demonstrate the effectiveness of distributed MPC for CPS management. Furthermore, a decentralized predictive control scheme is practically implemented on a smart building testbed. The building's features (surveillance, humidity, temperature, light intensity, and data streaming) are managed in real-time, through the model-based controller.

3.1 Model Predictive Control

Model Predictive Control (MPC) is an effective model-based control technique that has been applied in many areas due to its ability to handle constrained control problems [26]. MPC uses the system model to predict the future states and make optimal control decisions through its path. In every step, an optimization problem, including the current and future states and operating constraints, is solved, and control signals from the current step up to

the prediction horizon H, are generated. The first element of the control input sequence is injected into the system at instant k, and the process is repeated in each instant [26]. It is worth mentioning that MPC's performance is highly dependent on the accuracy of system model. The structure of MPC is depicted in Fig. 3.1 [26].

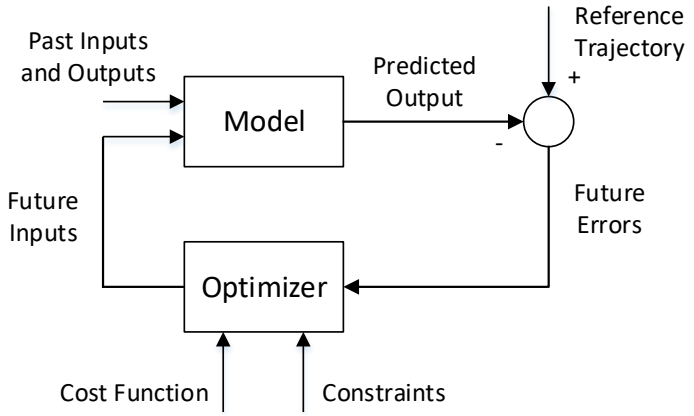

Figure 3.1: Structure of MPC [26]

3.2 Centralized Model Predictive Control

Consider a state-space model of a system as (3.1).

$$x(k+1) = f(x(k), u(k)) \tag{3.1}$$

where $x(k)$ and $u(k)$ denote the system states and control inputs, respectively, and k is the time step. The global MPC cost function for system (3.1) is stated as (3.2):

$$J = \sum_{k=0}^{K-1} J(k) \tag{3.2}$$

where K is the final time step. As though, in every time step k, the objective function $J(k)$ is minimized with the predicted parameters up to the horizon H:

$$J(k) = \sum_{h=1}^{H} L(x(k+h), u(k+h-1)) \tag{3.3}$$

In MPC, typically, an objective function that reflects a "cost" is minimized, considering the constraints on the states, system dynamics, and inputs. The cost function usually contains the deviation of the states from the desired states, control inputs, and control input changes (as in (3.4)) [26, 42].

$$L(x(k), u(k-1)) = \|x(k) - x^*(k)\|_P^2 + \|u(k-1)\|_Q^2 + \|\Delta u(k-1)\|_R^2 \tag{3.4}$$

where P, Q, and R are the weighting matrices. $x^*(k)$ is the desired value of state $x(k)$ at time step k. $u(k)$ and $\Delta u(k)$ denote the control input and control input changes at time step k, respectively. By solving the optimization problem in each time step k, over the prediction horizon H, the summation of objective terms in (3.4) from time step $k+1$ to $k+H$ is minimized. The objective of MPC is to drive the system to the desired state $x^*(k)$ (minimizing the deviation of the states from the desired states) while minimizing the control inputs and their changes. The centralized MPC algorithm is as follows:

Algorithm 1 Centralized MPC algorithm

Step 0: Get the system model at the current time.

Step 1: At $k = 0$; initialize $x(0)$, $x^*(0)$, $\Delta u(0)$, and $u(0)$.

Step 2: At time $k > 0$; apply $u(k-1 : k+h-1)$ to the system model, and determine the current and future values of the states $x(k : k+h)$.

Step 3: At time $k > 0$; determine $x(k : k+h)$, and solve the optimization problem (3.3) to calculate $u^*(k-1 : k+h-1)$.

Step 4: $k = k + 1$, go back to step 2, and repeat the algorithm.

For solving the optimization problem (minimizing the cost function), an appropriate optimization solver is required. In this research, we utilize two optimization solvers, *CasADi* and *fmincon* solvers, to solve the optimization problem throughout the MPC algorithm. *CasADi* is an open-source software tool for nonlinear optimization and algorithmic differentiation. *CasADi* is available for C++, Python, and MATLAB/Octave. This tool provides almost all the building blocks for optimal control and is used by several high-level optimization packages, such as MPCTools, ACADOS, do-mpc, FORCES Pro, JModelica.org, and Casiopeia [9]. MATLAB *fmincon* solver is used for the nonlinear multivariable optimization problems. This solver includes four optimization algorithms; interior-point (default), trust-region-reflective, SQP, and active-set, which can be chosen by setting *options* in *fmincon* function. Note that *fmincon* is a gradient-based method that is designed to work on problems

where the objective and constraint functions are both continuous and have continuous first derivatives [27].

3.3 Distributed Model Predictive Control

Distributed MPC approach is known to be effective in CPS management since large-scale CPSs consist of large number of complex subsystems [34, 91]. In a distributed MPC approach, local controllers are assigned to each subsystem of the plant, and they coordinate together to achieve a specific global performance of the entire system [118, 39]. Fig. 3.2 presents the block diagram of a distributed MPC for a CPS with N subsystems. Each local MPC controller solves a local objective function, which contains the tracking error (between the future states and the desired states), control inputs, and control inputs increments.

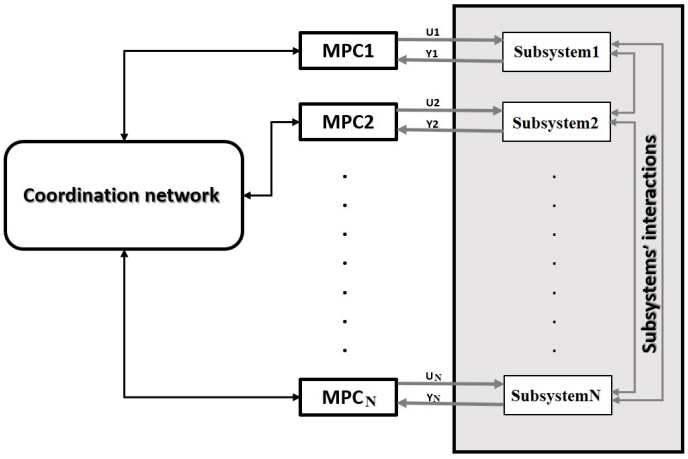

Figure 3.2: Distributed MPC on N interacted subsystems

The state-space model of each subsystem i, $\quad 1 \leq i \leq N$, is as (3.5).

$$x_i(k+1) = f_i(x_i(k), u_i(k), v_i(k)), \quad i = 1, \cdots, N \tag{3.5}$$

where $x_i(k)$ and $u_i(k)$ denote the states and control inputs of subsystem i, respectively, and k is the time step. $v_i(k)$ is a vector containing all the states of neighboring subsystems that can influence the dynamics of subsystem i. The local objective function, J_i, for each subsystem i is expressed as follows:

$$J_i = \sum_{k=0}^{K-1} J_i(k), \quad i = 1, \cdots, N \tag{3.6}$$

where K is the final time step. At each time step k, the cost function in (3.7) is minimized over the prediction horizon, considering the constraints on the system dynamics and states.

$$J_i(k) = \sum_{h=1}^{H} L_i(x_i(k+h), u_i(k+h-1), w_i(k+h)), \quad i = 1, \cdots, N$$

$$L_i(x_i(k), u_i(k-1)), w_i(k)) = \|x_i(k) - x_i^*(k)\|_{P_i}^2 + \|u_i(k-1)\|_{Q_i}^2 + \|\Delta u_i(k-1)\|_{R_i}^2 \tag{3.7}$$

where $w_i(k)$ is a vector containing all the states of neighboring subsystems that can influence subsystem i through its cost. P_i, Q_i, and R_i are the weighting matrices. $x_i^*(k)$ is the desired value of state $x_i(k)$ at time step k. $u_i(k)$ and $\Delta u_i(k)$ are the control input and control input changes of subsystem i at time step k, respectively. The constraints of the local optimization problem are stated as follows.

$$\hat{x}_i(k+1) = f_i(\hat{x}_i(k), \hat{u}_i(k), \hat{v}_i(k))), \quad \hat{x}_i(k) = x_i(k)$$

$$\hat{v}_i(k) = v_i(k), \quad \hat{w}_i(k) = w_i(k), \quad i = 1, \cdots, N \tag{3.8}$$

where $\hat{x}_i(k)$, $\hat{u}_i(k)$ are the predicted states and inputs of subsystem i at time instant k, respectively. $\hat{v}_i(k)$ and $\hat{w}_i(k)$ denote the predicted values of the states in the subsystems that influence subsystem i's dynamics and cost, respectively.

Utilizing the dual decomposition approach, we incorporate the optimization constraints (3.8) into the objective function formulation (3.7). The idea is to impose the interconnecting constraints into the objective function by the Lagrangian multipliers and solve the approximated dual cost function (duality theory is explained in [73]). Thus, the optimization problem for each local controller is the minimization of augmented function, Φ_i (stated in (3.9)).

$$\Phi_i(k) = L_i(\hat{x}_i(k), \hat{u}_i(k-1)), w_i(k) + \lambda_i(k)^T(v_i(k) - \hat{v}_i(k)) + \rho_i(k)^T(w_i(k) - \hat{w}_i(k)) \tag{3.9}$$

where λ_i and ρ_i are the Lagrangian coefficients of subsystem i, that are being updated in each iteration through (3.10).

$$\begin{aligned} \lambda_i^{s+1}(k) &= \lambda_i^s(k) + {\alpha_i}^s({v_i}^s(k) - \hat{v}_i^s(k)) \\ \rho_i^{s+1}(k) &= \rho_i^s(k) + {\beta_i}^s({w_i}^s(k) - \hat{w}_i^s(k)) \end{aligned} \tag{3.10}$$

where α_i and β_i are gradient ascent step sizes for updating the Lagrangian multipliers. Thus, the optimization problem for the entire system is as follows.

$$\begin{aligned} &\max_{\lambda_i,\rho_i} \sum_{i=1}^{N} \min_{\hat{u}_i,v_i,w_i} \sum_{k=0}^{K-1} \sum_{h=1}^{H} [L_i(x_i(k+h), u_i(k+h-1)), w_i(k+h)) + \lambda_i(k)^T v_i(k+h) \\ &+ \rho_i(k)^T(w_i(k+h) - \sum_{(i,j)} \lambda_{j,i}(k)^T \hat{x}_i(k+h) - \sum_{(i,j)} \rho_{j,i}(k)^T \hat{x}_i(k+h)] \end{aligned} \tag{3.11}$$

where i and j are the two neighboring subsystems that can have interactions. Therefore, our proposed distributed MPC strategy for CPS is as follows.

Algorithm 2 Distributed MPC algorithm

Step 1:

- Initialize the Lagrangian multipliers (${\lambda_i}^0(k:k+h)$, ${\rho_i}^0(k:k+h)$).

Step 2:

- Send $u_i(k-1:k+h-1)$ and $\hat{x}_i(k:k+h)$ to the neighboring subsystems.
- Determine the values of $\hat{v}_i(k:k+h)$, $\hat{w}_i(k:k+h)$, $\hat{x}_i(k:k+h)$, and $\hat{u}_i(k-1:k+h-1)$ in each subsystem i.
- Determine the current and future values of the desired trajectory $x^*(k:k+h)$.

Step 3:

- Solve the augmented optimization problem (3.9), and attain the optimal control input $u_i(k:k+h)$.
- Apply the first element of the optimal control $u_i(k:k+h)$ to the system.

Step 4:

- Update the Lagrangian multipliers (λ_i and ρ_i), from (3.10).

Step 5:

- $k = k+1$, go to step 2, and repeat the algorithm until $k = K$.

Fig. 3.3 shows the complete flowchart of distributed MPC.

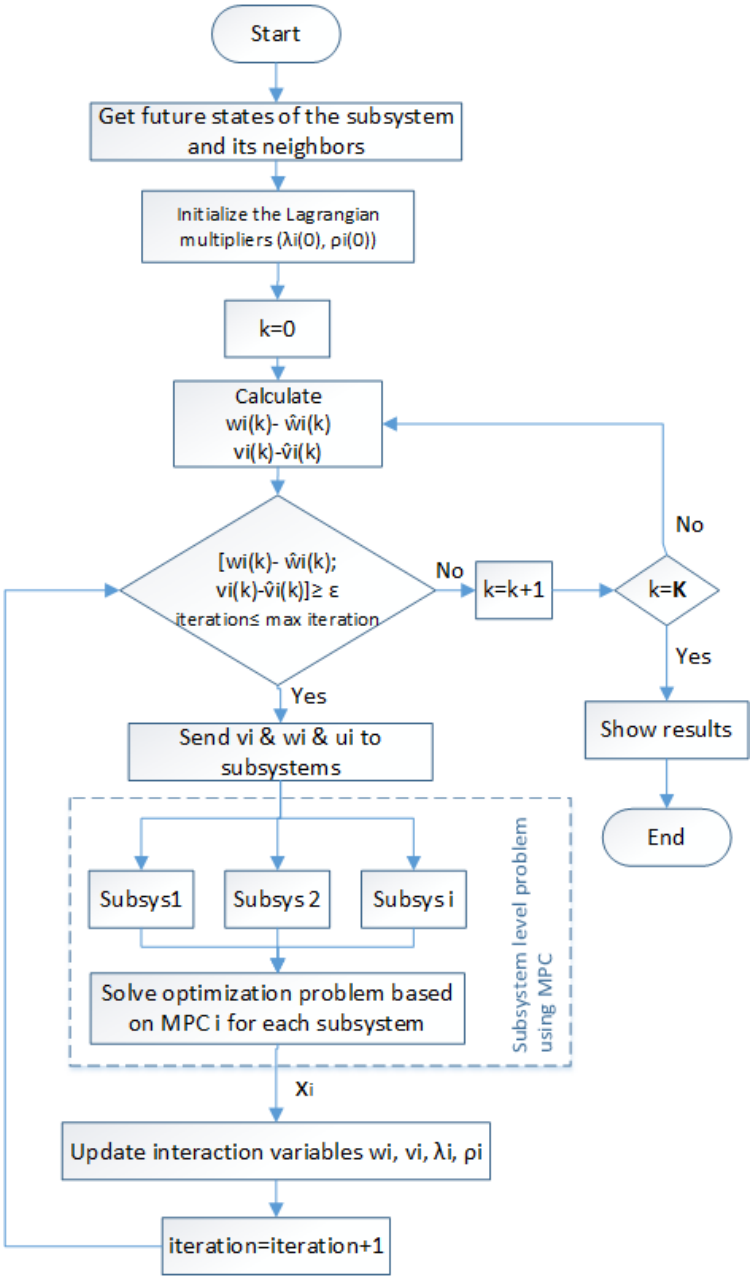

Figure 3.3: Distributed MPC algorithm flowchart

3.4 Stability Analysis

The finite-horizon MPC cost function introduced in the previous sections imposes no stability requirements by itself; therefore, inappropriate choices of design parameters (prediction horizon H, wights P, Q, and R, and optimization constraints) may result in unstable closed-loop system. In this section, we discuss on how to ensure stability in the proposed MPC approaches.

Considering discrete-time system model (3.1), and assuming that the control objective is regulation to the origin, we express the optimization problem as:

$$\begin{aligned} &\min_{u} J(x(k:k+h), u(k-1:k+h-1)) = \sum_{h=1}^{H} [\|x(k+h)\|_Q^2 + \|u(k+h-1)\|_R^2] \\ &\text{subject to } G(x(k:k+h), u(k-1:k+h-1)) \leq 0 \;\; h = 1, \cdots, H \end{aligned} \tag{3.12}$$

where $G(x(k:k+h), u(k-1:k+h-1))$ denotes the constraints on the system states and inputs. We define a compact and convex terminal set Ω, as follows:

$$\Omega = \{x \in \mathbb{R}^n | x^T P x \leq \alpha\} \tag{3.13}$$

where $P = P^T > 0$ and $\alpha > 0$. Assume that $u^*(k-1:k+h-1)$ is the optimal solution to the optimization problem (3.12), and define the set of H-step feasible initial states as (3.14).

$$X_F = \{x \in \mathbb{R}^n | G(x(k:k+h), u(k-1:k+h-1)) \leq 0 \;\; \text{for some} \;\; u(k-1:k+h-1)\} \tag{3.14}$$

Assuming that Ω is a control invariant set, then X_F is an H-step subset of stabilizable set. To determine P and α values, we design a linear feedback for the system such that Ω

is positively invariant under this feedback. The system is first linearized around the origin (equilibrium point).

$$A = \frac{\partial f}{\partial x}(0,0), \quad B = \frac{\partial f}{\partial u}(0,0) \tag{3.15}$$

Assume that (A, B) are stabilizable, and weights of the cost function (Q, R) are positive. If there exists a $P > 0$ that satisfies the Lyapunov equation (3.16) for some values of $\kappa > 0$;

$${A_0}^T P A_0 - P = -\kappa P - Q - K^T R K \tag{3.16}$$

then, there exists an $\alpha > 0$ such that the Ω set in (3.13), satisfies:

1. $\Omega \subset \Theta = \{x \in \mathbb{R}^n | u_{min} \leq -Kx \leq u_{max}, x_{min} \leq x \leq x_{max}\}$,

   where the parameters with min and max indices represent the lower and upper constraints on the states and inputs.

2. Nonlinear system $x(k+1) = f(x(k), -Kx(k))$ is asymptotically stable for all $x(0) \in \Omega$; Ω is a positive invariant set.

3. The cost function (3.12) is bounded ($J(x,u) \leq x^T P x$) for all $x \in \Omega$.

The proof of the arguments above is explained in detail in [73]. Therefore, the proposed MPC approaches guarantee asymptotic stability with region of attraction equal to the feasible set X_F. An algorithm for selecting the values of P, κ, and α is proposed in [4].

3.5 Centralized and Distributed MPC on CPS Case Study

Model Predictive Control strategies have been extensively applied to control and manage smart buildings [70, 11, 21, 74, 39, 44]. MPC is proven to be efficient in solving the

buildings' constrained optimization problems; to optimize the energy efficiency of buildings while providing maximum comfort for the residents. Various control scenarios and objective functions can be formulated for a building management problem. Building energy consumption, occupants' comfort, indoor air temperature, and indoor air humidity are some factors that can be included in the cost function. In a centralized MPC approach, one global objective function is defined for the building management system. Using centralized MPC is not practical for the buildings management, because these infrastructures are large-scale with complex components and requirements, and a centralized building management system may demand large computational overhead.

In a distributed MPC approach, local objective functions are defined for each smart building component. Local objective functions are then optimized by the local controllers, which coordinate together to achieve a specific global performance of the entire system. Therefore, various building's properties, such as thermal and lighting conditions, and energy consumption, can be managed with less computation and complication through a distributed MPC structure. In this section, we implement the proposed centralized and distributed MPC on CPS case study (multi-zone building), and analyze the simulation results.

3.5.1 Model definition

The CPS under study is a building consisting of six rooms (subsystems) with thermal exchange between the inner walls and inner doors. The rooms also have thermal exchanges with the environment. The physical system layout is shown in Fig. 3.4. In this system,

each room is equipped with a heater (AC). Based on the electro-thermal model presented in chapter II, the zonal thermal model of room $i, i = 1, \cdots, 6$, is as follows:

$$\frac{dx_i}{dt} = (\frac{1}{m_i C})[\frac{T_o - x_i}{R_{walls-outi}} + \frac{T_{roomi-j} - x_i}{R_{walls-ini}} + wc_{outdoori}\frac{T_o - x_i}{R_{outdoori}} + wc_{windowi}\frac{(T_o - x_i)}{R_{windowi}}$$
$$+ wf_{outdoori}M_{outdoori}C(T_o - x_i) + wf_{aci}M_{aci}C(T_{aci} - x_i) + wc_{indoori}\frac{T_{roomi-j} - x_i}{R_{indoori}}$$
$$+ wf_{indoori}M_{indoori}C(T_{roomi-j} - x_i) + wf_{windowi}M_{windowi}C(T_o - x_i)] \tag{3.17}$$

where x_i is the temperature of room i, and T_o is the outside temperature. $R_{walls-outi}$ and $R_{walls-ini}$ are the thermal resistance of walls from the outside and inside layers of room i, respectively. wc_{indoor} and $wc_{outdoor}$ are the conduction weight between two rooms, and between the rooms and outside, respectively. $wc_{winodwi}$ and $R_{windowi}$ are the thermal conduction and thermal resistance of windows in room i, respectively. $T_{roomi-j}$ is the heat exchange between room i and j. $M_{outdoor}$, M_{indoor} , and M_{window} are the amount of airflow from outside to inside, the amount of airflow indoors, and the amount of airflow from the windows, respectively. M_{ac} is the amount of airflow of the heater. C is the thermal capacity of air. Control variables are T_{aci}, M_{aci}, and wf_{aci}. The numerical values used in the system simulations are stated in Table 3.1.

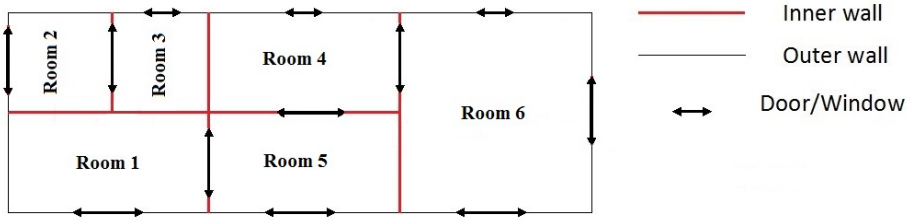

Figure 3.4: Six-room model plan

Table 3.1: Thermal model numerical values

Parameter	Value	Parameter	Value
C	1005.4	$R_{window3}$, $R_{window4}$, $R_{window6}$	0.0000593542
$m_i, \quad i = 1, \cdots, 6$	102.0425	$wc_{window3}$, $wc_{window4}$, $wc_{window6}$	1
$M_{indoori}$	20	$wf_{window3}$, $wf_{window4}$, $wf_{window6}$	0
$R_{indoori}$	0.000208	$wc_{outdoor1}$, $wc_{outdoor2}$, $wc_{outdoor5}$, $wc_{outdoor6}$	1
$R_{walls-ini}$	0.0000696	$wf_{outdoor1}$, $wf_{outdoor2}$, $wf_{outdoor5}$, $wf_{outdoor6}$	0
$R_{walls-outi}$	0.0000321	$T_{room2-3}, T_{room1-5}, T_{room4-5}, T_{room4-6}(initial)$	10
$R_{outdoori}$	0.000208	$M_{outdoori}, M_{window3}$, $M_{window4}$, $M_{window6}$	35
$wc_{indoori}$	0	$wf_{indoori}, wf_{aci}$	1

3.5.2 Centralized MPC

Considering a discrete state-space model, state variables (zonal temperature) predictions P steps ahead of the current time are stated as (3.18).

$$\hat{x}(k|k) = A\hat{x}(k|k-1) + Bu(k-1) + Ed(k-1) + L(\hat{y}(k) - \hat{y}(k|k-1))$$
$$Y(k|k) = TH\hat{x}(k|k) + TG\Delta U(k|k) + TFu(k-1) + TVW(k|k) \tag{3.18}$$

In (3.18), A, B, and E are the state-space representation matrices. d is the disturbance, and Y, G, T, F, H, V, and W are defined as follows.

$$Y^T(k) = \begin{bmatrix} y(k+1|k)^T & y(k+2|k)^T & \cdots & y(k+P|k)^T \end{bmatrix}$$

$$G = \begin{bmatrix} B & 0 & \cdots & 0 \\ (A+I)B & B & \cdots & 0 \\ \vdots & \vdots & \cdots & \vdots \\ \sum_{i=1}^{M} A^{i-1}B & \sum_{i=1}^{M-1} A^{i-1}B \cdots & & B \\ \sum_{i=1}^{M+1} A^{i-1}B & \sum_{i=1}^{M} A^{i-1}B & \cdots & (A+I)B \\ \vdots & \vdots & \cdots & \vdots \\ \sum_{i=1}^{P} A^{i-1}B & \sum_{i=1}^{P-1} A^{i-1}B \cdots & & \sum_{i=1}^{P-M+1} A^{i-1}B \end{bmatrix} \quad T = \begin{bmatrix} C & 0 & \cdots & 0 \\ 0 & C & \ddots & \vdots \\ \vdots & \ddots & \ddots & 0 \\ 0 & \cdots & 0 & C \end{bmatrix}$$

$$F^T = \begin{bmatrix} B & (A+I)B \cdots \sum_{i=1}^{M} A^{i-1}B & \sum_{i=1}^{M+1} A^{i-1}B \cdots \sum_{i=1}^{P} A^{i-1}B \end{bmatrix}$$

$$H^T = \begin{bmatrix} A & A^2 \cdots A^P \end{bmatrix} \qquad V = \begin{bmatrix} E & 0 & \cdots & 0 \\ AE & E & \cdots & 0 \\ \vdots & \vdots & \cdots & \vdots \\ A^{P-1}E & A^{P-2}E & \cdots & E \end{bmatrix}$$

$$W^T(k) = \begin{bmatrix} d(k|k)^T & d(k+1|k)^T & \cdots & d(k+P-1|k)^T \end{bmatrix} \tag{3.19}$$

The cost function $J(k)$ in (3.20) penalizes the deviations of the predicted outputs $\hat{y}(k+i|k)$ from a reference trajectory $y_r(k+i|k), \quad i = 1, 2, \cdots, P$. Maximizing the thermal comfort and minimizing the cooling/heating energy consumption of the building is the optimization problem.

$$J(k) = \sum_{i=1}^{P} \|(\hat{y}(k+i|k) - y_r(k+i|k))\|_Q^2 + \sum_{i=1}^{M} \|u(k+i-1|k)\|_{R_1}^2 + \|\Delta u(k+i-1|k)\|_{R_2}^2 \tag{3.20}$$

In (3.20), P and M are the prediction and control horizons, respectively. Q, R_1, and R_2 are the weight matrices. $y(k)$, and $y_r(k)$ denote the indoor temperature and desired

temperature at time step k, respectively. $u(k)$ and Δu are the cooling/heating power consumption and its increments at time step k, respectively. To minimize the cost function (3.20) subject to the system model description and prediction equations, the centralized MPC algorithm in Algorithm 1 is utilized. Using the centralized MPC, the whole system is monolithic, and only one MPC controller is assigned to the system. Therefore, there is one complicated large optimization problem with various variables being calculated at each time step.

3.5.3 Distributed MPC

Our proposed distributed MPC algorithm in this dissertation considers not only the future output and manipulated input predictions of the neighbor zones but also the disturbance predictions in each local controller. The goal is to attain a satisfactory global performance with minimum computation demand. The cost function for our case study is defined as follows.

$$J_i(k) = \sum_{p=1}^{P} \|(\hat{y}_i(k+p) - {y_i}^d(k+p))\|_{Q_i}^2 + \sum_{m=1}^{M} \|u_i(k+m-1|k)\|_{R_{1i}}^2 + \|\Delta u_i(k+m-1|k)\|_{R_{2i}}^2 \tag{3.21}$$

In (3.21), P and M are the prediction and control horizons, respectively. Q_i, R_{1i}, and R_{2i} are the weight matrices of subsystem i. ${y_i}^d$, u_i, and Δu_i are the desired temperature, heating/cooling energy consumption, and energy consumption increments in room i, respec-

tively. ${y_i}^d$ is obtained by a smooth approximation from the current value of output $y_i(k)$ towards the known reference $r_i(k)$ in (3.22).

$$\begin{aligned} &{y_i}^d(k) = y_i(k), \\ &{y_i}^d(k+p) = \alpha_i w_i(k+p-1) + (1-\alpha_i) r_i(k+p), \quad p = 1, \cdots, P \end{aligned} \tag{3.22}$$

The control inputs, $u_i(k+m|k)$, are attained by minimizing the local objective function (3.21) at each time step k. Then, the global objective function at each time step k is as (3.23).

$$J(k) = \sum_{i=1}^{N} J_i(k) \tag{3.23}$$

Above, $N = 6$ is the total number of subsystems. The system's predicted outputs and states are calculated through (3.24), and then substituted in the cost function.

$$\begin{aligned} &\hat{x}_i(k+p|k) = {A_{ii}}^p \hat{x}_i(k|k) + \sum_{s=1}^{p} {A_{ii}}^{s-1} B_{ii} u_i(k+p-1|k) + \sum_{s=1}^{p} {A_{ii}}^{s-1} \hat{w}_i(k+p-1|k-1) \\ &\hat{y}_i(k+p|k) = C_{ii} \hat{x}_i(k+p|k) + \hat{v}_i(k+p|k-1) \end{aligned} \tag{3.24}$$

The states and inputs interaction equations are stated as (3.25).

$$w_i(k) = \sum_{j=1}^{m} A_{ij} x_j(k) + \sum_{j=1}^{m} B_{ij} u_j(k) \qquad v_i(k) = \sum_{j=1}^{m} C_{ij} x_j(k) \tag{3.25}$$

where we assume that m neighboring subsystems are interacting with subsystem i.

Defining the following matrices;

$$\tilde{A}_i = \Big[\text{diag}_P\{A_{i,1}\} \cdots \text{diag}_P\{A_{i,i-1}\} 0 \text{diag}_P\{A_{i,i+1}\} \cdots \text{diag}_P\{A_{i,m}\} \Big]$$

$$\tilde{B}_i = \Big[\text{diag}_P\{B_{i,1}\} \cdots \text{diag}_P\{B_{i,i-1}\} 0 \text{diag}_P\{B_{i,i+1}\} \cdots \text{diag}_P\{B_{i,m}\} \Big]$$

$$\tilde{C}_i = \left[\text{diag}_P\{C_{i,1}\}\cdots\text{diag}_P\{C_{i,i-1}\}0\text{diag}_P\{C_{i,i+1}\}\cdots\text{diag}_P\{C_{i,m}\}\right]$$

$$\tilde{\Gamma}_i = \begin{bmatrix} 0_{(M-1)n_{ui}n_{ui}} & I_{(M-1)n_{ui}} \\ 0_{n_{ui}(M-1)n_{ui}} & I_{n_{ui}} \\ \vdots & \vdots \\ 0_{n_{ui}(M-1)n_{ui}} & I_{n_{ui}} \end{bmatrix} \qquad \tilde{\Gamma} = \text{diag}\{\tilde{\Gamma}_1 \cdots \tilde{\Gamma}_m\} \qquad \tilde{B}_i = \tilde{\tilde{B}}_i\tilde{\Gamma} \tag{3.26}$$

The predictions of interacting parameters, system states, and outputs are as (3.27) and (3.28), respectively.

$$\hat{W}_i(k,P|k-1) = \tilde{A}_i\hat{X}(k,P|k-1) + \tilde{B}_iU(k-1,M|k-1)$$

$$\hat{V}_i(k,P|k-1) = \hat{C}_i\hat{X}(k,P|k-1) \tag{3.27}$$

$$\hat{X}_i(k+1,P|k) = \bar{S}_i[\bar{A}_ix_i(\hat{k}|k) + \bar{B}_iU_i(k,M|k) + \hat{W}_i(k,P|k-1)]$$

$$\hat{Y}_i(k,P|k-1) = \bar{C}_i[\hat{X}_i(k+1,P|k) + T_i\hat{V}_i(k,P|k-1)] \tag{3.28}$$

where matrices T_i, $\bar{S}_i$, $\bar{A}_i$, $\bar{B}_i$, and $\bar{C}_i$ are stated as (3.29).

$$T_i = \begin{bmatrix} 0_{(P-1)n_{yi}n_{yi}} & I_{(P-1)n_{yi}} \\ 0_{n_{yi}(P-1)n_{yi}} & I_{n_yi} \end{bmatrix} \qquad \bar{S}_i = \begin{bmatrix} {A_{ii}}^0 & \cdots & 0 \\ \vdots & \ddots & \vdots \\ {A_{ii}}^{P-1} & \cdots & {A_{ii}}^0 \end{bmatrix}$$

$$\bar{A}_i = \begin{bmatrix} A_{ii} \\ 0_{Pn_{yi}n_{yi}} \end{bmatrix} \qquad \bar{B}_iT = \begin{bmatrix} \text{diag}_M\{B_{ii}\} & & & \\ 0_{n_{ui}} & \cdots & 0_{n_{ui}} & B_{ii} \\ \vdots & \ddots & \vdots & \vdots \\ 0_{n_{ui}} & \cdots & 0_{n_{ui}} & B_{ii} \end{bmatrix} \qquad \bar{C}_i = \text{diag}_P\{C_{ii}\}$$

Therefore, the control solution for the optimization problem is stated as (3.29).

$$U_i(k,M|k) = {\Gamma_i}'u_i(k-1) + \bar{\Gamma}_i\bar{K}_i[Y_i^d(k+1,P|k) - \hat{Z}_i(k+1,P|k)] \tag{3.29}$$

where K_i, and $\hat{Z}_i$ are defined in (3.30).

$$\hat{Z}_i(k+1,P|k) = S_i[\bar{B}_i\Gamma_i{}'u_i(k-1) + \bar{A}_i\hat{x}_i(k|k) + \hat{W}_i(k,P|k-1)] + T_i\hat{V}_i(k,P|k-1)$$

$$\bar{K}_i = {H_i}^{-1}{N_i}^T\bar{Q}_i \qquad H_i = {N_i}^T\bar{Q}_iN_i + \bar{R}_i \qquad S_i = \bar{C}_i\bar{S}_i$$

$$\bar{Q}_i = \text{diag}_P\{Q_i\} \qquad \bar{R}_i = \text{diag}_P\{R_i\} \qquad N_i = S_i\bar{B}_i\bar{\Gamma}_i$$

$$\Gamma_i{}' = \begin{bmatrix} I_{n_{ui}} \\ \vdots \\ I_{n_{ui}} \end{bmatrix} \qquad \bar{\Gamma}_i = \begin{bmatrix} I_{n_{ui}} & \cdots & 0 \\ \vdots & \ddots & \vdots \\ I_{n_{ui}} & \cdots & I_{n_{ui}} \end{bmatrix} \tag{3.30}$$

The subsystems' interactions (heat exchange) are included in the cost function as follows.

$$\Phi_i(P) = \min\{\|x_i(K)\|^2_{P_i} + \sum_{k=0}^{K-1}(\|(x_i(k) - {x_i}^d(k))\|^2_{Q_i} + \|z_i(k)\|^2_{S_i} + \|(T_{ac}(k))\|^2{}_{R_i}$$
$$+ {P_i}^T(k)[A_ix_i(k) + B_iu_i(k) + C_iz_i(k) - x_i(k+1)] + {\lambda_i}^T(z_i - \sum_{j=1}^{m} L_{ij}x_j))\} \tag{3.31}$$

where L_{ij}s are the coefficients used for connecting the states of neighboring subsystems. λ_i and ${P_i}^T$ are the interactions and system model constraints coefficients, respectively. Using the Hamiltonian function H_i, defined in (3.32), (3.31) is converted to (3.33).

$$H_i(x_i,u_i,z_i,k) = \|(x_i(k) - {x_i}^d(k))\|^2_{Q_i} + \|z_i(k)\|^2_{S_i} + \|(T_{ac}(k))\|^2_{R_i} + {P_i}^T(k)[A_ix_i(k)$$
$$+ B_iu_i(k) + C_iz_i(k) - x_i(k+1)] + {\lambda_i}^T(z_i - \sum_{j=1}^{m} L_{ij}x_j) \tag{3.32}$$

$$\Phi_i(P) = \min\{\|x_i(K)\|^2_{P_i} - P_i(K-1)^Tx_i(K) + \sum_{k=0}^{K-1}(H_i(k) - P_i(k-1)^Tx_i(k)))\} \tag{3.33}$$

In each instant, the following proposed three-level algorithm is applied iteratively up to the prediction horizon, until the optimum input is attained.

Algorithm 3 Distributed MPC algorithm for thermal control of buildings

Step 1: $k = 0$; minimize $H_i(x_i(0), u_i(0), z_i(0))$ with partial derivatives with respect to $u_i(0)$ and $z_i(0)$.

Step 2: $k = 1, 2, ..., K-1$; minimize $H_i(x_i(k), u_i(k), z_i(k), k) - P_i(k-1)^T x_i(k))$ with respect to $x_i(k)$, $u_i(k)$ and $z_i(k)$.

Step 3: $k = K$; minimize $\|(x_i(K))\|^2_{P_i} - P_i{}^T(K-1)x_i(K)$ with respect to $x_i(K)$.

Coordination mechanism in the distributed control approach avoids global communication in the whole network, which enhances the closed-loop system stability and feasibility. Assuming the existence of a feasible input sequence for each subsystem i at $k = 0$, the optimization problem has a feasible solution for each subsystem i at all $k \geq 0$. For stability analysis, (3.34) is defined as the Lyapunov function which will be solved off-line.

$$A^T P A - P = -F, \qquad P = \begin{bmatrix} P_{11} & P_{12} & \cdots & P_{1m} \\ P_{21} & P_{22} & \cdots & P_{2m} \\ \vdots & \vdots & \ddots & \vdots \\ P_{m1} & P_{m2} & \cdots & P_{mm} \end{bmatrix}$$

$$F = \text{diag}(F_1, F_2, \cdots, F_m), \quad F_i(0) = F_i(1) = \cdots = F_i(N-1) = F_i \tag{3.34}$$

Having relationship (3.35) from [73],

$$J(k)(x(k)) \leq J(0)(x(0)) - \sum_{k=0}^{K-1} \sum_{i=0}^{m} J_i(k)(x_i(k), u_i(k)) \leq J(0)(x(0)) \tag{3.35}$$

(3.36) is attained.

$$\frac{1}{2}\lambda_{min}(F)\|x(k)\|^2 \leq J(k)(x(k))$$

$$J(k)(x(k)) \leq J(k)(x(0)) = \frac{1}{2}x(0)^T P x(0) \leq \frac{1}{2}\lambda_{max}(P)\|x(0)\|^2 \tag{3.36}$$

Thus, it is proved that $\|x(k)\| \leq \sqrt{\frac{\lambda_{max}(P)}{\lambda_{min}(F)}}\|x(0)\|$, which shows that the closed-loop system is asymptotically stable.

3.5.4 Simulation results

The desired trajectory for each room's temperature is between 5 $^{\circ}C$ to 25 $^{\circ}C$ in 5 different periods (0-6 AM, 6-12 AM, 12-6 PM, 6-9 PM, and 9-12 PM), regarding the occupancy status. To maintain the occupants' comfort, temperature set points during occupied hours (0-6 AM and 6-12 PM) are higher than the vacant periods (6-12 AM and 0-6 PM). The environment temperatures are assumed to be between -6 to 4 $^{\circ}C$. The weighting matrices Q_i and R_i are chosen as $1.5I_{12\times 12}$ and $(\frac{1}{1600})I_{6\times 6}$, respectively.

Fig.s 3.5 and 3.6 show the six rooms' temperatures using centralized and distributed MPC, respectively. Fig. 3.7 shows the control input trajectories from the centralized and distributed MPC. Table 3.2 compares the numerical values from the two rooms' temperature trajectories and input signals using centralized and distributed MPC. From Fig.s 3.5 and 3.6, the distributed MPC functions better compared to the centralized MPC strategy in terms of reference tracking performance. From Table 3.2, the overshoots and peak values of room 1 and 2 temperatures using distributed MPC are significantly smaller than the same values in centralized case. From Fig. 3.7, the control input using the distributed MPC approach shows lower overshoot and stabilizes sooner than the centralized MPC control trajectory.

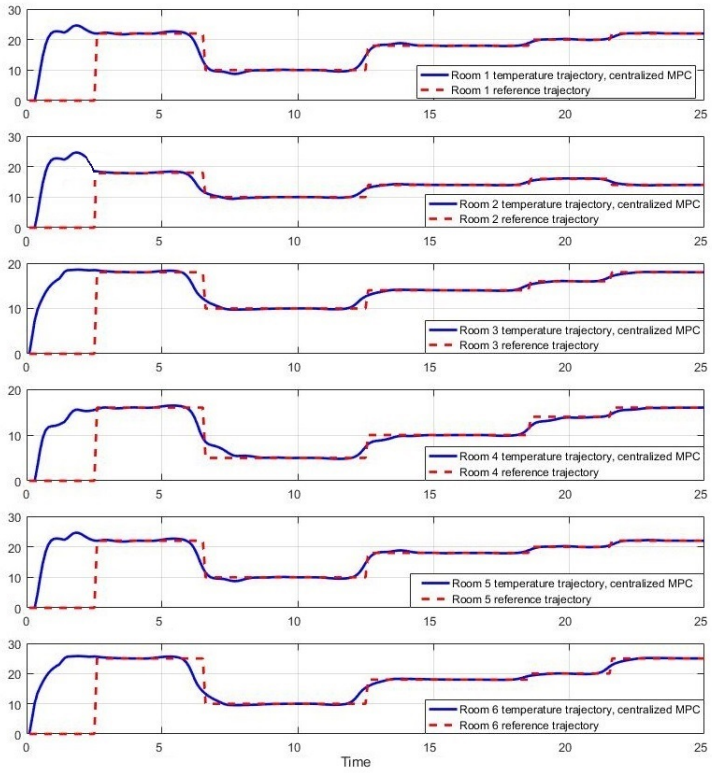

Figure 3.5: Six rooms' temperature using centralized MPC

Comparing the areas under the control input trajectories (7th column in Table 3.2), the energy consumption using distributed MPC is 25.42% lower than that of the centralized one. Besides, the optimization time for distributed MPC controller is 60 times lower than the centralized MPC (last column in Table 3.2). As the system gets larger, the computation time in the centralized approach gets relatively higher. Another important innovation of the proposed distributed MPC algorithm is that it considers the disturbances predictions and it provides system stability. The proposed controller is applied to a practical smart building testbed as well. Using the proposed scheme for buildings, not all the agents need

to be connected to each other; therefore, the communication effort is significantly lower compared to the centralized scheme.

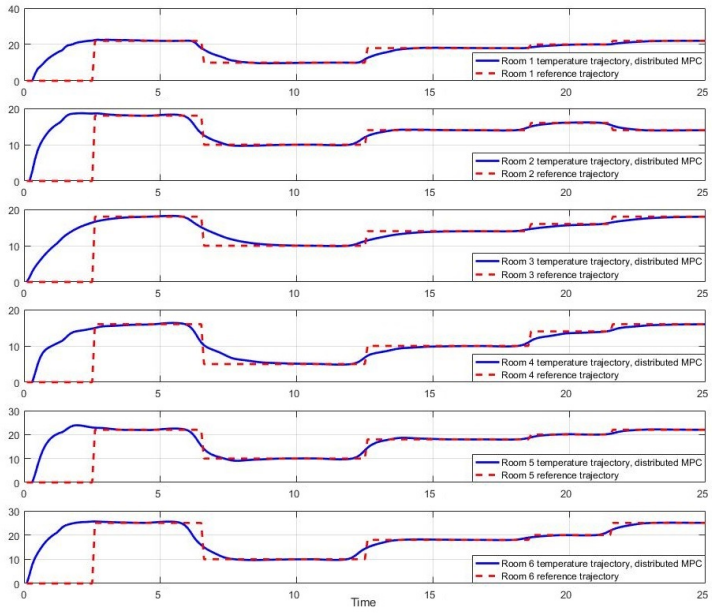

Figure 3.6: Six rooms' temperature using distributed MPC

Table 3.2: Numerical characteristics of the state and control signals of the two rooms using centralized and distributed MPC

	T_1 overshoot	T_1 peak	T_2 overshoot	T_2 peak	control overshoot	control area	run time
CMPC	89.95	22.39	80.96	25.03	78.66	7.4138e+3	1120 sec
DMPC	11.65	20.33	15.70	17.28	31.90	5.5291e+3	52 sec

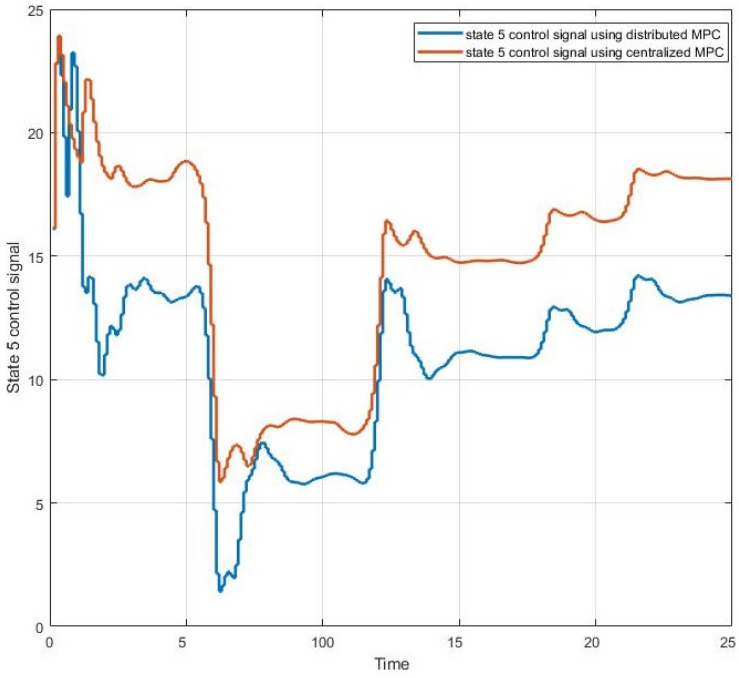

Figure 3.7: Control signal 5 using centralized and distributed MPC

3.5.5 Practical implementation

This section provides experimental results on a smart building management system. The testbed is a four-story building equipped with sensors and actuators. Fig. 3.8 shows the 3D plan of building prototype, and Fig. 3.9 shows the position of all the actuators and sensors in the structure. The sensors and actuators mounted on the walls, doors, windows, elevator, and ceilings. Each room of the building has at least one strip of LEDs as a light source, a DTH22 as a temperature/humidity sensor, a Peltier tile as a heat source, a fan for heat dissipation, PIR sensors to detect the movements, and micro servos to operate the doors and windows.

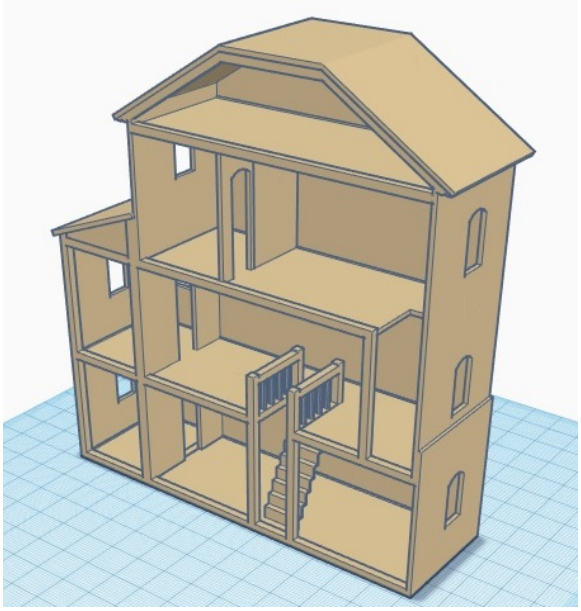

Figure 3.8: The smart home's CAD plan

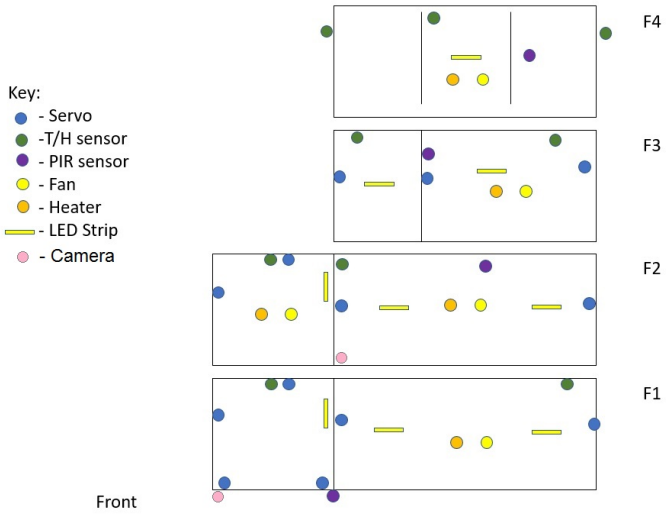

Figure 3.9: The position of all the sensors and actuators in each floor (top view)

Fig. 3.10 shows a selected sample of the actuators and sensors (e.g., PIR sensor, DHT22 sensor, servo motor, fan, heater, LEDs, and camera) mounted in a room. Sensor readings are collected and sent to a central server by Adafruit HUZZAH ESP8266 breakout boards. Some

actuators, such as the micro servos, are also connected to the ESP boards. LEDs, relays, cameras, and fans are connected directly to the computation node (Raspberry Pi). The camera records videos/capture pictures when the near-by PIR sensor detects movement. The camera can also stream videos and pictures upon the resident's command. The controller unit (Raspberry Pi module), interface modules (e.g., the voltage regulator modules, power isolation modules, and Wifi modules), and the power supplies are mounted at the back of the building. Fig. 3.11 shows the actuators, sensors, voltage sources, and control boards used in the testbed. The circuits for the 12V and 5V components are kept isolated by relays, and as a precaution in the event of high current, all micro-controllers are isolated from each other with fuses. Power can be supplied to any combination of individual floors.

Figure 3.10: Picture of one room including its actuators and sensors

Figure 3.11: Picture of sensors, actuators, sources, and control boards used in the smart building

For the lighting system, each LED strip contains 5 LEDs. Different voltage levels are applied to generate different colors for each of the living areas. The voltage range required is between 1.4 to 5 V, and the maximum current needed per LED strip is 0.29 A. The temperature and humidity in each floor are regulated based on the residents' desired levels. A decentralized model-based predictive control is developed in Python 3.6 and loaded on the micro-controller through Raspbian. The modules that are most used are numpy, csv, pylab, matplotlib, time, RPi.GPIO, string, and scipy. The sensors' data is updated every 5 seconds, and the control inputs are generated at the same rate. Fig. 3.12 shows the trajectories of the first-floor temperature versus the desired temperature. Fig. 3.13 shows the humidity trajectory and the desired humidity signal. The average temperature error and

average humidity error are 2.5% and 10%, respectively. Fig. 3.14 illustrates the control law and the input signal generated for the actuators (fan and heater).

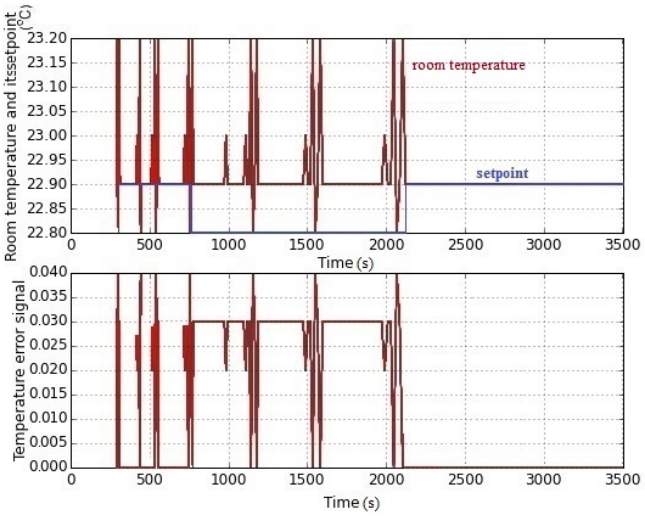

Figure 3.12: First-floor temperature trajectory

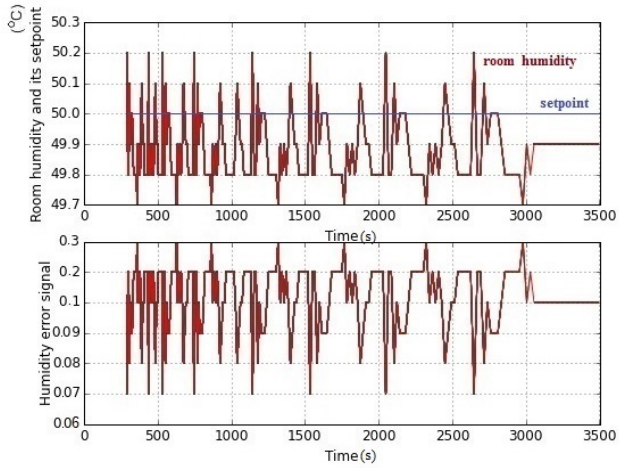

Figure 3.13: First-floor humidity trajectory

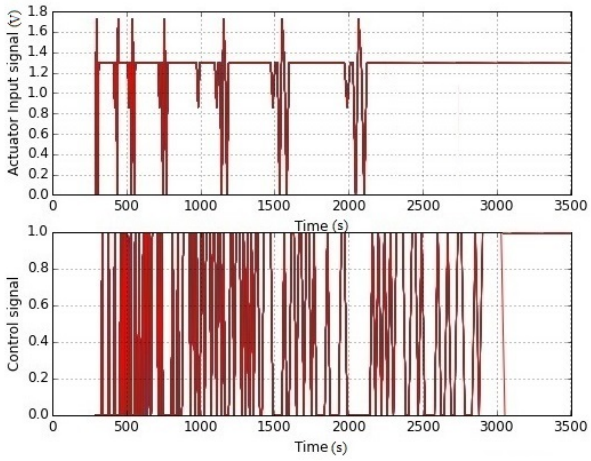

Figure 3.14: First-floor actuator input and control signal

3.6 Conclusion

In this chapter, we designed centralized and distributed predictive control approaches for the management of cyber-physical systems. To evaluate the performance of distributed and centralized MPC on the building, we applied these two control methods to regulate the thermal condition of a six-zone building and minimize energy consumption. The heat exchange between rooms, and between the outer and inner spaces are all considered in the control design. The control variables are the heat flow amount and the heater temperature in the zones. The proposed distributed predictive controller was able to predict the model inputs, states, thermal exchanges, and disturbances, to rapidly compensate the system outputs. From the simulation results, the distributed MPC approach showed better performance in signal tracking, energy consumption, and computation time compared with the centralized MPC. The control performance is improved by utilizing the disturbances' predictions in the proposed MPC approach. Besides, the feasibility of the solution is

guaranteed if the initial solution is feasible, and the controlled closed-loop system is asymptotically stable at the system's equilibrium point.

CHAPTER IV

LEARNING-BASED MODEL PREDICTIVE CONTROL FOR CYBER-PHYSICAL SYSTEMS

In this chapter, we incorporate the model-based predictive control approach with machine learning for the management and control of cyber-physical systems. Besides, we implement our proposed learning-based control strategy to manage visual, thermal, and olfactory performances, and energy consumption in a building. Artificial Neural Network (ANN) is utilized to learn the parameters associated with the building's energy consumption data, environmental conditions, comfort, and occupant-related information. Learned parameters are then used in the model-based controller (MPC) to generate the optimal control inputs for HVACs, lighting systems, blinds, and ventilators. The training data for NNs are generated by simulating an actual building in EnergyPlus software, considering the indoor temperature, time of the day, weather data, energy consumption data, and desired temperatures. The model-based controller generates the optimum control inputs at each time step, with the aim of conserving energy and improving residents' comfort. Performance of the proposed learning-based MPC approach is analyzed by comparing its simulation results with the results of a baseline controller on the building under the same conditions.

4.1 Learning-based Prediction

This section explains the learning-based approach to predict CPS parameters. The goal of the learning-based algorithm is to predict the information, which can not be modeled, in the long-term, and investigate its influence on CPS performance. Artificial neural network (ANN) is well-known for its ability to approximate nonlinear systems without prior knowledge of the system dynamics [105]. ANN is highly applicable and efficient for the approximation of building nonlinear parameters [30]. In this study, a nonlinear autoregressive exogenous (NARX) neural network is utilized to learn and estimate the parameters associated with three performance indexes (thermal, visual, and olfactory conditions) in a building. The reason we used the NARX neural network as the learning approach is that the parameter we try to learn is a time series parameter, and one of the primary applications of NARX is predicting the time series models [33]. Moreover, the parameter that we try to learn is highly nonlinear, and the NARX model is suitable for nonlinear models of this type. The NARX network can be implemented in two different architectures, parallel and series-parallel architectures. In a series-parallel architecture, the past measurements are utilized in a feed-forward architecture to train ANN and get the predictions one step ahead. However, in a parallel architecture, the predictions for multi-steps ahead (e.g., i steps ahead) can be attained through a feedback structure [86]. The series-parallel and parallel architectures' equations are presented in (4.1) and (4.2), respectively. Three main layers, i.e., input, output, and hidden layer, exist in both NARX architectures [86].

$$\hat{y}(k) = f(u(k-1), ..., u(k-n_a), y(k-1), ..., y(k-n_b)) \tag{4.1}$$

$$\hat{y}(k+i) = f(u(k+i-1), ..., u(k+i-n_a), y(k+i-1), ..., y(k+i-n_b)) \qquad (4.2)$$

Above, u and y are the system's input and output variables. n_a and n_b denote the order of inputs and outputs, respectively, and f is a nonlinear function. Thus, the output signal in the next step is estimated based on its previous values and those of the exogenous inputs.

The parallel architecture can provide predictions for a long time horizon; however, the accumulative prediction error using this architecture can be very high because all the past predicted outputs are utilized in every step of the algorithm. In this study, the estimations of building parameters over a long-term prediction horizon are required; therefore, the parallel architecture is chosen for the NARX network. A training algorithm need to be chosen to train the network. In this study, Levenbegrg-Marquardt backpropagation algorithm is used for training. This algorithm is a well-known and efficient method to train networks with several hidden layers [105]. After training, the network is validated. Test data is used to evaluate the stopping criterion and expected performance of the predicted data. To evaluate the training performance, the mean squared errors (MSE)s of the training data are calculated. The sum of all the errors between the measured and predicted outputs over the training stack size is defined as the MSE criterion. Thus, the NARX neural network algorithm is as follows:

- Define input and output datasets.
- Define three sets of training, validation, and testing data.
- Choose a network architecture and a training algorithm by the trial and error method.
- Train the network and evaluate its performance.
- If the network performance is satisfactory, the problem is solved, otherwise, change the network size, retrain, or use a larger dataset.

4.2 Model-based Control Incorporated with Learning

In the proposed approach, online model learning is integrated within the control approach to provide self-adaptive models that are robust to the environment changes. By integrating machine learning with model-based control technique, we will obtain a high-fidelity model of the building system and its environment with less training data and higher model certainty. Also, the integrated structure allows run-time reconfiguration and adaptation in response to the changing models, specifications, and operating conditions. The integrated building management system is shown in Fig. 4.1. The system consists of three main blocks; environmental module, system model module, and management module. In the environmental module, environment variables, such as climatic conditions, are predicted through environment models or learning algorithms. In this regard, the predicted environment variables are represented by a vector, $\hat{\lambda}_k$, as follows:

$$\hat{\lambda}_k = \begin{bmatrix} \hat{\lambda}_k^M \\ \\ \hat{\lambda}_k^D \end{bmatrix} \tag{4.3}$$

where λ_k^M denotes the variables estimated using an environment model (e.g., Kalman filter estimation method), and λ_k^D denotes the variables learned using data analytics and machine learning algorithms. The general representation of an environment model is as follows:

$$\hat{\lambda}_{k+1}^M = \phi(\lambda_k^M, \theta_k^\phi, r), \tag{4.4}$$

where $\hat{\lambda}_{\mathbf{k}}^{\mathbf{M}} \in \Lambda_k^M$ is the environment variable, θ_k^ϕ is the parameter of the environment model that needs to be learned, and r denotes a set of previously observed variables. The environment inputs and building's historical data are sampled and fed into the prediction

filter. The model parameters, θ_k^{ϕ}, are updated in the prediction filters (through ARIMA modeling or Kalman filtering [110, 56]). The predicted environmental parameters obtained in this module are used for updating the formulations in the system module and management module.

Dynamics of the building components (models defined in subsection 2.1) are included in the system module. The general representation of a component model is considered as follows:

$$\hat{x}_{k+1} = f(x_k, u_k, \hat{\lambda}_{k+1}, \theta_k) \tag{4.5}$$

where x_k and u_k are the state variables and control inputs of the building component, respectively. $\hat{x}_k$ is the predicted state variable, $\hat{\lambda}_{k+1}$ is the predicted environmental variable, and θ_k denotes model parameters that need to be learned. For example, for linear systems $\dot{x}_{k+1} = Ax_k + Bu_k$, θ_k can be matrices A and B that need to be learned (i.e., $\theta_k = \begin{bmatrix} A^T B^T \end{bmatrix}^T$). The model can be tuned through model-based forecasting strategies or machine learning. The estimated state values generated at each time instant are sent to the management module.

The management module consists of optimization block and objective function block. In this module, an objective function, containing the building's performance specifications (in terms of safety, cost-effectiveness, and comfort criteria) and its operating constraints, is formulated. Some building's specifications (such as energy consumption) are mathematically modeled, and some other requirements (such as the personal parameters of the comfort models defined in section 2.2) are learned using machine learning approaches.

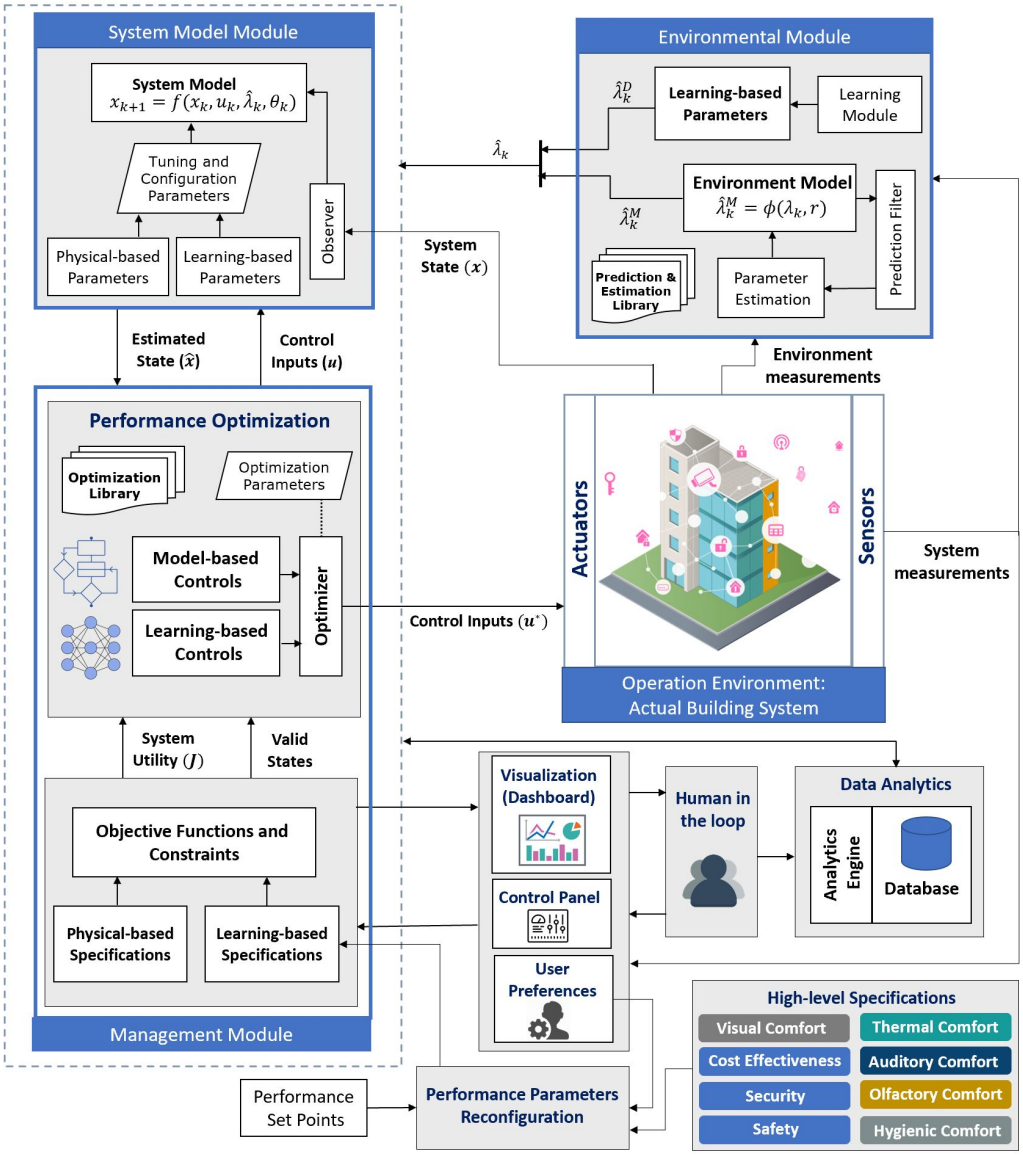

Figure 4.1: An integrated model-based control and data analytics approach for buildings management

A general set-point cost function equation for formulating the building's performance specifications is as follows:

$$J(x_k, u_{k-1}) = \|x_k - x_k^*\|_P^2 + \|u_{k-1}\|_Q^2 + \|\Delta u_{k-1}\|_R^2 \tag{4.6}$$

where x_k^* is the desired operating state (such as the desired comfort criteria, or thermal condition), Δu_{k-1} denotes the changes in the control inputs. P, Q, and R are the weighting matrices. In the objective function (4.6), the first term expresses the set-point regulation problem (for example, regulating the indoor temperature), and the second and third terms denote the cost of control inputs and their changes (for example, the cost of lighting energy).

The operating constraints define the feasible domains on both the state variables and control inputs. The general representation of the constraints is as:

$$\psi(x_k) \leq 0, \quad U(x_k) \subseteq U \tag{4.7}$$

where $U(x_k)$ denotes the admissible input set in state x and $\psi(x_k)$ represents the reachable states. Depending on the type of state variables (e.g., comfort criteria, thermal conditions), control inputs, and hardware limitations, specific operating constraints are defined. Considering the system constraints and objective functions, the optimal control inputs are generated through a learning-based and model-based optimizer. Control inputs are then injected to the actual building system to minimize the operating costs and meet the desired performance metrics. The incorporated model-based control with learning approaches are utilized for CPS management for three main purposes: (1) to model the CPS components more accurately through learning-based approximations (2) to learn the control laws from the training data instead of solving the actual model-based optimization problem (3) to attain the cost function equation by learning its parameters.

Table 4.1: Building materials description

	4 inch dense face brick	2 inch insulation	4 inch concrete block	3/4 inch plaster board	1/8 inch hardwood	8 inch concrete block	acoustic tile	1/2 inch stone	3/8 inch membrane
Roughness	Rough	Very rough	Medium rough	Smooth	Medium smooth	Rough	Medium smooth	Rough	Rough
Thickness (m)	0.1014684	0.050901	0.1014984	0.019050	0.003169	0.2033016	0.019050	0.012710	0.009540
Conductivity $(W/m-K)$	1.245296	0.043239	0.3805070	0.7264224	0.1591211	0.5707605	0.060535	1.435549	0.1902535
Density (kg/m^3)	2082.400	32.03693	608.7016	1601.846	720.8308	608.7016	480.5539	881.0155	1121.292
Specific heat $(J/kg-K)$	920.4800	836.8000	836.8000	836.8000	1255.200	836.8000	836.8000	1673.600	1673.600
Thermal absorptance	0.900000	0.900000	0.900000	0.900000	0.900000	0.900000	0.900000	0.900000	0.900000
solar absorptance	0.930000	0.500000	0.650000	0.920000	0.780000	0.650000	0.320000	0.550000	0.750000
Visible absorptance	0.930000	0.500000	0.650000	0.920000	0.780000	0.650000	0.320000	0.550000	0.750000

4.3 Learning-based MPC for Management of Case Study I

In this section, the proposed learning-based MPC approach is applied to manage thermal conditions in a four-zone building simulated in EnergyPlus software.

4.3.1 Case study I model definition

The building under study is a two-story office building with four zones and one HVAC system per zone. Each zone's thermostat is dual setpoint. Fig. 4.2 shows the CAD model of the building under study. The total floor area is $1600m^2$ with the orientation to the north. Windows include shadings, overhangs, and fins. Several materials are used in various layers of the walls (exterior and interior), window frames, door, roof, ceiling, and inter-zone walls. Table 4.1 contains the building materials' specifications.

4.3.2 Learning-based MPC on case study I

This subsection explains the proposed learning-based control approach to control the building's indoor temperature. Considering the thermal convection and conduction equa-

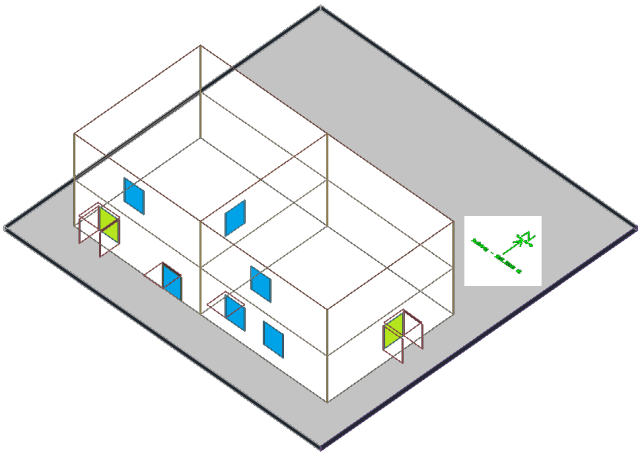

Figure 4.2: four-zone building CAD model

tions, the mathematical model of the indoor temperature is represented as (4.8) [39].

$$\hat{T}_{in}(t) = a[\hat{T}_{in}(t-1) + \frac{\Delta t}{C}[P(t-1) - U(\hat{T}_{in}(t-1) - T_{out}(t-1))]] + \hat{b}(t) \qquad (4.8)$$

where $\hat{T}_{in}$ and T_{out} are the estimated indoor temperature and outdoor temperature, respectively. Δt is the time step, and P is the heating power. a and U are the parameters to be identified. $\hat{b}(t)$ is the estimated occupancy at time t. In the learning-based simulation, the estimated value of occupancy is fed into the model-based predictor. In the model-based controller, the occupancy profile is chosen constant at its average value ($\bar{b}(t)$).

Parameters of the thermal model (4.8) are identified through the recursive least square (RLS) identification algorithm using the EnergyPlus input/output data. To evaluate the performance of the identification algorithm, the root mean square (RMS) criterion is used.

The RLS algorithm is presented in brief as follows [55].

$$\hat{F}(t+1) = \frac{1}{\lambda}[F(t) - \frac{F(t)\phi^T(t)F(t)}{\lambda + \phi^T(t)F(t)\phi(t)}]$$

$$e(t+1) = y(t+1) - \hat{\theta}(t)\phi(t)$$

$$\hat{\theta}(t+1) = \hat{\theta}(t) + F(t+1)\phi(t)e(t+1) \tag{4.9}$$

where F, λ, ϕ, and $\hat{\theta}$ are the gain, forgetting factor, observations and estimated parameter, respectively. e denotes the error between the measurements and identified outputs.

Having the weather and occupancy forecasts, the model predictive control (MPC) comes into play. At each time instant, an optimal control problem is solved to obtain the optimal control action over the time horizon. Using MPC, a plan for the HVAC system is generated

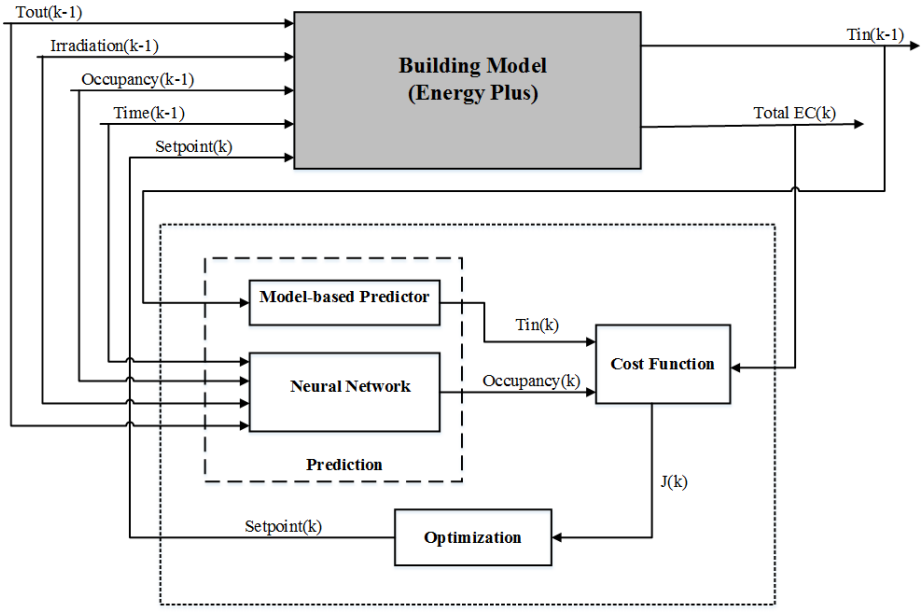

Figure 4.3: Learning-based model predictive control (MPC) for thermal management of buildings

based on the predicted weather conditions and occupancy profiles over the time horizon. The first control action that minimizes the energy consumption and satisfies the comfort is applied to the building's HVACs, then the control algorithm is repeated with the feedback information of building states and outputs at the next time instant. Fig. 4.3 presents the proposed learning-based MPC approach. The cost function of MPC is defined as (4.10), such that it penalizes the deviations from the comfort level and optimum energy consumption.

$$J(t) = \sum_{k=0}^{N} \|\hat{T}_{in}(t+k) - T_d\|_Q^{\,2} + \sum_{k=0}^{N} \|\Delta P(t+k-1)\|_R^{\,2} \tag{4.10}$$

where Q and R are the weighting factors associated with the states and inputs, respectively. N is the time horizon, and T_d is the desired temperature. Therefore, the MPC problem is to minimize (4.10) subject to the performance constraints (4.11), robustness constraints (4.12), and limit constraints ((4.13)). It is worth mentioning that equation (4.11) includes learning, while (4.12) is solely based on model-based design.

$$\hat{T}_{in}(t) = a[\hat{T}_{in}(t-1) + \frac{\Delta t}{C}[P(t-1) - U(\hat{T}_{in}(t-1) - T_{out}(t-1))]] + \hat{b}(t) \tag{4.11}$$

$$\bar{T}_{in}(t) = a[\bar{T}_{in}(t-1) + \frac{\Delta t}{C}[P(t-1) - U(\bar{T}_{in}(t-1) - T_{out}(t-1))]] + \bar{b}(t) \tag{4.12}$$

$$\begin{aligned} T_{in}^{min} \leq \bar{T}_{in}(t+k) \leq T_{in}^{max}, \\ P^{min} \leq P(t+k-1) \leq P^{max} \end{aligned} \tag{4.13}$$

4.3.3 Simulation results of learning-based MPC on case study I

In this section, all the simulation assumptions and results from the proposed learning-based MPC and the model-based controller are illustrated. The simulations are performed for

one year, with 6 time steps per hour. To provide the ANN dataset, EnergyPlus simulations on the building model of Fig. 4.2 were completed from the 1st of January to 31st of December. The simulation assumptions are as follows.

- The desired temperature of all zones are between $20°C$ and $25°C$.
- The control variables are the HVAC setpoints.
- The maximum and minimum supply air temperatures are $50°C$ and $13°C$, respectively.
- The maximum dry-bulb temperature for winter and summer days in Chicago Ohare location are considered $-16.6°C$ and $31.6°C$, respectively.
- The weather data at Chicago Ohare location is used.
- The number of people per zonal area is 0.1.
- The ANN input layer includes the environmental measures, e.g., the time of day, date, weather data, and the historical occupancy data.
- The input and output delays of the NARX model are both chosen 2.
- One output layer and 10 hidden layers are chosen.
- The Levenbegrg-Marquardt backpropagation training algorithm is chosen.

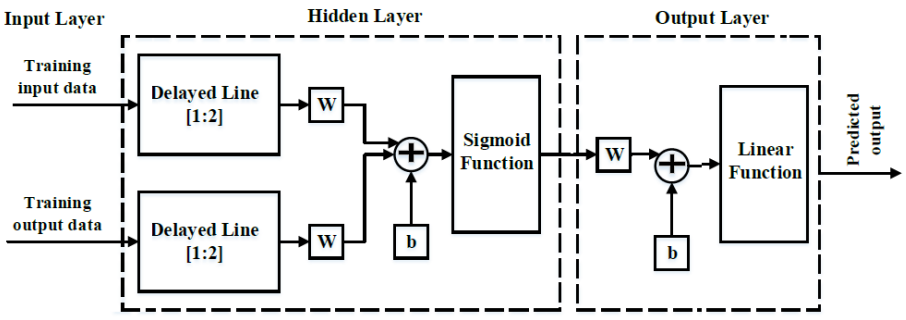

Figure 4.4: NARX neural network model

The NARX neural network implemented in MATLAB is presented in Fig. 4.4. Fig. 4.5 compares the network's response with the actual vacancy profile and shows the error values

between the occupancy predictions and the actual data throughout one month (To get a clear image, these plots are presented for a one-month period). The maximum error value at each time step is 1, i.e., the target occupancy profile is well-tracked. Fig. 4.6 presents the regression and performance plots of the training, validation, and testing datasets. The regression values are all close to 1, and the MSE error is 0.003189, i.e., the training performance is satisfactory. Fig. 4.7 shows the results of the indoor temperature identification throughout a one-month simulation. From Fig. 4.7, the identification error does not exceed 0.05, i.e., the identified outputs are very close to the actual indoor temperature values.

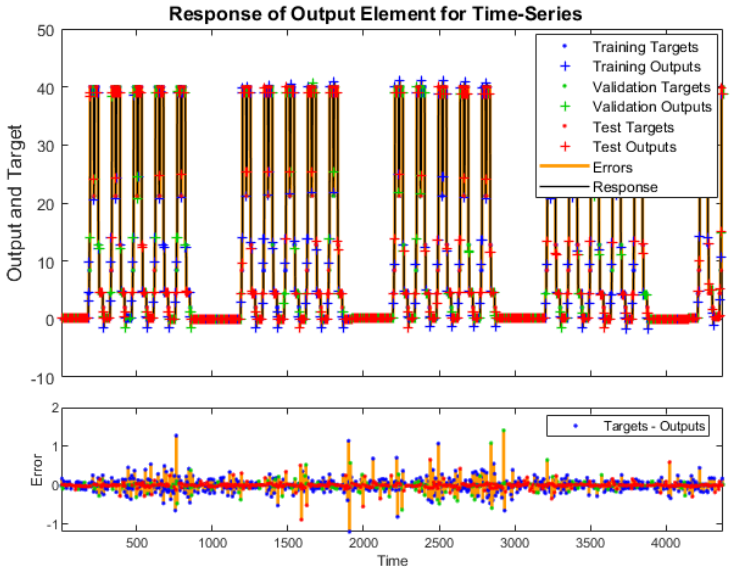

Figure 4.5: Neural network output response versus targets

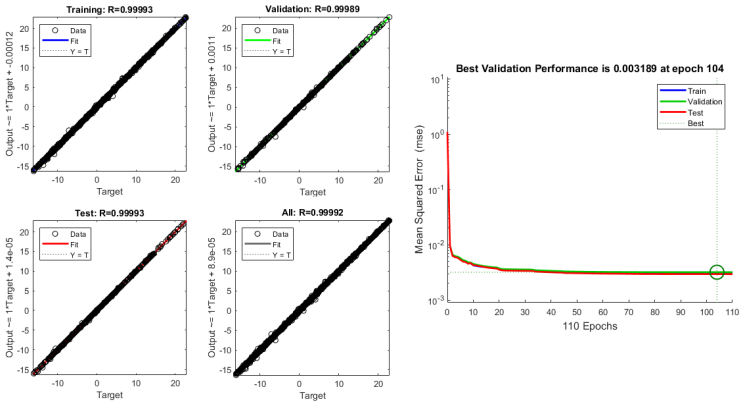

Figure 4.6: Regression and performance trajectories of datasets

Figs. 4.8 and 4.9 show the results of learning-based and model-based control approaches on the building. Comparing the power consumption graphs and the corresponding values in Table 4.2, the proposed method decreased the cooling and heating power consumption by 40.56% and 16.73%, respectively. The deviations from the comfort level in the model-based control method are extremely higher compared to the proposed method. The zone temperature using the model-based control approach even deviates from the lower comfort zone limit.

Table 4.2: Simulation results

Parameters	Conventional MPC	Learning-based MPC	Change
Average cooling power	396.28 W	235.55 W	$\downarrow 40.56\%$
Average heating power	2.43 KW	2.02 KW	$\downarrow 16.73\%$

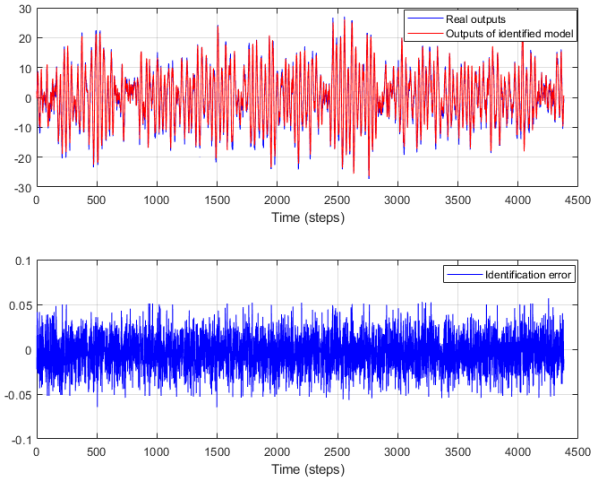

Figure 4.7: Identified model outputs versus real outputs, and the identification error

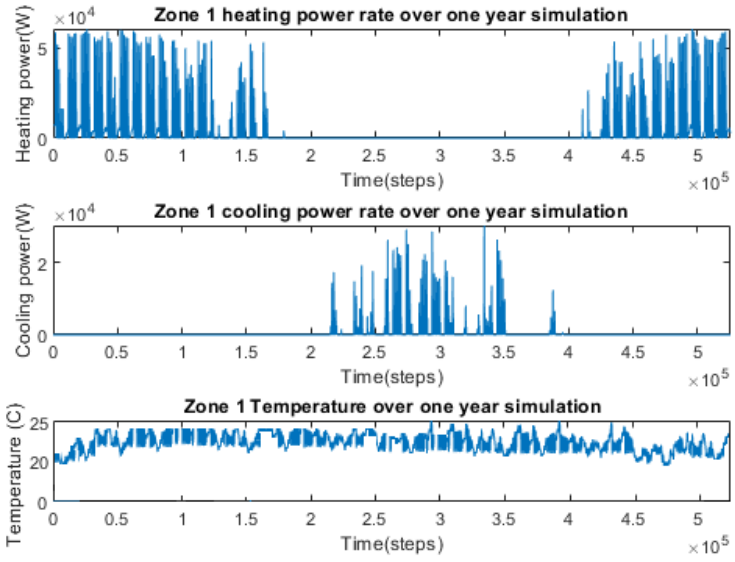

Figure 4.8: Power consumption and zone 1 temperature using learning-based MPC

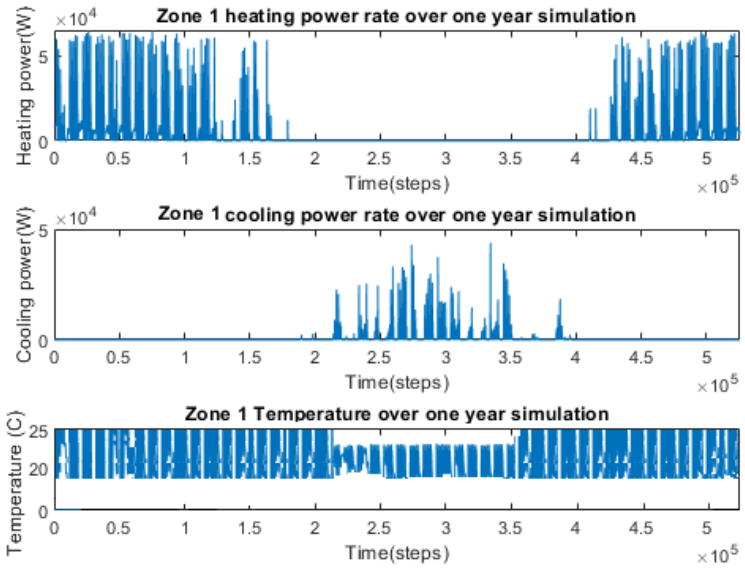

Figure 4.9: Power consumption and zone 1 temperature using conventional MPC

4.4 Learning-based MPC for Management of Case Study II

In this section, the proposed learning-based MPC approach is applied to manage thermal, visual, olfactory conditions in a building simulated in EnergyPlus software.

4.4.1 Case study II model definition

The building under study is a one-story, L-shaped building, with total area and volume of $130.06m^2$ and $396.44m^3$, respectively. The area and volume of the north, west, and east zones are ($55.74m^2$, $169.90m^3$), ($37.16m^2$, $113.27m^3$), and ($37.16m^2$, $113.27m^3$), respectively. The windows are double-pane, and the building is oriented to the north. The zones are equipped with air conditioners (HVACs), light dimming, and blind control systems. An illuminance detector is placed at the center of the west zone, at desk height.

4.4.2 Learning-based MPC on case study II

Three NARX networks, corresponding to three performance criteria, are utilized in this study. The network estimating the thermal comfort has five output variables, i.e., PMV, occupancy (Occ), cooling/heating power consumption (P), indoor air temperature (T_{ai}), and radiant temperature ($\bar{T}_r$) from time step k to $k+i$. The time of day, season, outdoor temperature (T_{out}), solar radiation (Sr), occupancy, radiant temperature, set-point temperature (T_{sp}), and indoor air temperature at time step k compose the input layer of ANN for estimating the thermal properties. The NARX network for estimating thermal properties is presented in (4.14).

$$\begin{aligned}
\hat{y}(k+i) &= f(u(k+i-1),...,u(k+i-n_a),y(k+i-1),...,y(k+i-n_b)) \\
u(k) &= [Time(k);T_{out}(k);Sr(k);\bar{T}_r(k);T_{sp}(k);T_{ai}(k);Occ(k)] \\
y(k) &= [PMV(k);Occ(k);P(k);T_{ai}(k);\bar{T}_r(k)]
\end{aligned} \tag{4.14}$$

For estimating the visual properties, visual comfort index ($PPDv$), occupancy, lighting power consumption, luminance ($L_{s,i}$) and illuminance level (E_v) from time step k to $k+i$ are the ANN outputs. The inputs of ANN for the visual comfort evaluation are the time of day, season, luminance, solid angle ($\omega_{s,i}$), position index (P_i), and occupancy at time step k. The NARX network for estimating visual properties is presented in (4.15).

$$\begin{aligned}
\hat{y}(k+i) &= f(u(k+i-1),...,u(k+i-n_a),y(k+i-1),...,y(k+i-n_b)) \\
u(k) &= [Time(k);L_{s,i}(k);\omega s,i(k);P_i(k);Occ(k)] \\
y(k) &= [PPDv(k);Occ(k);P(k);L_b(k);E_v(k)]
\end{aligned} \tag{4.15}$$

For learning the olfactory properties, the humidity level, CO2 concentration, air flow rate (L_p), and occupancy at time k are the inputs. The output layer of ANN for learning olfactory parameters is composed of the occupancy, $PPDo$ olfactory comfort index, pollutant concentration (C), humidity, and air flow rate from time step k to $k+i$. The NARX network for estimating olfactory properties is presented in (4.16).

$$\begin{aligned}
\hat{y}(k+i) &= f(u(k+i-1), ..., u(k+i-n_a), y(k+i-1), ..., y(k+i-n_b)) \\
u(k) &= [Time(k); Humidity(k); C(k); L_p(k); Occ(k)] \\
y(k) &= [PPDo(k); Humidity(k); C(k); L_p(k); Occ(k)]
\end{aligned} \tag{4.16}$$

In this study, to validate the performance of the proposed control strategy and for comparison purposes, we first designed a PID controller for the building. One PID controller is designed for each building zone. They are tuned such that they maintain desired thermal, visual, and olfactory set-points in the building with minimum violations of comfort bounds (comfort constraints satisfaction is not guaranteed). The PID parameters for each zone are computed using $pidtune$ in MATLAB (shown in Table 4.3). It is worth mentioning that the building energy trend and comfort criteria are not considered as inputs for the optimization problem (i.e., They are outputs of the PID controller). To achieve the highest (thermal, visual, olfactory) comfort level, a conservative reference (in the middle of lower and upper comfort limits) is chosen for PID tracking.

Table 4.3: PID parameters

Zone	P	I	D
North	215.1	0.172	103000
West	111.0	0.041	50300
East	117.0	0.033	49810

The control goals in this study are minimizing energy consumption in the HVACs and lighting systems, and maximizing occupants' comfort (thermal, visual, and olfactory comfort). In this regard, the objective function is formulated as (4.17).

$$\begin{aligned} \text{minimize } \ J(k) = \sum_{i=0}^{N} \|P\hat{M}V(k+i) - PMV_d\|_{Q_1}^2 + \|P\hat{P}D_v(k+i) - PPD_d\|_{Q_2}^2 \\ + \|P\hat{P}D_o(k+i) - PPD_d\|_{Q_3}^2 + \sum_{i=0}^{N} \|\Delta P(k+i)\|_R^2 \end{aligned} \tag{4.17}$$

$$\begin{aligned} \text{subject to } \ \hat{y}(k+i) = f(u(k+i-1), ..., u(k+i-n_a), y(k+i-1), ..., y(k+i-n_b), \\ \hat{\lambda}(k+i), \theta(k)) \end{aligned} \tag{4.18}$$

where Q_1, Q_2, Q_3, and R are the weighting factors associated with the thermal, visual, olfactory comfort indexes, and energy usage, respectively. N is the prediction horizon, and the d indices in comfort indexes represent the desired comfort levels. $\hat{y}(k)$ is the predicted output variable, $\hat{\lambda}(k)$ is the predicted environmental variable, and $\theta(k)$ denotes model parameters that need to be learned. Therefore, the MPC problem is to minimize (4.17)

subject to the system model (4.18), and system constraints (4.19).

$$
\begin{aligned}
PMV^{min} \leq PMV(k+i) \leq PMV^{max}, \\
{PPD_v}^{min} \leq PPD_v(k+i) \leq {PPD_v}^{max}, \\
{PPD_o}^{min} \leq PPD_o(k+i) \leq {PPD_o}^{max}, \\
T_{ai}^{min} \leq \bar{T}_{ai}(k+i) \leq T_{ai}^{max}, \\
P^{min} \leq P(k+i) \leq P^{max}
\end{aligned} \tag{4.19}
$$

Above, PMV^{max} and PMV^{min} denote the upper and lower constraints of the thermal comfort index. ${PPD_v}^{max}$ and ${PPD_v}^{min}$ denote the upper and lower constraints of the visual comfort index. ${PPD_o}^{max}$ and ${PPD_o}^{min}$ denote the upper and lower constraints of the olfactory comfort index. T_{ai}^{max} and T_{ai}^{min} are the upper and lower limits of the indoor air temperature. P^{max} and P^{min} are the upper and lower limits of power consumption.

The performance of MPC is highly dependent on the accuracy of the prediction model [26]. To improve model accuracy, in this work, NNs are utilized to learn the building parameters, i.e., energy consumption, comfort indexes, and their associated parameters. The learned data is then fed into the model-based controller (MPC). The control algorithm generates control inputs for the heating/cooling systems, lighting systems, blinds, and ventilators in each step.

Fig 4.10 shows the block diagram of our proposed integrated learning-based control strategy. The environmental conditions, comfort parameters, and energy consumption of the building are learned through NNs. Learned parameters are then injected into the cost function block of MPC. In each step, MPC computes the current and future optimal control

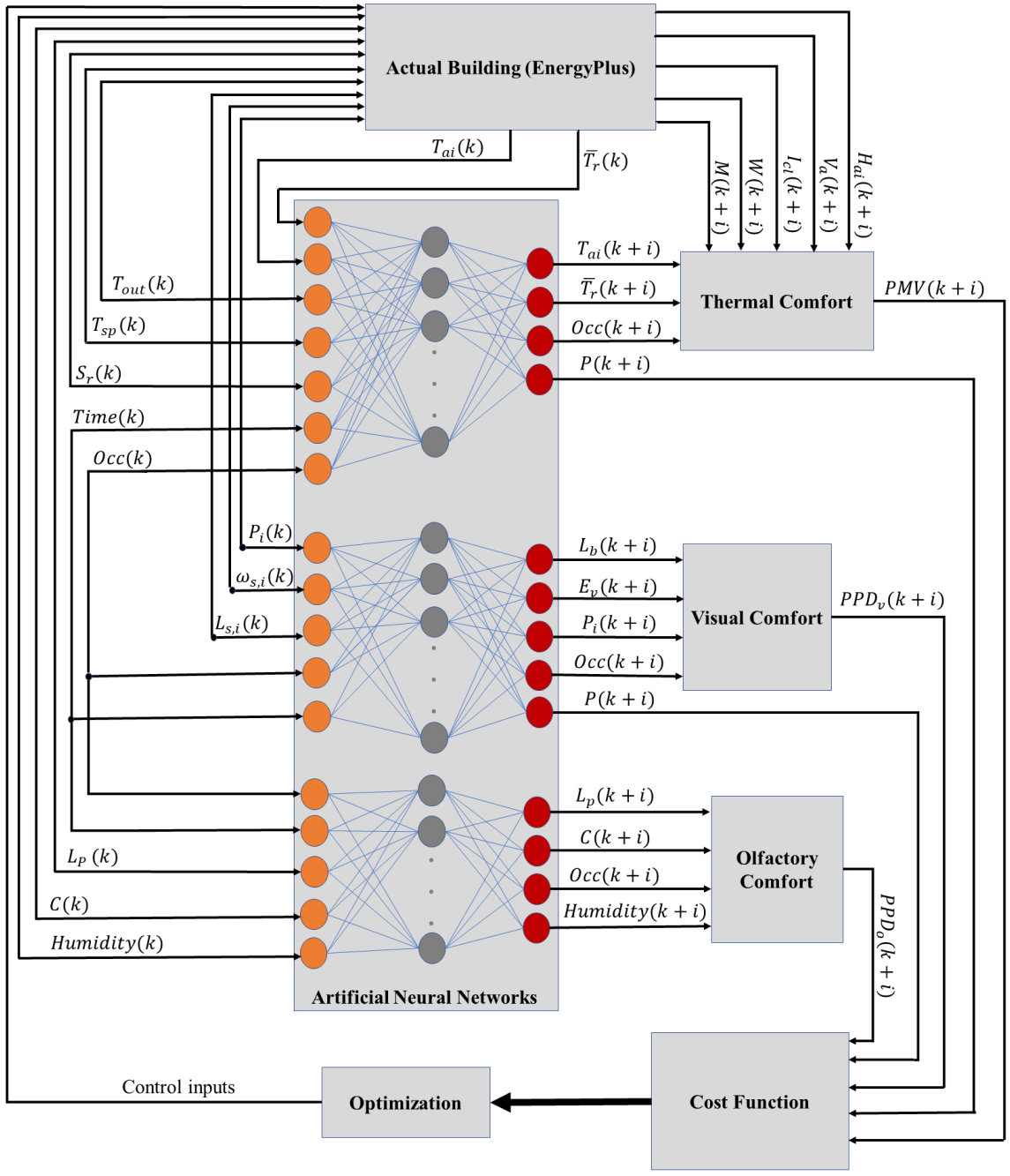

Figure 4.10: Proposed learning-based building control system

inputs that can minimize the accumulated power consumption and maximize the residents' comfort. Control inputs are then applied to the building actuators, such as the blinds,

heating/cooling systems, artificial lights, and ventilators. Our proposed learning-based MPC approach for managing case study is as follows:

Algorithm 4 Proposed learning-based control approach for building management

Step 1: Set the time step $n = 1$.

Step 2: Reset optimization iteration $k = 0$.

Step 3: Initialize the system state and control input values.

Step 4: Get the ANN outputs, i.e., approximations of the power consumption, environmental conditions, and comfort indexes.

Step 5: Build the cost function with the learned data, and compute the current and future control inputs (heating/cooling set-points, airflow of the ventilator, light intensity, and blind angle) by solving the optimization problem (4.17) subject to (4.18) and (4.19).

Step 6: Increment k, $k = k + 1$, and continue until $k \leq k_{max}$. If $k \geq k_{max}$, go to step 4.

Step 7: Apply the first control inputs to the building simulated in EnergyPlus.

Step 8: Increment n, $n = n + 1$, and go to step 2.

4.4.3 Simulation results of learning-based MPC on case study II

Fig. 4.11 shows the general block diagram of the simulations. To provide learning datasets, the building model is simulated in EnergyPlus building simulation software. The proposed control strategy is coded in MATLAB. EnergyPlus transfers the datasets to the MATLAB code, in which the NARX network learns the comfort indexes, environmental

conditions, and energy consumption. Based on the learned and estimated parameters, HVAC systems' energy consumption, lighting energy consumption, and residents' comfort are optimized. For comparison purposes, a PID controller is also applied to the case study under the same conditions. The simulation assumptions are as follows:

- Simulation is performed for one year period, from the 1st of January to 31st of December.
- Sampling time is 10 minutes.
- Location (weather data) is San Francisco, Intl Ap, CA, USA.
- The thermal constraint is between 20 °C and 27 °C.
- The maximum dry-bulb temperature for winter and summer days are -17.30 °C and 31.50 °C, respectively.
- The average number of occupants per zonal area is 2.18, and the total occupancy count in the whole area is 10.
- The temperature set-points for the PID controller are set in the middle of thermal comfort limits (20 °C).
- The luminance and glare set-points for the PID controller are set slightly under their upper comfortable limits ($2000cd/m^2$ and 30, respectively).
- For the PID case, the highest contaminant concentration level is set at 800 ppm.
- Input delays of ANNs are chosen to be 2 for learning the thermal, 1 for learning the visual, and 10 for learning the olfactory comfort.
- Output delays of ANNs are chosen 10 for learning the thermal, 20 for learning the visual, and 70 for learning the olfactory comfort.
- The number of hidden layers for thermal, visual, and olfactory comfort learning are 10, 10, and 30, respectively.
- Training algorithm is Levenbegrg-Marquardt backpropagation.
- Control variables are the heating/cooling temperature, humidity, air flow, blind status, and light illuminance.

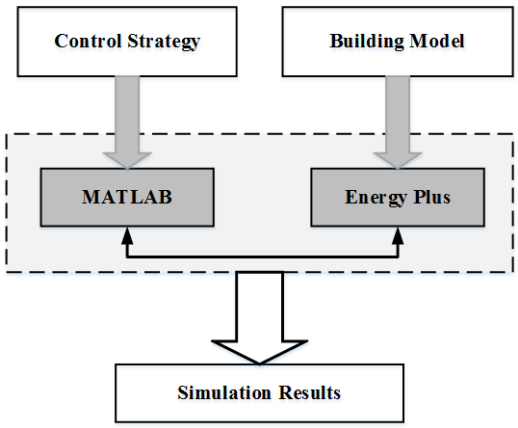

Figure 4.11: General block diagram of the simulations

Network training, testing, and validation are performed over a one year period, and the learning results are shown over a 36-day period (for a clear illustration). Besides, for the sake of clarity, simulation results are shown only for the north zone of the building. The other zones show similar behavior. Fig. 4.12 shows the time-series trajectory of learning the temperature. Based on the error trajectory in Fig. 4.12, the absolute value of the temperature learning error does not exceed 0.5. The mean squared error (MSE) of the most optimum temperature learning (where the testing, training, and validation curves converge) is 0.0067, which depicts satisfying performance of the network. The time-series trajectory of learning the clothing factor is shown in Fig. 4.13. According to Fig. 4.13, the absolute value of the clothing learning error is less than 0.05. Moreover, the training, testing, and validation curves converge at MSE of 3.552×10^{-6}. Fig. 4.14 shows the time-series trajectory of learning PMV thermal comfort index. The absolute value of MSE for learning the PMV index does not exceed 0.02, which is satisfying considering the PMV values that do not exceed the desired thermal comfort limits (± 1).

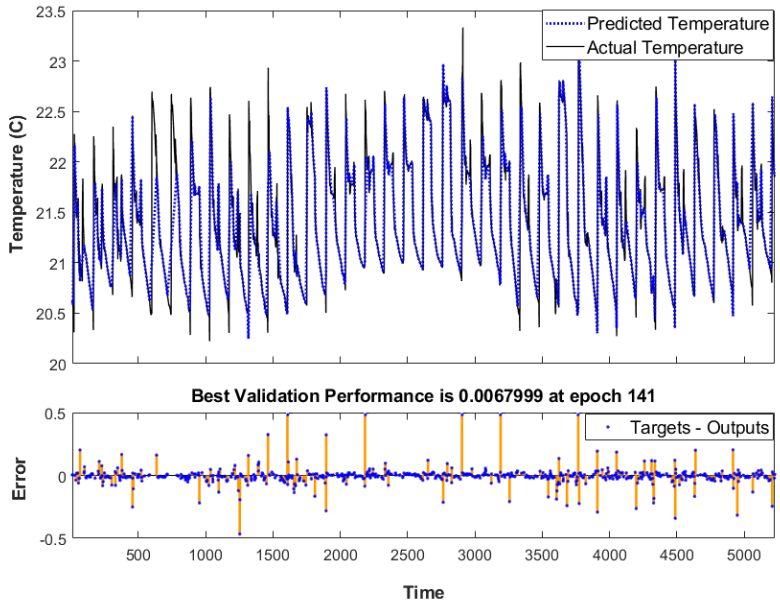

Figure 4.12: Learned temperature versus targets

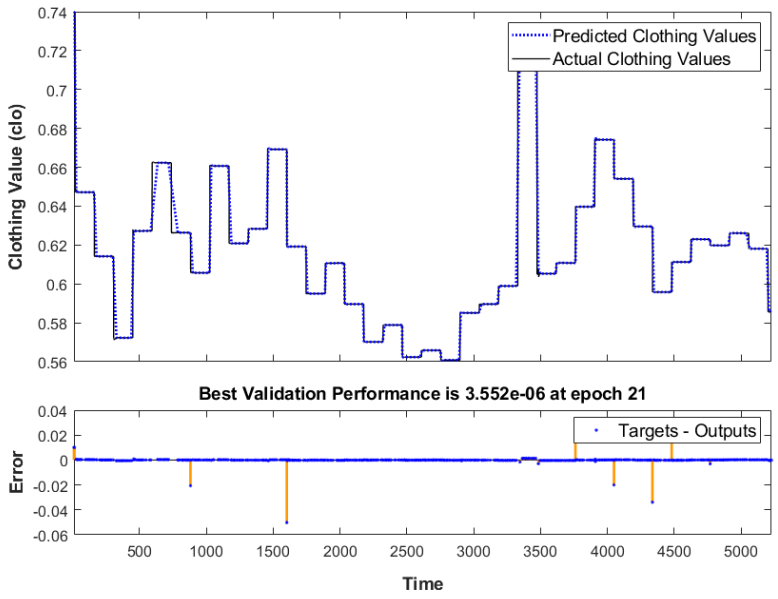

Figure 4.13: Learned clothing versus targets

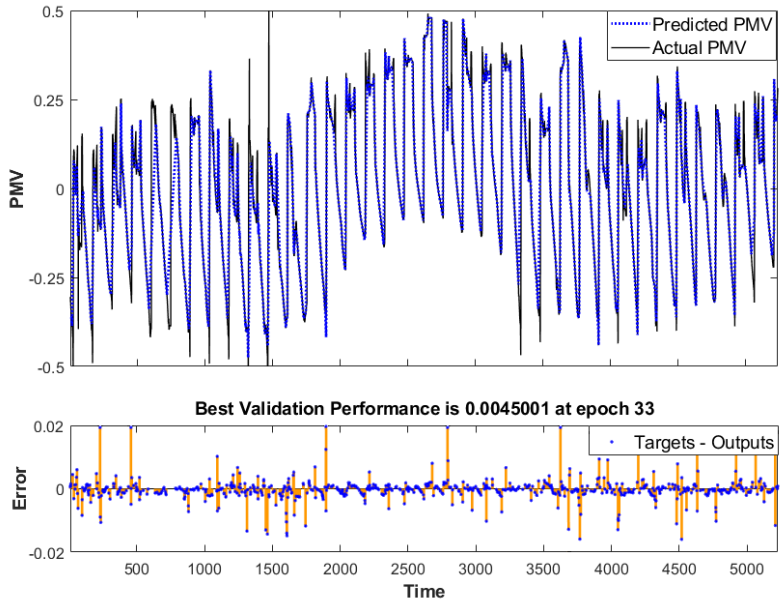

Figure 4.14: Learned PMV thermal comfort index versus targets

Results of learning the visual properties are shown in Figs. 4.15 to 4.17. The time-series trajectory of learning the illumination is shown in Fig. 4.15, in which the maximum value of error for learning the illumination data is 0.5, with the best MSE performance of 0.0045. According to the time-series plots in Fig. 4.16, the error between the observed and learned glare data is 0.5. Moreover, The best validation performance value for the glare learning is 0.0023. Fig. 4.17 shows the actual and learned values for the visual comfort index ($PPDv$). The maximum error and the best performance MSE for learning $PPDv$ are 0.5 and 0.0043, respectively. Results of learning the olfactory properties are shown in Figs. 4.18 and 4.19. Fig. 4.18 shows the actual and learned values for the CO2 concentration. From Fig. 4.18, the maximum absolute error between the targeted and learned values is 6 (which is satisfactory considering the average value of CO2 level over the simulation period), and the MSE value is 0.0046. Fig. 4.19 shows the time-series trajectory of learning

the olfactory comfort index ($PPDo$). The MSE and maximum absolute error values of learning the $PPDo$ index are 0.0084 and 0.8, respectively.

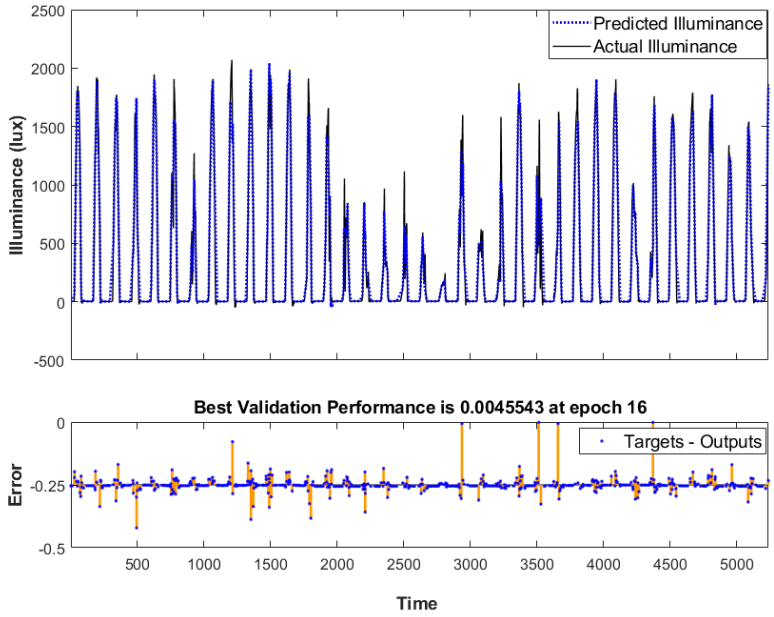

Figure 4.15: Learned illumination versus targets

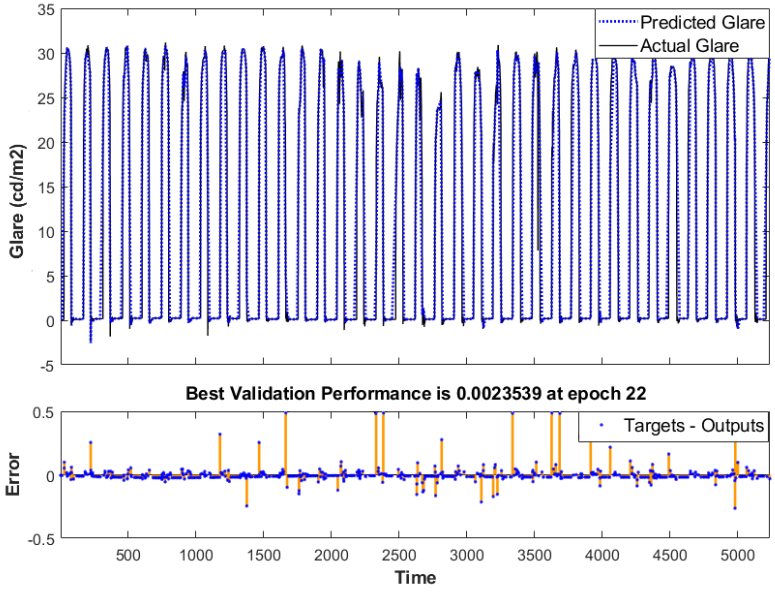

Figure 4.16: Learned glare versus targets

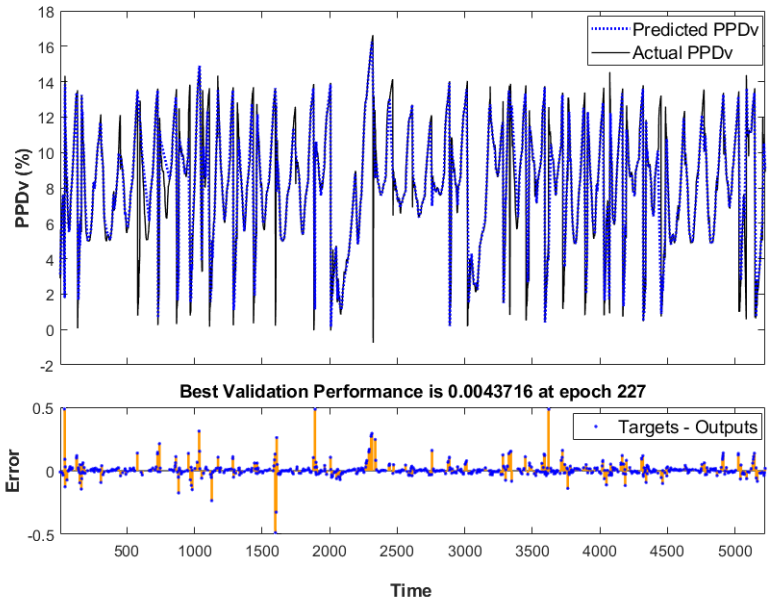

Figure 4.17: Learned PPD visual comfort index versus targets

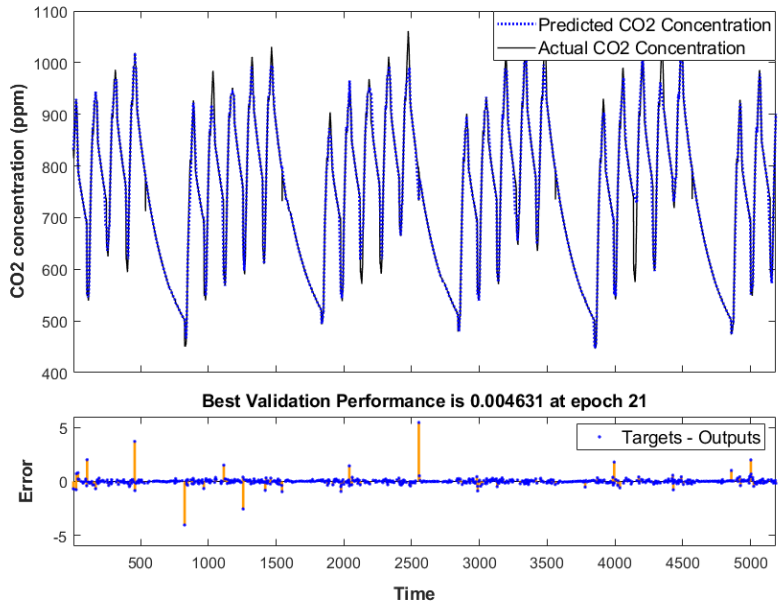

Figure 4.18: Learned CO2 concentration versus targets

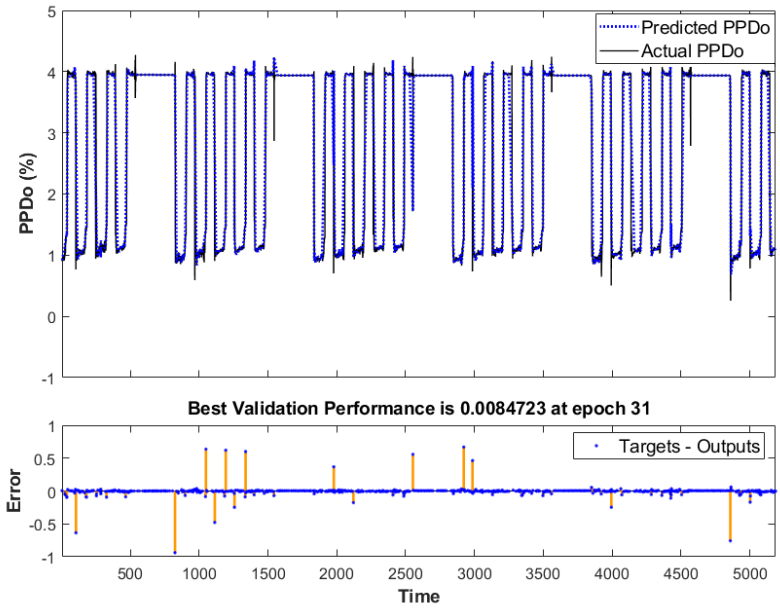

Figure 4.19: Learned PPD olfactory comfort index versus targets

Figs. 4.20 and 4.21 show thermal properties of the building using the proposed control strategy and baseline controller, respectively. The clothing factor trajectories present higher values during the winter seasons (two sides of the plots), which is expected since the residents' thermal perceptions are dependant on the environmental changes. In Fig 4.20, the PMV index trajectory varies between -1 and 1, which represents slight cool (-1), neutral (0), and slight warm (1) conditions. Moreover, thermal comfort values are lower during the cold seasons than the hot seasons. The zonal temperature using the proposed controller fluctuates between 20 °C and 27 °C (desired zonal temperature values), and it is slightly higher during summer seasons than winter seasons. Therefore, it is conceived that the thermal comfort is maintained using the proposed control strategy. According to Fig. 4.21, the PMV profile using PID controller oscillates between -0.5 and 2.5 (i.e., it reaches

uncomfortable thermal conditions). Likewise, the temperature profile in Fig. 4.21 shows large oscillations and time-lags. Thus, in spite of choosing a conservative temperature set-point (slightly under the upper comfort bound) for PID, it fails to maintain thermal comfort constraints. According to the heating/cooling power consumption plots in Figs. 4.20 and 4.21, an average of 888.68 W less heating power, and 872.78 W less cooling power are consumed using the proposed control approach compared to the baseline. Thus, the conventional controller is not capable of minimizing energy consumption; because unlike the proposed learning-based controller, PID is not adaptive to the environmental changes nor predictive, and it does not take into account the energy saving aspect as an input for the decision-making process.

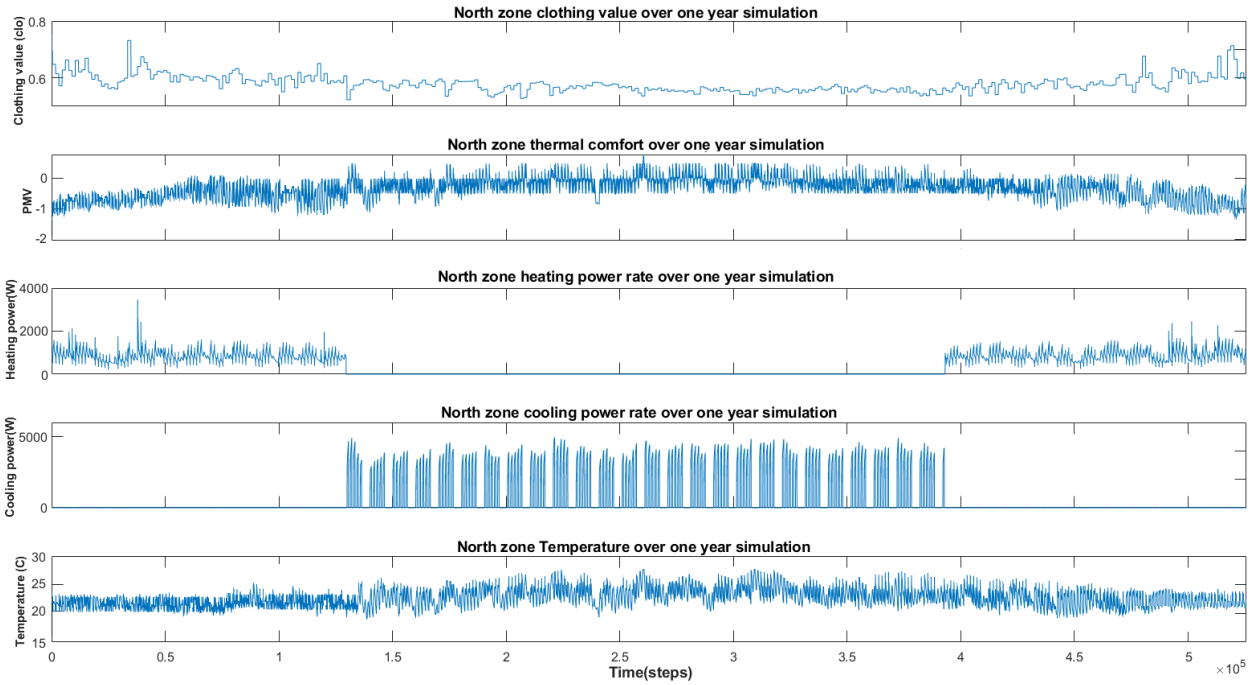

Figure 4.20: Thermal properties using the proposed control strategy

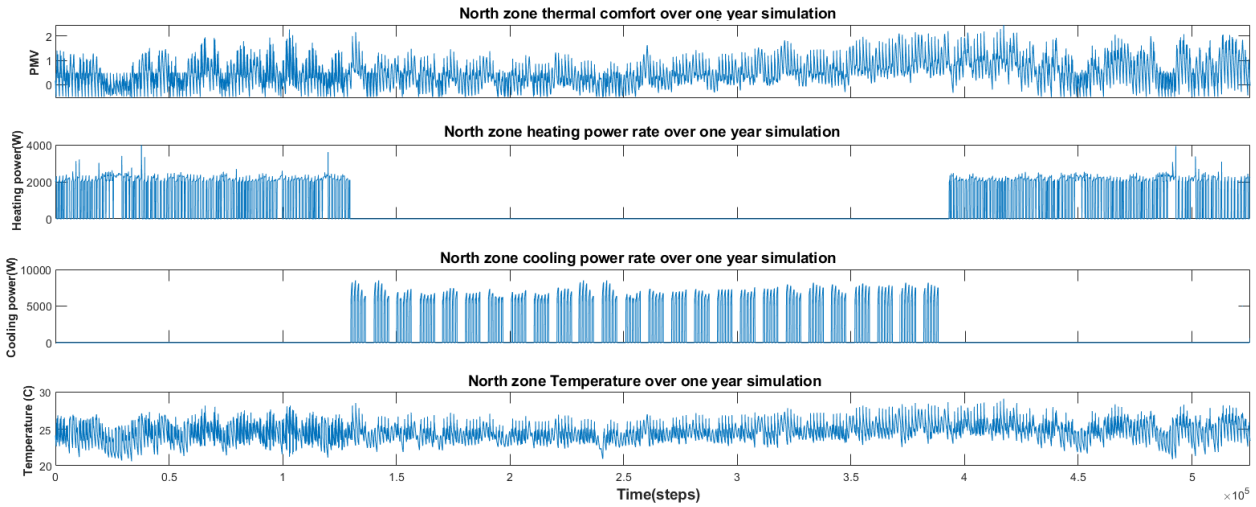

Figure 4.21: Thermal properties using PID control

Figs. 4.22 and 4.23 show the building's visual properties using the proposed control strategy and baseline, respectively. According to the lighting energy consumption plots, an average of 1012.30 J less lighting energy is consumed using the proposed control approach compared to the baseline. The lighting energy and occupancy count trajectory curves are proportional in Fig. 4.22, indicating that the predictions of occupancy is utilized to save energy using the learning-based controller. From Figs. 4.22 and 4.23, the illumination and glare levels fluctuate significantly over the simulation period. During the hot seasons, illuminance level and lighting consumption are lower than the cold seasons. According to section II. B, the illuminance and glare values in Figs. 4.22 and 4.23 (using both controllers) are within the comfortable limits. The average of $PPDv$ index using the proposed control approach is 7.25 %; however, $PPDv$ average using PID is 15.20%. Although the PID controller did not violate the comfort limits, the proposed control approach has shown better

visual comfort index by learning historical comfort data and forecasting occupancy and environmental conditions.

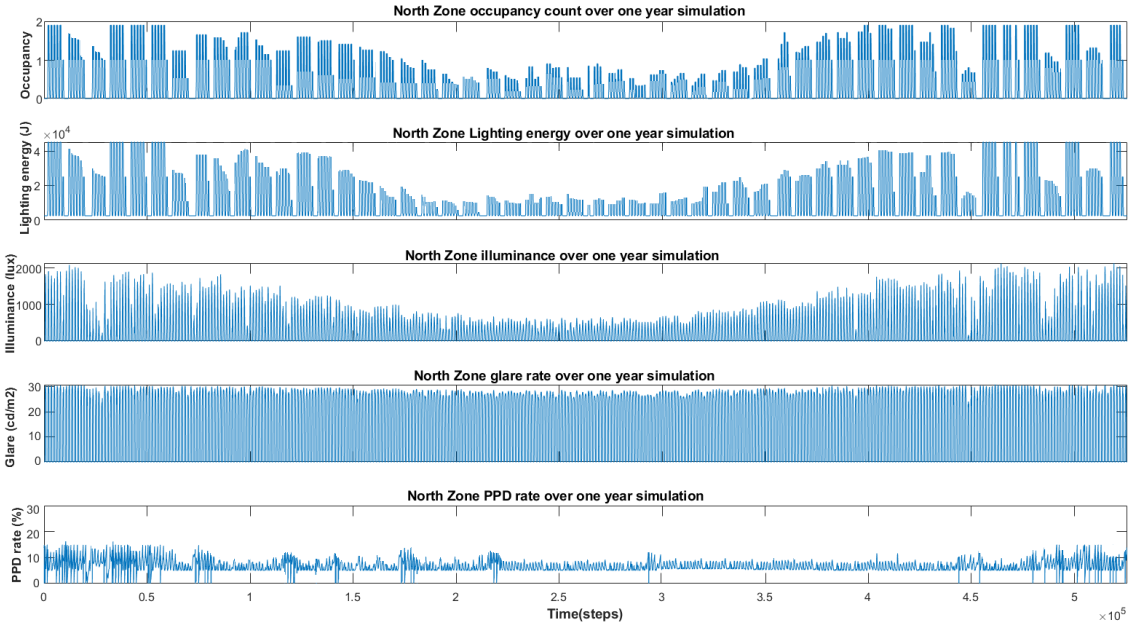

Figure 4.22: Visual properties using the proposed control strategy

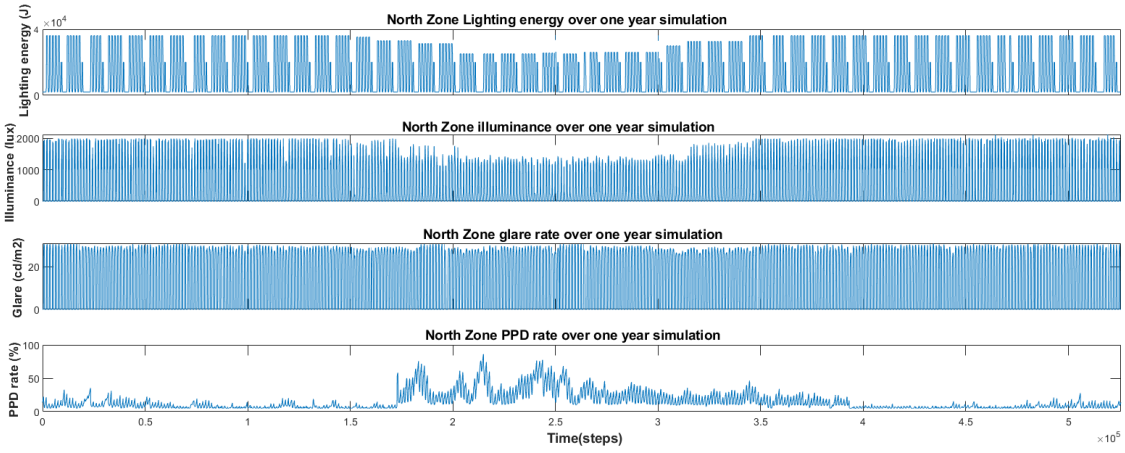

Figure 4.23: Visual properties using PID control

Figs. 4.24 and 4.25 show olfactory properties of the building using the proposed control strategy and baseline, respectively. From the air flow rate and contaminant concentration plots in Figs. 4.24 and 4.25, it is conceived that higher air flow rates are applied to the higher levels of CO2 and contaminant concentration. Furthermore, $PPDo$ is lower (corresponding to a higher comfort level) with higher air flow intake. The olfactory comfort index ($PPDo$) in both figures (Figs. 4.24 and 4.25) varies from 0 to 4 (desired levels). However, the average $PPDo$ is slightly lower using the proposed control approach (higher olfactory comfort satisfaction) compared to the baseline. Furthermore, Table 4.4 compares the simulation results of the baseline and proposed control approaches. In particular, Table 4.4 summarizes all the analysis mentioned above on the simulation results. In summary, our proposed learning-based controller ensures the highest possible overall thermal, visual, and olfactory comfort in the building with the lowest possible energy usage in the corresponding subsystems.

Table 4.4: Performance comparison of baseline and proposed control methods

Approach	Thermal energy consumption	Thermal comfort	Lighting energy consumption	Visual comfort	Olfactory comfort]
Baseline	7463.71 W	75.52%	18052 J	84.8%	86.50%
Proposed	5702.25 W	99.86%	17039.7 J	92.75%	97.89%

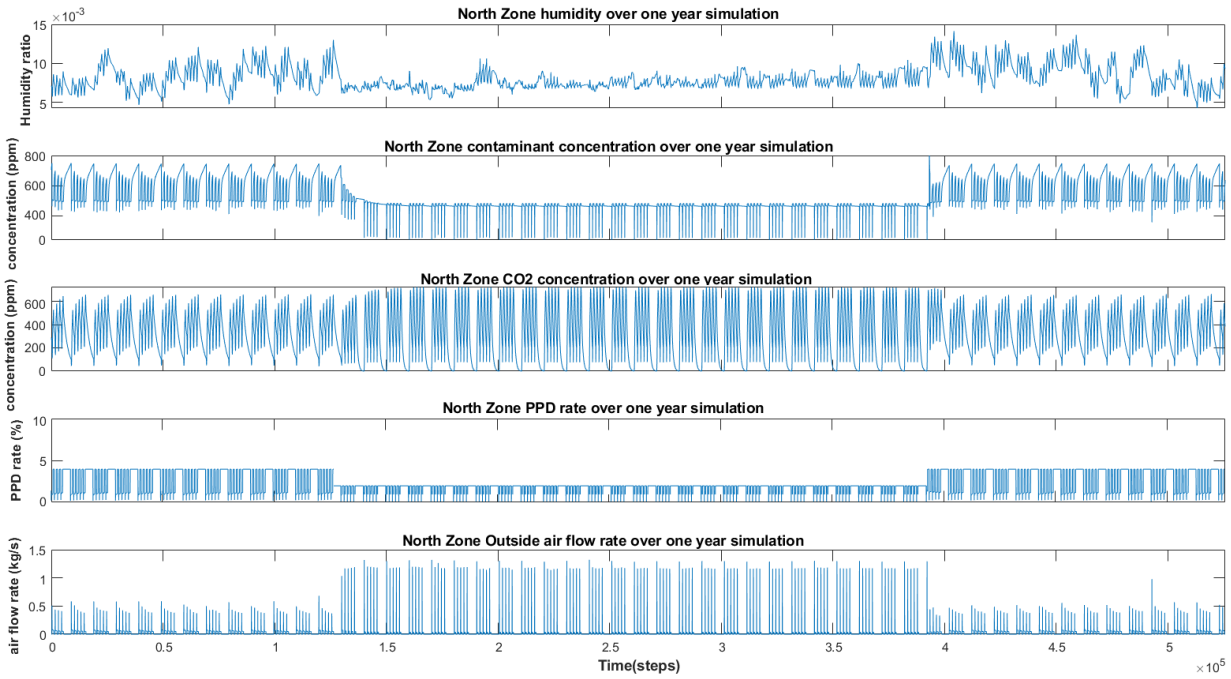

Figure 4.24: Olfactory properties using the proposed control strategy

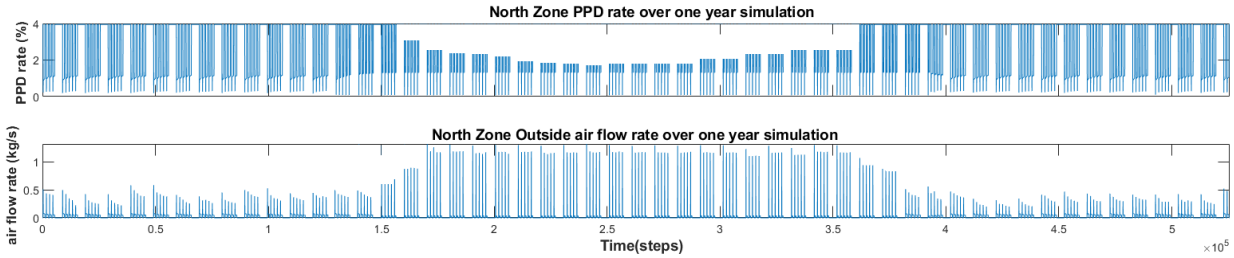

Figure 4.25: Olfactory properties using PID control

4.5 Conclusion

In this chapter, a learning-based modeling strategy incorporated with a model-based predictive control approach is proposed for CPS management and control. The proposed approach is applied to two case studies; (1) to manage the thermal comfort and energy

consumption in a four-zone building simulated in EnergyPlus software, and (2) to manage visual, thermal, and olfactory conditions in a building simulated in EnergyPlus software. Predicting the building parameters is a challenging part of MPC since the building's subsystems are nonlinear, associated with uncertainties, and strongly coupled. ANN is incorporated with the model-based control approach to address the mentioned issues. The predictions of building's energy consumption data, environmental conditions, occupant-related parameters, and comfort criteria are generated through ANN, and then fed into the model-based controller (MPC). EnergyPlus software is used to simulate a building with real materials and components, and to test the proposed approach on it. Results from the proposed learning-based approach in both case studies, showed significantly better performance in maintaining residents' comfort and minimizing energy usage, compared to the baseline approach. From the simulation results of case study I, the proposed learning-based control approach proved the significantly better performance in energy savings (40.56%less cooling power consumption and 16.73%less heating power consumption), and residents' comfort over the conventional MPC approach. From the simulation results of case study II, the proposed learning-based building management system performs significantly better than the baseline controller in maintaining residents' thermal, visual, and olfactory comfort and energy efficiency. The average thermal, visual, and olfactory comfort rates are 92%, 88%, and 98%, respectively, throughout the simulation. The learning algorithm is over 90% accurate in predicting building comfort parameters, environmental conditions, and energy consumption patterns. Moreover, compared to the baseline, an average of 67.53% less heating power, 62.14% less cooling power, and 5.6% less lighting energy are consumed

using our proposed control approach. It is worth mentioning that while most of the previous studies on building management applications focused on optimizing one single aspect of buildings, such as thermal aspect, our proposed building management system is set out to address simultaneous energy and comfort management in three main components of buildings; thermal, visual, and olfactory components. The proposed management system ensures the highest possible overall thermal, visual, and olfactory comfort in buildings with the lowest possible energy usage in the corresponding subsystems.

CHAPTER V

CONCLUSIONS AND FUTURE RESEARCH

This chapter concludes the contributions of this dissertation and states the future research directions.

5.1 Conclusions

In this dissertation, we proposed and implemented control approaches for cyber-physical systems management. The information revealed in this dissertation is expected to contribute to the design, development, and evaluation of model-based and learning-based controllers for CPSs management (smart buildings management).

Developing appropriate models has always been a significant challenge in designing and implementing model-based controllers for CPSs management. Suitable models (thermal, humidity, and occupants behavior models for a building) are required to be chosen based on the application. For instance, mathematical models are typically accurate in predicting the system's dynamics, but they are not computationally efficient for real-time control purposes. Other than mathematical models, learning-based models can be advantageous when insufficient information about the physical properties is available. Learning-based models also have the advantage of being self-adaptive/self-growing over time, for instance, for learning the building occupants' feedback or their perception of comfort. The second

chapter of this dissertation is dedicated to CPS models description, specifications, and constraints. Models of the building indoor conditions, and performance criteria (thermal, visual, auditory, olfactory, hygienic comfort) are provided.

One of the most debated aspects of cyber-physical systems is their control and management. The first step to design a controller for a CPS is to define its control objectives. For a building control problem, improving the residents' comfort, and minimizing building energy consumption can be the control objectives. Model predictive control (MPC) is known to be excellently suited for CPSs control and management due to its predictive properties. Moreover, MPC takes into account the constraints and disturbances associated with the optimal problem, which usually exists in CPS control problems. For our problem, MPC can be utilized in a centralized or distributed control architecture. In a centralized MPC approach, one objective function, including the system constraints, dynamics, and control objectives, is formulated. Clearly, if the system is large-scale, the optimal control problem will contain so many variables, and solving it demands a huge computation. In a distributed MPC approach, the system is split into smaller subsystems; each subsystem is controlled by a local controller through the local state and input variables. There also exists a coordinator that shares the interaction variables with the other subsystems. The computation overhead for solving the distributed control problem is expected to be lower than the centralized structure.

In the third chapter of this dissertation, we provided centralized and distributed MPC architectures, as a general guide, for the management of CPSs. We applied our proposed MPC approaches to a CPS case study; smart building. In the building control problem,

achieving optimal energy consumption and thermal comfort are the control objectives. Comparing the simulation results of the distributed and centralized MPC demonstrate the effectiveness of the distributed MPC approach for the systems under study. Distributed MPC resulted in a good overall performance with significantly less computational complexity. Our implemented smart building testbed is also illustrated at the end of this chapter, which was utilized to analyze the performance of our proposed management schemes.

By incorporating learning with the model-based control approach, we are capable of controlling two types of systems, i.e., systems with available mathematical models, and the ones with unavailable models (due to complex non-linearity or high order). In the integrated approach, the model-based controller allows to formulate system management tasks as optimal control problems in terms of performance metrics. Online model learning is utilized within the control approach to adapt the system to the changing environmental conditions over time. The controller is integrated with the machine learning algorithm to update formal specifications over time. Therefore, this approach integrates control and learning algorithms into one management structure that enables systems to adapt to the variations in their environment.

In the fourth chapter of this dissertation, we proposed a learning-based predictive control strategy for the management and control of thermal, visual, and olfactory properties of smart buildings. The comfort criteria, energy trends, and environmental parameters of the underlying building are learned using neural networks. Based on the learned parameters, a predictive model-based controller is then utilized to achieve the desired comfort levels and energy savings. Compared to the previous building management systems presented

in the literature, the proposed management system combines learning with model-based control design to include the changing occupant-related data and environmental conditions in the control loop. The proposed control strategy learns building dynamics and adapts to the changing environment, to balance the performance of three subsystems in buildings (thermal, visual, and olfactory components), in terms of cost-effectiveness and comfort. Two controllers, the proposed control approach and a baseline controller, are implemented on a building simulated in EnergyPlus building simulation software, and their results are compared. The simulation results (in MATLAB and EnergyPlus) proved that the proposed control structure is very effective for simultaneous optimization of visual, thermal, and olfactory performances, by considering the forecasts of environmental conditions, comfort parameters, and energy profiles in the control loop. Therefore, the learning-based control strategy has shown better control performance in maintaining occupants' comfort and reducing building energy consumption over the baseline. An average of 92.66% comfort (thermal, visual, and olfactory comfort) is attained using the proposed control approach. Besides, compared to the baseline, an average of 67.53% less heating power, 62.14% less cooling power, and 5.6% less lighting energy are consumed using the proposed control approach. The configured learning algorithm is also over 90% accurate in predicting building comfort parameters, environmental conditions, and energy consumption patterns. The key findings of this dissertation are summarized as follows:

1. Existing model-based building control schemes typically require a sufficiently accurate model of the building mechanism in order to achieve a desired control performance. In situations where finding a suitable mathematical model for the building

is difficult (due to measurement errors, lack of information, and poor understanding of the system mechanism), machine learning techniques can be used to represent the underlying dynamics. However, learning-based building control strategies can not be generalized and analyzed easily, and they suffer from limitations in verifying their accuracy. In this study, we combined the concepts of model-based control with learning-based techniques to provide a real-time building management structure that can learn complex dynamics and adapt to achieve optimal performance while satisfying the problem constraints.

2. Five categories of building comfort (including thermal, thermal, visual, auditory, olfactory, and hygienic comfort), their constraints, specifications, and requirements are modeled and included in the proposed building management system. In addition, building cost-effectiveness requirements are formulated and included in the control scheme.

3. In the proposed building control scheme, estimations from the data-driven and model-based building models are utilized to build the optimization problem. In each instance, the dynamic information of users, energy usage, and ambient conditions are fed back to the model-based controller to update the objective function for the next time sample. This ensures that the system disturbances are taken into account. In particular, in the proposed approach, a learning-based design is utilized for computing the objective function, learning the building uncertainties and its dynamics, and solving the optimization problem.

4. While most of the previous studies on building management applications focused on buildings thermal control, to optimize the energy consumption, this study is set out to address energy and comfort management in all the subsystems in a building. The proposed management system ensures the highest possible overall thermal, visual, auditory, olfactory, and hygienic comfort in buildings with the lowest possible energy usage in the corresponding subsystems.

5.2 Future Research

In this dissertation, we have proposed predictive control approaches for CPSs management and control, assuming that the actuators are free of fault. However, an actuator malfunction in a plant may corrupt the behavior of the whole system and lead to critical degradation in the system stability and closed-loop performance. Compensating the actuator faults in a system is difficult since the control re-computation and reconfiguration are the only remedies to address this issue. Studies in [52, 28] used back-up fault approaches, in which they use back-up states of control inputs in terms of a fault. Literature [3, 119] implemented fault-free decentralized MPC architectures on smart plants, in which no coordination exists in the algorithm. For future research, fault tolerance properties can be incorporated into the distributed MPC approach to handle the actuator faults in CPS. In the fault-tolerant method, the faulty subsystem's sates should be considered in the optimization cost function of the neighboring subsystems. When a failure happens, control inputs are computed considering the effects of the faulty subsystem on its neighboring subsystems; the neighboring subsystems can sacrifice their performance to recover the faulty subsystem.

This way, the system's overall stability and performance can be preserved. Furthermore, the plant response to some unpredicted failures, such as actuator failures, can be practically surveyed on CPS testbeds for future research.

Cyber-physical systems are innately fragmented structures with heterogeneous components. As though CPS control tools being developed for various types of CPSs' requirements, and disciplines are not necessarily compatible with each other. In this regard, the most prominent challenge in the CPS control and management area is the lack of a generic and integrated control tool, i.e., a framework in which different models and tools can be integrated, combined, and modified. For instance, there are a number of simulation software for modeling the building components, such as Energy Plus, TRNSYS, HVACSIM, BSim, and BLAST, which are required to be linked with the programming software, like Python, to run the specific controller on these models. All of the mentioned software requires interfaces to be linked to other programming software. It would be easier and more user-friendly if the designer can develop both the model and controller in one framework. The integrated simulation software should provide the ability to quantify and compare all the aspects of the CPS performance and costs relevant to its design, construction, operation, and controls. In a smart building context, the simulations can be the thermal simulations, lighting simulations, energy consumption calculations, airflow simulations, building modeling/architecture, visual comfort trends, and load trends. The benefits of using building simulation software are as follows:

- Get a real-time view of the building operating performances by collecting all the analytics data.

- Instead of relying on the previous projects' experiences, run hundreds of full building simulations to save millions of dollars by designing efficient optimization methods.
- Get a clear understanding of the climate that the building is being constructed in and how to best leverage passive strategies to move into the world of active and renewable optimization.
- By updating the models as the building design changes, the designer can keep track of the building performance with each design decision.

The inputs of this software can be the local climatic data (temperature, humidity, solar radiation, wind speed and direction), building shape and geometry, shadings and surroundings of the building, building plan (inside and outside), building envelope, building materials characteristics (such as the walls thermal conductivity and resistivity), building appliances characteristics, building operation/occupancy schedules, and type of the control approach. Various parameters can be quantified and analyzed using the tool, such as the zonal/surface/water/construction layer temperature trends, zonal/whole heat balances, load profiles, energy demands of the building devices, and comfort measures (e.g., PPD or PMV comfort standards). As though an integrated building management software can be developed in the future, that contains the mentioned features above. The management tool is required to include all the components with their specific constraints and attributes. This tool should be developed generic and configurable, i.e., the user can conveniently utilize the components to simulate and analyze a management system. Furthermore, the tool should be developed open-source, i.e., the user can modify and configure the tool components.

CHAPTER VI

PUBLICATIONS

1. **Roja Eini**, Lauren Linkous, Nasibeh Zohrabi, and Sherif Abdelwahed, "Smart Building Management System: Performance Specifications and Design Requirements," *Journal of Building Engineering,* 2021.

2. **Roja Eini**, and Sherif Abdelwahed, "A Learning-based Control Approach for Comfort Management and Energy Efficiency in Smart Buildings," *ACM Transactions on Cyber-Physical Systems*, under review.

3. **Roja Eini**, and Sherif Abdelwahed, "A Neural Network-based Model Predictive Control Approach for Buildings Comfort Management," *2020 IEEE International Smart Cities Conference (ISC2)*, Piscataway, NJ, October 2020.

4. **Roja Eini**, and Sherif Abdelwahed, "Learning-based Model Predictive Control for Smart Building Thermal Management," *2019 IEEE 16th International Conference on Smart Cities: Improving Quality of Life Using ICT IoT and AI (HONET-ICT),* Charlotte, NC, October 2019.

5. **Roja Eini**, and Sherif Abdelwahed, "Distributed Model Predictive Control for Intelligent Traffic System," *: 2019 International Conference on Green Computing and Communications (GreenCom),* Atlanta, GA, July 2019.

6. **Roja Eini**, and Sherif Abdelwahed, "Rotational Inverted Pendulum Controller Design using Indirect Adaptive Fuzzy Model Predictive Control," *2019 IEEE International Conference on Fuzzy Systems (FUZZ-IEEE),* New Orleans, LA, June 2019.

7. Adam Morrissett, **Roja Eini**, Mostafa Zaman, Nasibeh Zohrabi, and Sherif Abdelwahed, "A Physical Testbed for Intelligent Transportation Systems," *2019 12th International Conference on Human System Interaction (HSI),* Richmond, VA, June 2019.

8. **Roja Eini**, Lauren Linkous, Nasibeh Zohrabi, and Sherif Abdelwahed, "A Testbed for a Smart Building: Design and Implementation," *Proceedings of the Fourth Workshop on International Science of Smart City Operations and Platforms Engineering (SCOPE '19),* Montreal, QC, Canada, April 2019.

9. **Roja Eini**, and Sherif Abdelwahed, "Distributed Model Predictive Control Based on Goal Coordination for Multi-Zone Building Temperature Control," *2019 IEEE Green Technologies Conference (GreenTech),* Lafayette, LA, April 2019.

10. **Roja Eini**, and Sherif Abdelwahed, "Indirect Adaptive Fuzzy Controller Design for a Rotational Inverted Pendulum," *2018 Annual American Control Conference (ACC),* Milwaukee, WI, August 2018.

REFERENCES

[1] *International Organization for Standardization. ISO 140: acoustic – measurement of sound insulation in buildings and of building elements (parts 1 - 14).*

[2] *International Organization for Standardization. ISO 16283 (Part 1: Airborne sound insulation, Part 2: Impact soundinsulation, Part 3: Facade sound insulation).*

[3] B. Aguiar, D. Berdjag, B. Demaya, and T.-M. Guerra, "A robust and fault tolerant approach for automatic train stop control system design," *IFAC-PapersOnLine*, vol. 50, no. 1, 2017, pp. 8549–8554.

[4] W. Al-Gherwi, H. Budman, and A. Elkamel, "Selection of control structure for distributed model predictive control in the presence of model errors," *Journal of Process Control*, vol. 20, no. 3, 2010, pp. 270–284.

[5] S. Altomonte and S. Schiavon, "Occupant satisfaction in LEED and non-LEED certified buildings," *Building and Environment*, vol. 68, 2013, pp. 66–76.

[6] R. Alur, *Principles of cyber-physical systems*, MIT Press, 2015.

[7] R. American Society of Heating and A.-C. Engineers, "ANSI/ASHRAE Standard 62.1-2019,", 2019.

[8] R. American Society of Heating and A.-C. Engineers, "ANSI/ASHRAE Standard 62.2-2019,", 2019.

[9] J. A. Andersson, J. Gillis, G. Horn, J. B. Rawlings, and M. Diehl, "CasADi: a software framework for nonlinear optimization and optimal control," *Mathematical Programming Computation*, vol. 11, no. 1, 2019, pp. 1–36.

[10] G. Antonelli, "Interconnected dynamic systems: An overview on distributed control," *IEEE Control Systems Magazine*, vol. 33, no. 1, 2013, pp. 76–88.

[11] F. Ascione, N. Bianco, C. De Stasio, G. M. Mauro, and G. P. Vanoli, "Simulation-based model predictive control by the multi-objective optimization of building energy performance and thermal comfort," *Energy and Buildings*, vol. 111, 2016, pp. 131–144.

[12] A. ASHRAE, "Standard 62.1-2004 Ventilation for Acceptable Indoor Air Quality," *American Society of Heating, Refrigerating and Air-Conditioning Engineers, Atlanta, GA, USA 2004*, 2004.

[13] J. Bai and X. Zhang, "A new adaptive PI controller and its application in HVAC systems," *Energy Conversion and Management*, vol. 48, no. 4, 2007, pp. 1043–1054.

[14] G. Ballou, *Handbook for sound engineers*, Taylor & Francis, 2013.

[15] F. Barata, N. Felix, and R. Neves-Silva, "Distributed MPC for green thermally comfortable buildings based on an electro-thermal modular approach," *Procedia Technology*, vol. 17, 2014, pp. 772–780.

[16] F. Barata and R. Neves-Silva, "Distributed model predictive control for thermal house comfort with auction of available energy," *2012 International Conference on Smart Grid Technology, Economics and Policies (SG-TEP)*. IEEE, 2012, pp. 1–4.

[17] F. Belić, Ž. Hocenski, and D. Slišković, "Thermal modeling of buildings with RC method and parameter estimation," *2016 International Conference on Smart Systems and Technologies (SST)*. IEEE, 2016, pp. 19–25.

[18] M. Benosman, *Learning-based adaptive control: An extremum seeking approach–theory and applications*, Butterworth-Heinemann, 2016.

[19] B. Berglund, T. Lindvall, D. H. Schwela, W. H. Organization, et al., "Guidelines for community noise," 1999.

[20] G. Bianchini, M. Casini, D. Pepe, A. Vicino, and G. G. Zanvettor, "An integrated model predictive control approach for optimal HVAC and energy storage operation in large-scale buildings," *Applied Energy*, vol. 240, 2019, pp. 327 – 340.

[21] E. Biyik, J. D. Brooks, H. Sehgal, J. Shah, and S. Gency, "Cloud-based model predictive building thermostatic controls of commercial buildings: Algorithm and implementation," *2015 American Control Conference (ACC)*. IEEE, 2015, pp. 1683–1688.

[22] E. Biyik and A. Kahraman, "A predictive control strategy for optimal management of peak load, thermal comfort, energy storage and renewables in multi-zone buildings," *Journal of building engineering*, vol. 25, 2019, p. 100826.

[23] M. Boduch and W. Fincher, "Standards of human comfort: relative and absolute," *TSoA-Seminar in Sustainable Architecture, Meadows Seminar Fall*, 2009.

[24] D. Boyd, *Intelligent buildings*, Alfred Waller, 1994.

[25] J. Bradley, "Deriving acceptable values for party wall sound insulation from survey results," *Proceedings of Inter-Noise*. Citeseer, 2001.

[26] E. F. Camacho and C. B. Alba, *Model predictive control*, Springer Science & Business Media, 2013.

[27] M. D. Center, "Optimization toolbox, constrained optimization, fmincon,".

[28] M. R. Chen, Y. L. Pei, and L. W. Hu, "A Model of the Driving Fault Tolerance of Traffic Management and Control Facilities at Urban Intersections," *Applied Mechanics and Materials*. Trans Tech Publ, 2014, vol. 496, pp. 2751–2755.

[29] G. Clausen, L. Carrick, P. O. Fanger, S. W. Kim, T. Poulsen, and J. H. Rindel, "A comparative study of discomfort caused by indoor air pollution, thermal load and noisec," *Indoor Air*, vol. 3, no. 4, 1993, pp. 255–262.

[30] C. H. Dagli, *Artificial neural networks for intelligent manufacturing*, Springer Science & Business Media, 2012.

[31] R. J. De Dear and G. S. Brager, "Thermal comfort in naturally ventilated buildings: revisions to ASHRAE Standard 55," *Energy and buildings*, vol. 34, no. 6, 2002, pp. 549–561.

[32] T. Dewson, B. Day, and A. Irving, "Least squares parameter estimation of a reduced order thermal model of an experimental building," *Building and Environment*, vol. 28, no. 2, 1993, pp. 127–137.

[33] E. Diaconescu, "The use of NARX neural networks to predict chaotic time series," *Wseas Transactions on computer research*, vol. 3, no. 3, 2008, pp. 182–191.

[34] D. Doan, T. Keviczky, I. Necoara, M. Diehl, and B. De Schutter, "A Distributed Version of Han's Method for DMPC of Dynamically Coupled Systems with Coupled Constraints," *IFAC Proceedings Volumes*, vol. 42, no. 20, 2009, pp. 240–245.

[35] A. I. Dounis and C. Caraiscos, "Advanced control systems engineering for energy and comfort management in a building environment—A review," *Renewable and Sustainable Energy Reviews*, vol. 13, no. 6-7, 2009, pp. 1246–1261.

[36] J. Drgoňa and M. Kvasnica, "Comparison of MPC strategies for building control," *2013 International Conference on Process Control (PC)*. IEEE, 2013, pp. 401–406.

[37] J. Drgoňa, D. Picard, M. Kvasnica, and L. Helsen, "Approximate model predictive building control via machine learning," *Applied Energy*, vol. 218, 2018, pp. 199–216.

[38] R. Eini and S. Abdelwahed, "Indirect Adaptive fuzzy Controller Design for a Rotational Inverted Pendulum," *2018 Annual American Control Conference (ACC)*. IEEE, 2018, pp. 1677–1682.

[39] R. Eini and S. Abdelwahed, "Distributed model predictive control based on goal coordination for multi-zone building temperature control," *2019 IEEE Green Technologies Conference (GreenTech)*. IEEE, 2019, pp. 1–6.

[40] R. Eini and S. Abdelwahed, "Distributed model predictive control for intelligent traffic system," *2019 International Conference on Internet of Things (iThings) and IEEE Green Computing and Communications (GreenCom) and IEEE Cyber, Physical and Social Computing (CPSCom) and IEEE Smart Data (SmartData)*. IEEE, 2019, pp. 909–915.

[41] R. Eini and S. Abdelwahed, "Learning-based model predictive control for smart building thermal management," *2019 IEEE 16th International Conference on Smart Cities: Improving Quality of Life Using ICT & IoT and AI (HONET-ICT)*. IEEE, 2019, pp. 038–042.

[42] R. Eini and S. Abdelwahed, "Rotational inverted pendulum controller design using indirect adaptive fuzzy model predictive control," *2019 IEEE International Conference on Fuzzy Systems (FUZZ-IEEE)*. IEEE, 2019, pp. 1–6.

[43] R. Eini and S. Abdelwahed, "A Neural Network-based Model Predictive Control Approach for Buildings Comfort Management," *2020 IEEE International Smart Cities Conference (ISC2)*. IEEE, 2020, pp. 1–7.

[44] R. Eini, L. Linkous, N. Zohrabi, and S. Abdelwahed, "A testbed for a smart building: design and implementation," *Proceedings of the Fourth Workshop on International Science of Smart City Operations and Platforms Engineering*, 2019, pp. 1–6.

[45] R. Eini, L. Linkous, N. Zohrabi, and S. Abdelwahed, "Smart building management system: Performance specifications and design requirements," *Journal of Building Engineering*, vol. 39, 2021, p. 102222.

[46] G. W. Evans and J. M. McCoy, "When buildings don't work: The role of architecture in human health," *Journal of Environmental psychology*, vol. 18, no. 1, 1998, pp. 85–94.

[47] P. O. Fanger, J. Lauridsen, P. Bluyssen, and G. Clausen, "Air pollution sources in offices and assembly halls, quantified by the olf unit," *Energy and Buildings*, vol. 12, no. 1, 1988, pp. 7–19.

[48] M. P. Fanti, A. M. Mangini, and M. Roccotelli, "A simulation and control model for building energy management," *Control Engineering Practice*, vol. 72, 2018, pp. 192–205.

[49] M. Finnegan, C. Pickering, and P. Burge, "The sick building syndrome: prevalence studies.," *Br Med J (Clin Res Ed)*, vol. 289, no. 6458, 1984, pp. 1573–1575.

[50] A. Ghofrani, S. D. Nazemi, and M. A. Jafari, "HVAC load synchronization in smart building communities," *Sustainable Cities and Society*, vol. 51, 2019, p. 101741.

[51] A. Guerrieri, V. Loscri, A. Rovella, and G. Fortino, *Management of cyber physical objects in the future internet of things*, Springer, 2016.

[52] J. Haddad and B. Mirkin, "Distributed fault tolerant perimeter control for urban road networks," *IFAC-PapersOnLine*, vol. 50, no. 1, 2017, pp. 4234 – 4239, 20th IFAC World Congress.

[53] F. Haldi and D. Robinson, "Interactions with window openings by office occupants," *Building and Environment*, vol. 44, no. 12, 2009, pp. 2378 – 2395.

[54] A. A. W. Hawila and A. Merabtine, "A statistical-based optimization method to integrate thermal comfort in the design of low energy consumption building," *Journal of Building Engineering*, vol. 33, p. 101661.

[55] S. Haykin, "Adaptive filter theory, ser," *Information and System Science. Prentice Hall*, 2002.

[56] S. Haykin, *Kalman filtering and neural networks*, vol. 47, John Wiley & Sons, 2004.

[57] I. Hazyuk, C. Ghiaus, and D. Penhouet, "Optimal temperature control of intermittently heated buildings using Model Predictive Control: Part I–Building modeling," *Building and Environment*, vol. 51, 2012, pp. 379–387.

[58] S. Herkel, U. Knapp, and J. Pfafferott, "Towards a model of user behaviour regarding the manual control of windows in office buildings," *Building and Environment*, vol. 43, no. 4, 2008, pp. 588 – 600, Part Special: Building Performance Simulation.

[59] R. G. Hopkinson, "Glare from daylighting in buildings," *Applied ergonomics*, vol. 3, no. 4, 1972, pp. 206–215.

[60] O. Howlett, L. Heschong, and J. McHugh, "Scoping study for daylight metrics from luminance maps," *Leukos*, vol. 3, no. 3, 2007, pp. 201–215.

[61] A. Jakubiec and C. Reinhart, "The use of glare metrics in the design of daylit spaces: recommendations for practice," *9th international Radiance workshop*, 2010, pp. 20–21.

[62] J. Jakubiec, "The use of visual comfort metrics in the design of daylit spaces," *Ph. D. in Architecture: Building Technology, Massachusetts Institute of Technology, Department of Architecture*, 2014.

[63] R. Jones, "Modelling water vapour conditions in buildings," *Building Services Engineering Research and Technology*, vol. 14, no. 3, 1993, pp. 99–106.

[64] R. Jones, "Indoor humidity calculation procedures," *Building Services Engineering Research and Technology*, vol. 16, no. 3, 1995, pp. 119–126.

[65] B. Karg and S. Lucia, "Deep learning-based embedded mixed-integer model predictive control," *2018 European Control Conference (ECC)*. IEEE, 2018, pp. 2075–2080.

[66] J. Klein, "Machine learning perspectives for smart buildings: an overview," 2017.

[67] D. Kleinbaum and M. Klein, "Survival Analysis: A Self-Learning Text (Statistics for Biology and Health). 2005,".

[68] J. Kleissl and Y. Agarwal, "Cyber-physical energy systems: Focus on smart buildings," *Design Automation Conference*. IEEE, 2010, pp. 749–754.

[69] T. Kletz, "Reducing Risks, Protecting People—HSE's Decision Making Process, HSE Books, 2001, 74 pp,£ 5, ISBN 0 7176 2151 0,", 2003.

[70] C. D. Korkas, S. Baldi, I. Michailidis, and E. B. Kosmatopoulos, "Occupancy-based demand response and thermal comfort optimization in microgrids with renewable energy sources and energy storage," *Applied Energy*, vol. 163, 2016, pp. 93–104.

[71] W. H. Kwon and S. H. Han, *Receding horizon control: model predictive control for state models*, Springer Science & Business Media, 2006.

[72] E. A. Lee, "Computing foundations and practice for cyber-physical systems: A preliminary report," *University of California, Berkeley, Tech. Rep. UCB/EECS-2007-72*, vol. 21, 2007.

[73] S. Li and Y. Zheng, *Distributed model predictive control for plant-wide systems*, John Wiley & Sons, 2016.

[74] B. Lim, M. Van Den Briel, S. Thiébaux, S. Backhaus, and R. Bent, "Hvac-aware occupancy scheduling," *Twenty-Ninth AAAI Conference on Artificial Intelligence*, 2015.

[75] D. Lim, B. P. Rasmussen, and D. Swaroop, "Selecting PID control gains for nonlinear HVAC&R systems," *HVAC&R Research*, vol. 15, no. 6, 2009, pp. 991–1019.

[76] F. Ljunggren, C. Simmons, and R. Öqvist, "Evaluation of impact sound insulation from 20 Hz," *24th International Congress on Sound and Vibration, London, 23-24 July, 2017*. International Institute of Acoustics and Vibration, 2017.

[77] Y. Long, S. Liu, L. Xie, and K. H. Johansson, "A scenario-based distributed stochastic MPC for building temperature regulation," *2014 IEEE international conference on automation science and engineering (CASE)*. IEEE, 2014, pp. 1091–1096.

[78] M. Luzi, M. Vaccarini, and M. Lemma, "A tuning methodology of Model Predictive Control design for energy efficient building thermal control," *Journal of Building Engineering*, vol. 21, 2019, pp. 28–36.

[79] Y. Ma, G. Anderson, and F. Borrelli, "A distributed predictive control approach to building temperature regulation," *Proceedings of the 2011 American Control Conference*. IEEE, 2011, pp. 2089–2094.

[80] M. Macarulla, M. Casals, N. Forcada, and M. Gangolells, "Implementation of predictive control in a commercial building energy management system using neural networks," *Energy and Buildings*, vol. 151, 2017, pp. 511–519.

[81] J. M. Maestre, R. R. Negenborn, et al., *Distributed model predictive control made easy*, vol. 69, Springer, 2014.

[82] R. Mahmoud, T. Yousuf, F. Aloul, and I. Zualkernan, "Internet of things (IoT) security: Current status, challenges and prospective measures," *2015 10th International Conference for Internet Technology and Secured Transactions (ICITST)*. IEEE, 2015, pp. 336–341.

[83] M. Manic, K. Amarasinghe, J. J. Rodriguez-Andina, and C. Rieger, "Intelligent Buildings of the Future: Cyberaware, Deep Learning Powered, and Human Interacting," *IEEE Industrial Electronics Magazine*, vol. 10, no. 4, 2016, pp. 32–49.

[84] M. Manic, D. Wijayasekara, K. Amarasinghe, and J. J. Rodriguez-Andina, "Building Energy Management Systems: The Age of Intelligent and Adaptive Buildings," *IEEE Industrial Electronics Magazine*, vol. 10, no. 1, 2016, pp. 25–39.

[85] T. F. Megahed, S. M. Abdelkader, and A. Zakaria, "Energy management in zero-energy building using neural network predictive control," *IEEE Internet of Things Journal*, vol. 6, no. 3, 2019, pp. 5336–5344.

[86] J. M. P. Menezes Jr and G. A. Barreto, "Long-term time series prediction with the NARX network: An empirical evaluation," *Neurocomputing*, vol. 71, no. 16-18, 2008, pp. 3335–3343.

[87] I. Milford, A. Lovestad, J. H. Rindel, and R. Klaeboe, "Socio-acoustic survey of sound quality in dwellings in Norway," *INTER-NOISE and NOISE-CON Congress and Conference Proceedings*. Institute of Noise Control Engineering, 2016, vol. 253, pp. 1606–1613.

[88] R. Ming, W. Yu, X. Zhao, Y. Liu, B. Li, E. Essah, and R. Yao, "Assessing energy saving potentials of office buildings based on adaptive thermal comfort using a tracking-based method," *Energy and Buildings*, vol. 208, 2020, p. 109611.

[89] R. Mitchell and I.-R. Chen, "A survey of intrusion detection techniques for cyber-physical systems," *ACM Computing Surveys (CSUR)*, vol. 46, no. 4, 2014, pp. 1–29.

[90] P.-D. Moroşan, R. Bourdais, D. Dumur, and J. Buisson, "Distributed model predictive control for building temperature regulation," *Proceedings of the 2010 American Control Conference*. IEEE, 2010, pp. 3174–3179.

[91] A. Morrissett, R. Eini, M. Zaman, N. Zohrabi, and S. Abdelwahed, "A Physical Testbed for Intelligent Transportation Systems," *2019 12th International Conference on Human System Interaction (HSI)*. IEEE, 2019, pp. 161–167.

[92] D. S. Naidu and C. G. Rieger, "Advanced control strategies for heating, ventilation, air-conditioning, and refrigeration systems—An overview: Part I: Hard control," *Hvac&R Research*, vol. 17, no. 1, 2011, pp. 2–21.

[93] D. S. Naidu and C. G. Rieger, "Advanced control strategies for HVAC&R systems—An overview: Part II: Soft and fusion control," *Hvac&R Research*, vol. 17, no. 2, 2011, pp. 144–158.

[94] K. Ogata and Y. Yang, *Modern control engineering*, vol. 5, Prentice hall Upper Saddle River, NJ, 2010.

[95] J. Page, D. Robinson, N. Morel, and J.-L. Scartezzini, "A generalised stochastic model for the simulation of occupant presence," *Energy and Buildings*, vol. 40, no. 2, 2008, pp. 83 – 98.

[96] A. Parisio, L. Fabietti, M. Molinari, D. Varagnolo, and K. H. Johansson, "Control of HVAC systems via scenario-based explicit MPC," *53rd IEEE conference on decision and control*. IEEE, 2014, pp. 5201–5207.

[97] L. Pérez-Lombard, J. Ortiz, and C. Pout, "A review on buildings energy consumption information," *Energy and buildings*, vol. 40, no. 3, 2008, pp. 394–398.

[98] J. Reynolds, Y. Rezgui, A. Kwan, and S. Piriou, "A zone-level, building energy optimisation combining an artificial neural network, a genetic algorithm, and model predictive control," *Energy*, vol. 151, 2018, pp. 729–739.

[99] R. Ruusu, S. Cao, B. M. Delgado, and A. Hasan, "Direct quantification of multiple-source energy flexibility in a residential building using a new model predictive high-level controller," *Energy Conversion and Management*, vol. 180, 2019, pp. 1109–1128.

[100] A. Schirrer, M. Brandstetter, I. Leobner, S. Hauer, and M. Kozek, "Nonlinear model predictive control for a heating and cooling system of a low-energy office building," *Energy and Buildings*, vol. 125, 2016, pp. 86–98.

[101] H. F. Society and A. N. S. Institute, "American national standard for human factors engineering of visual display terminal workstations," Human Factors Society, 1988.

[102] S. S. Stevens, "On the psychophysical law.," *Psychological review*, vol. 64, no. 3, 1957, p. 153.

[103] J. Y. Suk, M. Schiler, and K. Kensek, "Investigation of existing discomfort glare indices using human subject study data," *Building and Environment*, vol. 113, 2017, pp. 121 – 130, Advances in daylighting and visual comfort research.

[104] Y. Sutter, D. Dumortier, and M. Fontoynont, "The use of shading systems in VDU task offices: A pilot study," *Energy and Buildings*, vol. 38, no. 7, 2006, pp. 780 – 789, Special Issue on Daylighting Buildings.

[105] J. A. Suykens, J. P. Vandewalle, and B. L. de Moor, *Artificial neural networks for modelling and control of non-linear systems*, Springer Science & Business Media, 2012.

[106] W. Tempest, *The noise handbook*, Academic Press New York, 1985.

[107] A. TenWolde and I. S. Walker, "Interior moisture design loads for residences," *Performance of exterior envelopes of whole buildings VIII [electronic resource]: integration of building envelopes. Atlanta, GA: American Society of Heating, Refrigerating and Air-Conditioning Engineers, c2001: ISBN: 1883413966: 6 pages.*, 2001.

[108] J. J. Todd, "Urban air quality," *Environment Design Guide*, 2005, pp. 1–8.

[109] K. Van Den Wymelenberg and M. Inanici, "Evaluating a new suite of luminance-based design metrics for predicting human visual comfort in offices with daylight," *Leukos*, vol. 12, no. 3, 2016, pp. 113–138.

[110] K. M. Vu, *The ARIMA and VARIMA time series: their modelings, Analyses and Applications*, AuLac Technologies Inc., 2007.

[111] G. Walton and A. K. Persily, *Prototype Software for Contaminant-Based Design*, Tech. Rep., 2002.

[112] X. Wang, X. Mao, and H. Khodaei, "A multi-objective home energy management system based on internet of things and optimization algorithms," *Journal of Building Engineering*, vol. 33, p. 101603.

[113] J. Wienold and J. Christoffersen, "Towards a new daylight glare rating," *Lux Europa, Berlin*, 2005, pp. 157–161.

[114] J. Wienold and J. Christoffersen, "Evaluation methods and development of a new glare prediction model for daylight environments with the use of CCD cameras," *Energy and buildings*, vol. 38, no. 7, 2006, pp. 743–757.

[115] J. Xu and D. Nikovski, "A humidity integrated building thermal model," *2016 American Control Conference (ACC)*. IEEE, 2016, pp. 1492–1499.

[116] M. Zaheer-Uddin and G. Zheng, "Multistage optimal operating strategies for HVAC systems," *Ashrae Transactions*, vol. 107, 2001, p. 346.

[117] T. Zhang, M. P. Wan, B. F. Ng, and S. Yang, "Model Predictive Control for Building Energy Reduction and Temperature Regulation," *2018 IEEE Green Technologies Conference (GreenTech)*. IEEE, 2018, pp. 100–106.

[118] Y. Zhang and S. Li, "Networked model predictive control based on neighbourhood optimization for serially connected large-scale processes," *Journal of process control*, vol. 17, no. 1, 2007, pp. 37–50.

[119] H. Zhihong, Z. Yuan, and X. Chang, "A robust fault-tolerant control strategy for networked control systems," *Journal of Network and Computer Applications*, vol. 34, no. 2, 2011, pp. 708–714.

[120] J. Zhu, Y. Shen, Z. Song, D. Zhou, Z. Zhang, and A. Kusiak, "Data-driven building load profiling and energy management," *Sustainable Cities and Society*, vol. 49, 2019, p. 101587.

[121] Z. Zhu and J. Wu, "On the standardization of VDT's proper and optimal contrast range," *Ergonomics*, vol. 33, no. 7, 1990, pp. 925–932.